2Aticle

LMSC-D282873
VOL II
MSC-07040, DRL-3
CR 134327

FINAL REPORT FOR

DEVELOPMENT AND DESIGN APPLICATION OF RIGIDIZED SURFACE INSULATION THERMAL PROTECTION SYSTEMS

VOLUME II - APPENDIXES

30 DEC 1972

CONTRACT NAS9-12856

(NASA-CR-134327) DEVELOPMENT AND DESIGN APPLICATION OF RIGIDIZED SURFACE INSULATION THERMAL PROTECTION SYSTEMS. VOLUME 2: APPENDIXES (Lockheed Missiles and Space Co.) ~~164~~ 166 p CSCL 22B

N74-28340

Unclas G3/31 42825

LMSC

PREPARED FOR NATIONAL AERONAUTICS AND SPACE ADMINISTRATION,
MANNED SPACECRAFT CENTER,
BY LOCKHEED MISSILES & SPACE COMPANY, INC.,
MANNED SPACE SUPPORT SYSTEMS, SPACE SYSTEMS DIVISION

LOCKHEED MISSILES & SPACE COMPANY, INC.
A SUBSIDIARY OF LOCKHEED AIRCRAFT CORPORATION
SPACE SYSTEMS DIVISION • SUNNYVALE, CALIFORNIA

ATTENTION

AS NOTED IN THE NTIS ANNOUNCEMENT, PORTIONS OF THIS REPORT ARE NOT LEGIBLE. HOWEVER, IT IS THE BEST REPRODUCTION AVAILABLE FROM THE COPY SENT TO NTIS.

LMSC-D282673
Vol II
MSC-07040
DRL-3

FINAL REPORT FOR DEVELOPMENT AND DESIGN APPLICATION OF RIGIDIZED SURFACE INSULATION THERMAL PROTECTION SYSTEMS

Volume II – Appendixes

30 December 1972

Contract NAS 9-12856

Approved:

A. E. Trapp
Project Leader

Approved:

K. J. Forsberg, Assistant Director
Materials and Structures

J. F. Milton, Director
Manned Space Support Systems

Prepared for National Aeronautics and Space Administration, Manned Spacecraft Center, by Lockheed Missiles & Space Company, Inc., Manned Space Support Systems, Space Systems Division

1<

DISTRIBUTION

In accordance with contract requirements and instructions of the COR, this document has been distributed as follows:

	No. Copies
NASA Manned Spacecraft Center Orbiter Procurement Section Houston, Texas 77058 Attention: Paul W. Liebhardt/BC42	1
NASA Manned Spacecraft Center Technology Utilization Office Houston, Texas 77058 Attention: John Wheeler/JM7	1
NASA Manned Spacecraft Center Documentation Management Office Houston, Texas 77058 Attention: Charles M. Grant/JM2	3
Langley Research Center MD – Thermal Protection Mail Stop 206 Hampton, Virginia 23365 Attention: Andrew J. Chapman	1
George C. Marshall Space Flight Center S&E-ASTN-M Huntsville, Alabama 35812 Attention: Wilbur A. Riehl	1
NASA Ames Research Center Mail Stop 234-1 Moffett Field, California 94035 Attention: Howard Larson	1
Lewis Research Center Service Protection Br. MS49-1 Cleveland, Ohio 44135 Attention: S. J. Grisaffee	1

2<

	No. Copies
NASA Manned Spacecraft Center Structures and Mechanics Division Houston, Texas 77058 Attention: ES5/Don Tillian	41

ABSTRACT/FOREWORD

This final report presents the results of NASA Contract NAS 9-12856, "Development and Design Application of Rigidized Surface Insulation Thermal Protection Systems" performed by Lockheed Missiles and Space Company for the National Aeronautics and Space Administration, Manned Spacecraft Center, under the direction of the Thermal Technology Branch of the Structures and Mechanics Division, D. J. Tillian, COR.

The contract objective was to establish materials and design technology of the LMSC all-silica LI-900 rigid surface insulation (RSI) thermal protection system (TPS) concept for the Shuttle spacecraft. All results of contract development efforts to satisfy this objective are documented. Engineering design and analysis of RSI strain arrestor plate material selections, sizing, and weight studies are reported. A shuttle prototype test panel was designed, analyzed, fabricated, and delivered to NASA. Thermophysical and mechanical properties of LI-900 were experimentally established and reported. Environmental tests, including simulations of shuttle loads represented by thermal response, turbulent duct, convective cycling, and chemical tolerance tests are described and results reported. Descriptions of material test samples and panels fabricated for both NASA and LMSC testing are included. Descriptions of analytical sizing and design procedures are presented in a manner formulated to allow competent engineering organizations to perform rational design studies. Results of parametric studies involving material and system variables are reported. Material performance and design data are also delineated.

Areas requiring additional development effort are discussed and the conclusion drawn that no problems are foreseen that cannot be solved within the present NASA Shuttle time span. Based on the results of this contract effort, LMSC considers the LI-900 TPS to be sufficiently well developed to warrant use on the first Shuttle flight vehicle.

This report consists of two volumes. Volume I is the main body of the report and Volume II contains appendix material.

CONTENTS

Appendix A1

PROPOSED LI-900 FAILURE CONDITION

Appendix A1

PROPOSED LI-900 FAILURE CONDITION

The failure equation proposed by Hoffman (Ref. A1-1) to fit brittle fracture data has shown great utility for applications in composite materials. However, if applied to transversely isotropic materials, it does not satisfy invariance properties as it should for rotations about the axis of transverse isotropy. This condition is not of much importance in TPS tile analysis but nevertheless it should be handled properly.

To rectify the situation, the following equation is proposed.

$$\frac{\sigma_x^2 - \sigma_x\sigma_y + \sigma_y^2 + 3\tau_{xy}^2}{F_{tx}F_{cx}} + \frac{\sigma_z^2}{F_{tz}F_{cz}} + \left(\frac{1}{F_{tx}} - \frac{1}{F_{cx}}\right)(\sigma_x + \sigma_y) + \left(\frac{1}{F_{tz}} - \frac{1}{F_{cz}}\right)\sigma_z + \frac{\tau_{yz}^2 + \tau_{zx}^2}{F_{s_{xz}}^2} = 1$$

where

- F_{tx} = magnitude of in-plane tensile strength
- F_{cx} = magnitude of in-plane compressive strength
- F_{tz} = magnitude of cross-plane tensile strength
- F_{cz} = magnitude of cross-plane compressive strength
- $F_{s_{xz}}$ = magnitude of transverse shear strength

For application of this equation, it is assumed that the z-axis is the axis of transverse isotropy and that all directions in the x-y plane are equivalent. The equation satisfies the required invariance properties upon rotations about the z-axis.

This equation gives the same result as Hoffman's equation for σ_z and τ_{xz}, i.e., the case of most interest in TPS tile analysis.

If the compressive allowables are assumed to be equal to the measured tensile allowables, as suggested by J. Mueller (Ref. A1-2), then the following equation is proposed for combined stress states in the LI-900, LI-1500 family of RSI composite materials

$$\frac{\sigma_x^2 - \sigma_x\sigma_y + \sigma_y^2 + 3\tau_{xy}^2}{F_{tx}^2} + \frac{\sigma_z^2}{F_{tz}^2} + \frac{\tau_{yz}^2 + \tau_{xz}^2}{F_{s_{xz}}^2} = 1$$

subject to experimental verification.

With regard to such verification, the so-called off-axis testing can provide useful information on the cross-plane tension and transverse shear interaction on RSI failure. In Fig. A-1 are shown predictions for LI-900 based upon average values obtained under the present contract. The effect of off-axis testing is to introduce a third stress component which has a weakening effect but which does not seriously influence the results for angles up to 45 deg and hence can provide a lower bound on the interaction curve up to that point. To verify other portions of the curve, combined torsion-tension tests should be carried out on annular cylinders.

Qualitative verification of the predictions of Fig. A-1 is given in Fig. A-2, which shows the results of off-axis testing on some LI-1200 (12 lb/ft^3) material.

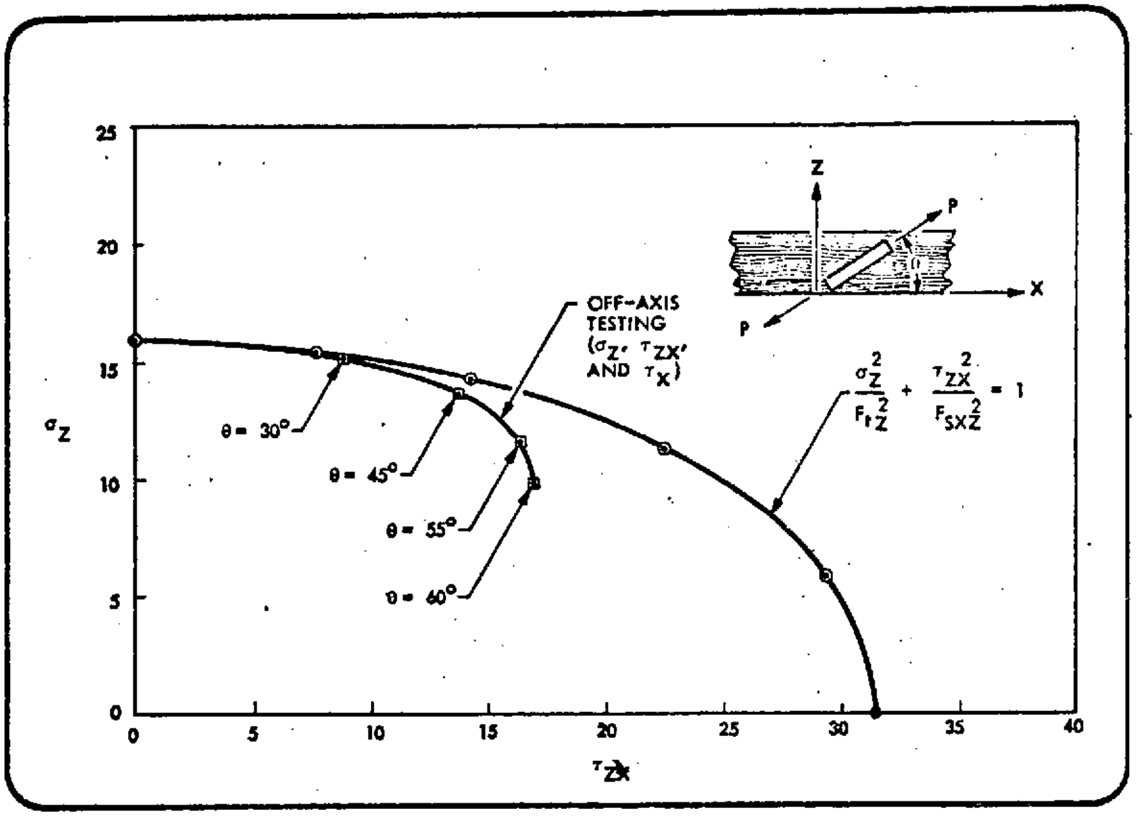

Fig. A1-1 Comparison of Combined Cross-Plane Tension and Transverse Shear With Off-Axis Testing

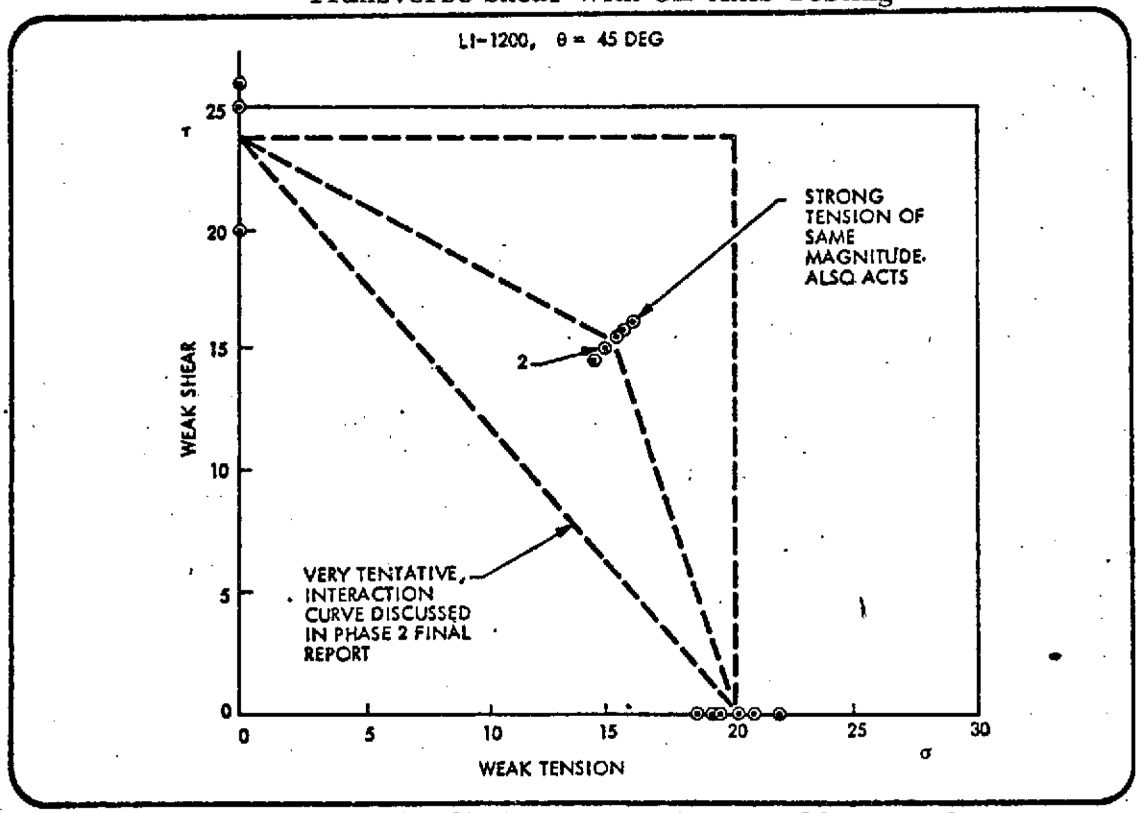

Fig. A1-2 Preliminary Investigation of Merits of "Off-Axis" Testing

REFERENCES

A1-1 Oscar Hoffman, "The Brittle Strength of Orthotropic Materials," J. Composite Materials, Vol. 1 (1967), p. 200

A2-2 J. Mueller, Private Communication

Appendix A2

PROTOTYPE TEST PANEL STRESS ANALYSIS OF PRIMARY STRUCTURE DESIGN OF EDGE STIFFENERS – STIFFENER SPRING RATES

PROTOTYPE PANEL
SECTION PROPERTIES

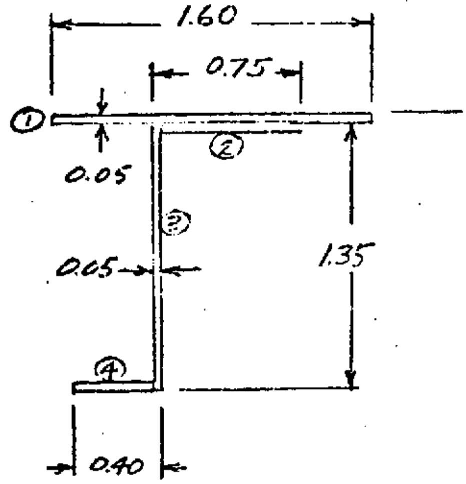

AREA

$$A = (1.60 + 1.35 + 0.75 - 0.05 + 0.40 - 0.05)(0.05)$$

$$= (4.0)(0.05) = 0.200 \text{ IN}^2$$

AREA MOMENT

$$A\bar{y} = (1.60)(0.05)(0.025) + (\overset{0.7}{0.75 - 0.05})(0.075)(0.05)$$

$$+ (1.35)(0.05)(\overset{0.725}{\frac{1.35}{2} + 0.05}) + (\overset{0.35}{0.40 - 0.05})(0.05)(\overset{1.375}{1.35 + 0.05 - 0.025})$$

$$= 0.077624 \text{ IN}^3$$

CENTROID LOCATION

$$\bar{y} = \frac{A\bar{y}}{A}$$

$$= \frac{0.077624}{0.200} = 0.388120 \text{ IN}$$

MOMENT OF INERTIA

$$I_{o,1} = \frac{(1.60)(0.05)^3}{12} = 0.000016666 \text{ IN}^4$$

$$I_{o,2} = \frac{(0.75-0.05)(0.05)^3}{12} = 0.0000072916 \text{ IN}^4$$

$$I_{o,3} = \frac{(0.05)(1.35)^3}{12} = 0.01025156$$

$$I_{o,4} = \frac{(0.40-0.05)(0.05)^3}{12} = 0.0000036458 \text{ IN}^4$$

$$\Sigma I_{o,i} = 0.0102791665 \text{ IN}^4$$

i	b_i	h_i	A_i	$\bar{Y}_i$	$A_i\bar{Y}_i$	$A_i\bar{Y}_i^2$
1	1.60	0.05	0.08	0.025	0.002	0.00005
2	0.7	0.05	0.035	0.075	0.002625	0.000196875
3	0.05	1.35	0.0675	0.725	0.0489375	0.0354797
4	0.35	0.05	0.0175	1.375	0.02406	0.033086
Σ						0.0688125

$$I_{cg} = \Sigma A_i \bar{Y}_i^2 + \Sigma I_{o,i} - (\bar{Y})^2 \Sigma A_i$$

$$= 0.0688125 + 0.0102792 - (0.38812)^2(0.200)$$

$$= 0.04896424 \text{ IN}^4$$

EQUIVALENT THICKNESS

$$\bar{t} = \frac{A}{b_s}$$

$$= \frac{0.200}{1.60} = 0.125 \text{ IN}$$

EFFECTIVE BENDING THICKNESS

$$\frac{b_s \bar{t}_b^3}{12} = I_{cg}$$

$$\bar{t}_b = \sqrt[3]{\frac{12\ I_{cg}}{b_s}}$$

$$\bar{t}_b = \left[\frac{(12)(0.04896424)}{1.6}\right]^{\frac{1}{3}}$$

$$= (0.3672318)^{\frac{1}{3}} = 0.71611 \text{ IN}$$

CONFIGURATION No. 2

MARGINS of SAFETY ~ ULTIMATE

1. MAX. COMPRESSION ON STIFFENER FREE LEG

$$M.S. = \frac{F_{cc}}{\sigma_{C\,MAX\,(ULT)}} - 1$$

COND. I: $M.S. = \frac{44.6}{36.70} - 1 = 1.215 - 1 =$ $\underline{\underline{+0.22}}$ CRIPPLING-ULT.

COND. II: $M.S. = \frac{44.6}{39.45} - 1 = 1.131 - 1 =$ $\underline{\underline{+0.13}}$ CRIPPLING-ULT.

COND. III: $M.S. = \frac{41.5}{28.22} - 1 = 1.471 - 1 =$ $\underline{\underline{+0.47}}$ CRIPPLING-ULT.

2. MAX. TENSION ON STIFFENER FREE LEG

$$M.S. = \frac{F_{tu}}{\sigma_{T\,MAX\,(ULT)}} - 1$$

COND. I: $M.S. = \frac{67}{42.17} - 1 = 1.589 - 1 =$ $\underline{\underline{+0.59}}$ TENS.-ULT.

COND. II: $M.S. = \frac{67}{38.96} - 1 = 1.720 - 1 =$ $\underline{\underline{+0.72}}$ TENS.-ULT.

COND. III: $M.S. = \frac{62.3}{55.29} - 1 = 1.127 - 1 =$ $\underline{\underline{+0.13}}$ TENS.-ULT.

CONFIGURATION No. 2

MAX. ULTIMATE STRESSES ~ APPLIED ~ STIFFENER FREE LEG

1. COMPRESSIVE N_x & BURST p ~ MAX. σ_c ON FREE LEG

COND. I: $\sigma_{I\,MAX} = \dfrac{2250}{.125} + \dfrac{554.4}{.02965} = 18{,}000 + 18{,}698 = 36{,}698$ psi (ULT.)

COND. II: $\sigma_{II\,MAX} = \dfrac{3000}{.125} + \dfrac{458.2}{.02965} = 24{,}000 + 15{,}454 = 39{,}454$ psi (ULT.)

COND. III: $\sigma_{III\,MAX} = \dfrac{3000}{.125} + \dfrac{125.2}{.02965} = 24{,}000 + 4223 = 28{,}223$ psi (ULT.)

2. TENSILE N_x & COLLAPSE p ~ MAX. σ_T ON FREE LEG

USE DIRECT SUPERPOSITION OF TENSION & BENDING

$$\sigma_{T\,MAX} = \frac{N_{xT}}{t} + \frac{M_{MAX}}{Z_{0\,MIN}} = \frac{N_{xT}}{t} + \frac{p_{MAX}\,l^2}{8 Z_{0\,MIN}} = \frac{N_{xT}}{t} + \frac{72\,p_{MAX}}{Z_{0\,MIN}}$$

COND. I: $\sigma_{T\,MAX} = \dfrac{3450}{.125} + \dfrac{72(6.0)}{.02965} = 27{,}600 + 14{,}570 = 42{,}170$ psi (ULT.)

COND. II: $\sigma_{II\,MAX} = \dfrac{4050}{.125} + \dfrac{72(2.7)}{.02965} = 32{,}400 + 6556 = 38{,}956$ psi (ULT.)

COND. III: $\sigma_{III\,MAX} = \dfrac{6000}{.125} + \dfrac{72(3.0)}{.02965} = 48{,}000 + 7285 = 55{,}285$ psi (ULT.)

ALLOWABLE CRIPPLING STRESSES ~ STIFFENER FREE LEG

REF. STRESS MEMO NO. 126: $b/t = (.40 - .12)/.05 = 5.6$

$\dfrac{F_{cc}}{MCF} = 37$ (FIG. 12, REF.) (CONSERVATIVE: $\pm$ IN t)

AT R.T.: $F_{cy}/E_c = 58/10{,}700 = .00542$

$K_m = .0208$ (FIG. 15, REF.)

$MCF = .0208(58) = 1.2064$

$F_{cc} = 1.206(37) = 44.6$ Ksi

AT 250°F: $F_{cy}/E_c = 52.2/10380 = .00502$

$K_m = .0215$ (FIG. 15, REF.)

$MCF = .0215(52.2) = 1.122$

$F_{cc} = 1.122(37) = 41.5$ Ksi

CONFIGURATION No. 2

MAX. ULTIMATE STRESSES ~ APPLIED

1. COMPRESSIVE N_x & BURST p ~ MAX. σ_c ON FREE LEG

REF.: TIMOSHENKO, THEORY of ELASTIC STABILITY, 2ND ED., CHAPTER 1

$$\sigma_{c\,MAX} = \frac{N_{xc}}{\bar{t}} + \frac{M_{MAX}}{\bar{Z}_{o\,MIN}}$$

$$M_{MAX} = \frac{p l^2}{8} \cdot \frac{2(1-\cos u)}{u^2 \cos u} = 144 p_B \cdot f(u) \quad \text{(EQ'N 1-23, REF.)}$$

$$u = \frac{l}{2}\sqrt{\frac{N_{xc}}{E_c \bar{I}_o}} \quad \text{(EQ'N 1-13, REF.)} \; ; f(u) = \frac{1-\cos u}{u^2 \cos u}$$

$$u = \frac{l}{2(I_o \times 10^{?})^{1/2}}\left(\frac{N_{xc}}{E_c \times 10^{-6}}\right)^{1/2} = \frac{24}{2(30{,}010)^{1/2}}\left(\frac{N_{xc}}{E_c \times 10^{-6}}\right)^{1/2} = \frac{1}{14.44}\left(\frac{N_{xc}}{E_c \times 10^{-6}}\right)^{1/2}$$

$$u_I = \frac{1}{14.44}\left(\frac{2250}{10.7}\right)^{1/2} = 1.0042 \; ; u_I^2 = 1.0085$$

$$u_{II} = \frac{1}{14.44}\left(\frac{3000}{10.7}\right)^{1/2} = 1.1596 \; ; u_{II}^2 = 1.3446$$

$$u_{III} = \frac{1}{14.44}\left(\frac{3000}{10.38}\right)^{1/2} = 1.1773 \; ; u_{III}^2 = 1.3861$$

LOAD COND.	u RAD.	u DEG.	$\cos u$	$1-\cos u$	$u^2 \cos u$	$f(u)$
I	1.0042	57°32′	.5368	.4632	.5414	0.8556
II	1.1596	66°26′	.3998	.6002	.5376	1.1164
III	1.1773	67°27′	.3835	.6165	.5316	1.1597

$M_{I\,MAX} = 144\,(4.5)(.8556) = 554.4$ in-lb/in (ULT.)

$M_{II\,MAX} = 144\,(2.85)(1.1164) = 458.2$ in-lb/in (ULT.)

$M_{III\,MAX} = 144\,(0.75)(1.1597) = 125.2$ in-lb/in (ULT.)

CONFIGURATION No. 2

DESIGN LOADS (AREA 2) (REF. No. 5)

COND.	$N_x \sim ppi$		$p \sim psi$	
	LIMIT	ULT.	LIMIT	ULT.
I (R.T.)	2300 -1500	3450 -2250	3.0 -4.0	4.5 -6.0
II (R.T.)	2700 -2000	4050 -3000	1.9 -1.8	2.85 -2.7
III (250°F)	4000 -2000	6000 -3000	0.5 -2.0	0.75 -3.0

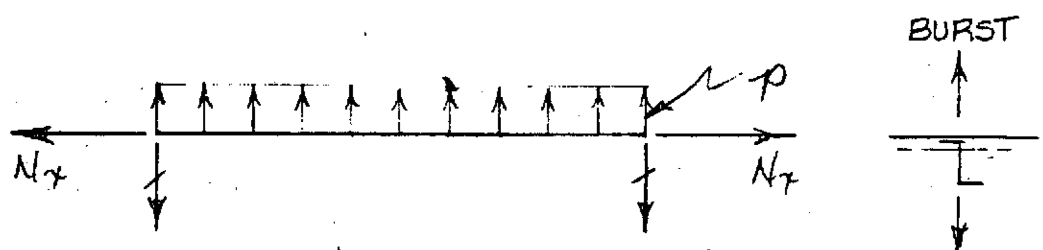

$+N_x \sim$ TENSION ; $-N_x \sim$ COMPRESSION
$+p \sim$ BURST ; $-p \sim$ COLLAPSE

ALLOW. COLUMN LOADS ~ EULER

$$\bar{P}_{CR} = \frac{\pi^2 E_c \bar{I}_o}{(1-\nu^2)\ell^2} = \frac{\pi^2 E_c (.03001)}{.91(24)^2} = \frac{E_c}{1770}$$

AT R.T.:

$$\bar{P}_{CR} = \frac{10,500}{1.770} = 5932 \text{ lb/in}$$

$$\sigma_{CR} = \frac{\bar{P}_{CR}}{\bar{t}} = \frac{5932}{.125} = 47,456 \text{ psi}$$

AT 250° F:

$$\bar{P}_{CR} = \frac{9660}{1.770} = 5458 \text{ lb/in}$$

$$\sigma_{CR} = \frac{5458}{.125} = 43,664 \text{ psi}$$

CONFIGURATION No. 2
SECTION PROPERTIES

FULL SCALE

D/N SK 90971

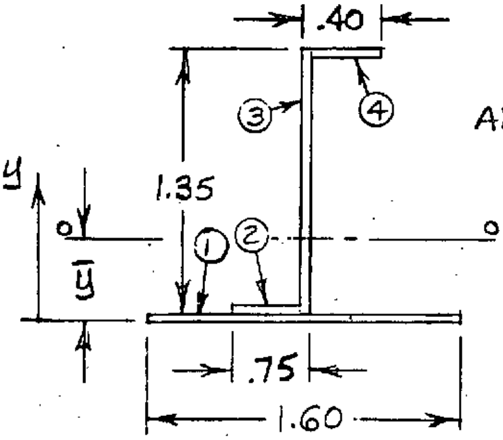

All $t = .050$ in

$R = 0.12$ in (MIN.)

$l = 24.0$ in

$W_T = 144\,\gamma\,\bar{t}$

$= 144(.101)(.1144)$

$W_T = 1.664$ lb/ft²

ELEM.	A	y	Ay	d	Ad²	I_i
1	.0800	.025	.00200	.36305	.01054	.00002
2	.035	.075	.00262	.2555	.00228	—
3	.0675	.725	.04893	.33695	.00766	.01048
4	.0175	1.375	.02406	.98695	.01704	—
Σ	.2000		.07761		.03752	.01050

$\bar{y} = \dfrac{.07761}{.2000} = 0.38805$ in ; $\bar{t} = \dfrac{.2000}{1.60} = 0.125$ in

$I_o = .03752 + .01050 = .04802$ in⁴ ; $\bar{I}_o = \dfrac{.04802}{1.60} = .03001$ in⁴/in

$\dfrac{I_o}{A} = \dfrac{.04802}{.2000} = 0.2401$ in²

$\rho = (.2401)^{1/2} = 0.490$ in

$\bar{Z}_{O\,MAX} = .03001/.388 = .07733$ in³/in

$\bar{Z}_{O\,MIN} = .03001/1.01195 = .02965$ in³/in

MATERIAL ~ 2024-T81 - ALUMINUM ALLOY : REF. MIL-HDBK-5A, SECT. 3.2.7

R.T. (TAB. 3.2.3.0 (b₂))		250 °F (5 HRS. EXPOSURE)	
F_{tu} = 67 Ksi	(.93)	62.3 Ksi	(FIG. 3.2.7.1.1 (a))
F_{ty} = 58 Ksi	(.96)	55.7 Ksi	(FIG. 3.2.7.1.1 (b))
F_{cy} = 58 Ksi	(.90)	52.2 Ksi	(FIG. 3.2.7.1.2 (a))
E = 10.5×10³ Ksi	(.97)	10.2 ×10³ Ksi	(FIG. 3.2.7.1.4)
E_c = 10.7×10³ Ksi	(.97)	10.4 ×10³ Ksi	(FIG. 3.2.7.1.4)
F_{bru} = 127 Ksi ($e/D = 2$)	(.95)	120.7 Ksi	(FIG. 3.2.7.1.3 (a))
F_{bry} = 94 Ksi ($e/D = 2$)	(.96)	90.2 Ksi	(FIG. 3.2.7.1.3 (b))

$\gamma = 0.101$ lb/in³

LOADS

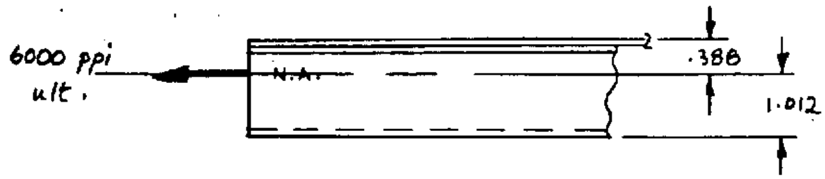

AREA TOP = .1319 in^2.
AREA BOT. = .0681 in^2.
.2000 in^2.

LOAD INTO UPPER SECTION $= (6000)\left(\frac{0.1319}{0.20}\right) = 3960$ ppi (ult.)

LOAD INTO LOWER SECTION $= (6000)\left(\frac{.0681}{0.20}\right) = 2040$ ppi. (ult.)

TOP SECTION:

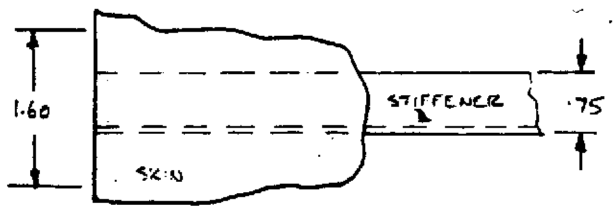

AREA SKIN $= (.85)(.05) = .0425$ in^2.
AREA STIFFENER & SKIN ABOVE $= (.75)(.10) + (.288)(.05) = .0894$ in.^{2}

LOAD INTO SKIN $= (3960)(1.60)\dfrac{(.0425)}{\underbrace{(.0425 + .0894)}_{.1319}} = 2040$ #

LOAD INTO STIFFENER & SKIN ABOVE $= (3960)(1.60)\dfrac{(.0894)}{\underbrace{(.0425 + .0894)}_{.1319}} = 4300$ #

BOTTOM SECTION:

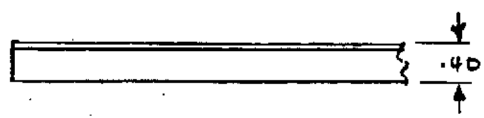

LOAD INTO STIFFENER $= (2040)(1.60) = 3270$ #

AREA $= (.40)(.05) + (0.962)(.05) = .068$ in.^{2}

PANEL STRESSES

@ 250°F, 2024-T81 $\hat{F}_{tu}$ = 62,500 psi.
" " $\hat{F}_{bru}$ = 117,000 psi.

SKIN: $f_t = \dfrac{2040}{(.0425)} = 48{,}000$ psi. M.S. = 0.30

STIFFENER & SKIN (TOP SECTION): $\hat{f}_t = \dfrac{4300}{(.0894)} = 48{,}000$ psi. M.S. = 0.30

STIFFENER (BOTTOM SECTION): $\hat{f}_t = \dfrac{3270}{(.068)} = 48{,}000$ psi. M.S. = 0.30

PANEL END DESIGN

SKIN: USE 5/32" STEEL JO-BOLTS, SHEAR STRENGTH = 1332#

USE 4 BOLTS

LOAD PER BOLT = $\dfrac{2040}{4}$ = 510# OK

BEARING ALLOWABLE = 924# IN .05 SHEET M.S. = 0.81

STIFFENER & SKIN (TOP SECTION):
USE 5/32" MONEL RIVETS, SHEAR STRENGTH = 973#

ASSUME EQUAL LOAD FIRST 4 RIVETS, TAPERED LOAD LAST 4.

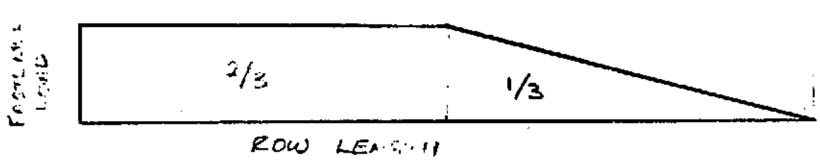

MAX. RIVET LOAD = $\left(\dfrac{2}{3}\right)\dfrac{(4300)}{(4)} = 716$# M.S. = 0.36

BEARING ALLOWABLE = 924# IN .05 SHEET. M.S. = 0.29

STIFFENER (BOTTOM SECTION):

USE 5/32" STEEL JO-BOLTS, SHEAR STRENGTH = 1822#

ASSUME TAPERED LOAD DISTRIBUTION, 7 RIVETS.

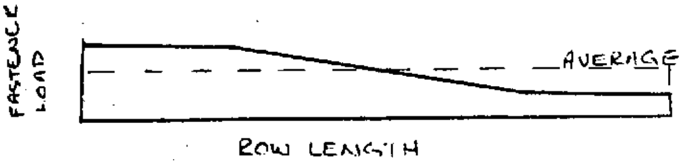

$$\text{MAX. BOLT LOAD} = \left(\frac{3}{2}\right)\frac{(3270)}{7} = 700^{\#}$$ OK

BEARING ALLOWABLE = 924# IN .25 SHEET. M.S. = 0.32

UPPER FINGER PLATE: @ 250°F, MAT'L: 2024-T81, $f_{tu} = 62{,}500$ psi, $f_{bru} = 117{,}000$ psi

AT FIRST ROW, LOAD = 3960 psi. (ult.)

$$\text{NET AREA} = (.16)\left[1.60 - (2)(.159)\right] = .205 \text{ in.}^2$$

$$f_t = \frac{(3960)(1.60)}{(.205)} = 30{,}900 \text{ psi.}$$ M.S. = 1.02

$$\text{BEARING IN RIVET HOLES} = \frac{(716)}{(.159)(.16)} = 28{,}200 \text{ psi}$$ OK

$$\text{BEARING IN } 3/4\text{" DIA BOLT HOLES} = \frac{(3960)(0.8)}{(.375)(.16)} = 52{,}800 \text{ psi.}$$ OK

AT FINGER ROOTS, LOAD = 4300 - (4)(528) = 2190#

$$\text{NET AREA} = (.16)\left[1.2 - .159\right] = .167 \text{ in.}^2$$

$$\sigma_t = \frac{2190}{(.167)} = 13{,}100 \text{ psi.}$$ OK

AT FINGER ENDS, LOAD = 716 #

NET AREA = $(.16)(.75 - .159) = .0946 \text{ in}^2$

$f_t = \dfrac{716}{.0946} = 7{,}570$ psi. OK

$C/D = \dfrac{[illegible]}{.159} = [illegible]$ OK

LOWER SHEAR SPLICE:

AT FIRST ROW, LOAD = 3270 # (ULT.)

NET AREA = $(.125)(1.2 - .159) = .13 \text{ in}^2$

$f_t = \dfrac{3270}{(.13)} = 25{,}200$ psi. M.S. = 1.48

BEARING IN 10-BOLT HOLE = $\dfrac{700}{(.159)(.125)} = 35{,}200$ psi. OK

BEARING IN 3/8" DIA BOLT HOLE = $\dfrac{(2040)(0.8)}{(.375)(.125)} = 34{,}800$ psi. OK

STRAIN COMPATIBILITY AT PANEL ENDS

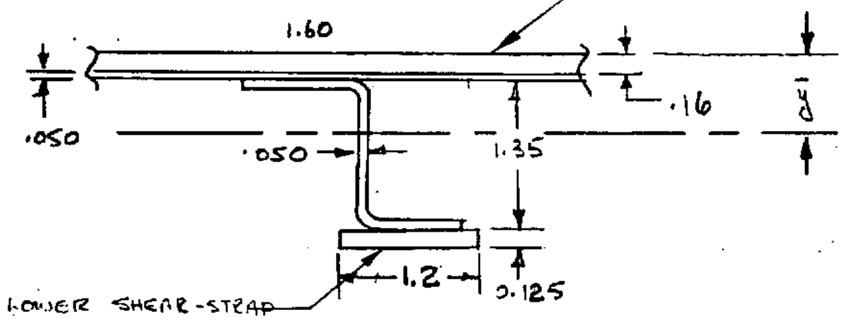

$$\bar{y} = \frac{\Sigma A y}{\Sigma A} = \frac{(1.60)(.21)(.105) + (2.75)(.05)(.885) + (1.2)(.125)(1.6225)}{(1.6)(.21) + (2.75)(.05) + (1.2)(.125)}$$

$$= \frac{.4003}{.6235} = 0.642 \text{ in.}$$

$\bar{y}$ for panel center $= 0.388 + .16 = .548$ in.

Offset axial load distance $= (.642 - .548) = .094$ in.

Bending moment $= (6000)(.094) = 564$ in-lb/in.

$$\text{Approx. } I_{cg} = \frac{(1.6)(.21)^3}{12} + (1.6)(.21)(.488)^2 + \frac{(1.2)(.125)^3}{12} + (1.2)(.125)(1.075)^2$$

$$= 0.26837 \text{ in}^4.$$

$$\sigma_b = \frac{Mc}{I} = \frac{(564)(1.6)(1.0745)}{(0.26837)} = 3613 \text{ psi.}$$ ok

END FITTING TOLERANCE

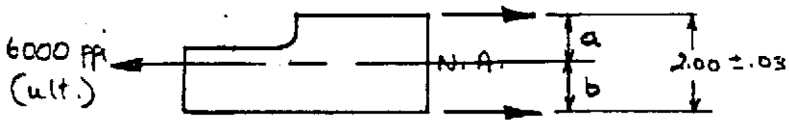

Assume $a = 1.00 \pm .03$

$a + b = 2.00 \pm .03$

Max. offset: $a = 0.97$

$a + b = 2.03 \qquad \therefore\ b = 1.06$

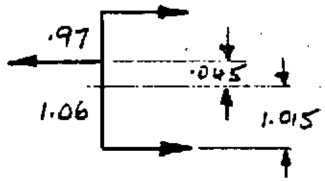

Bending Moment $= (.045)(6000)$

$= 270$ lb-in/in.

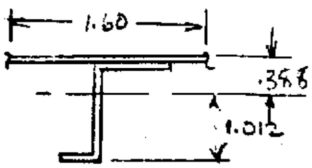

$I_o = .04896\ in^4$.

$$\sigma_b = \frac{Mc}{I} = \frac{(270)(1.012)(1.6)}{(.04896)} = 8920 \text{ psi}$$

$$\sigma_a = \frac{Mc}{I} = \frac{(270)(.388)(1.6)}{(.04896)} = 3420 \text{ psi}$$

Stiffener stress due to axial load = 48,000 psi.

Total = (48,000 + 8,920) = 56,920 psi.

Skin stress due to axial load = 48,000 psi

Total = (48,000 + 3420) = 51,420 psi.

2024-T81 f_{tu} = 62,500 psi.

M.S. = 0.10

EDGE STIFFENERS

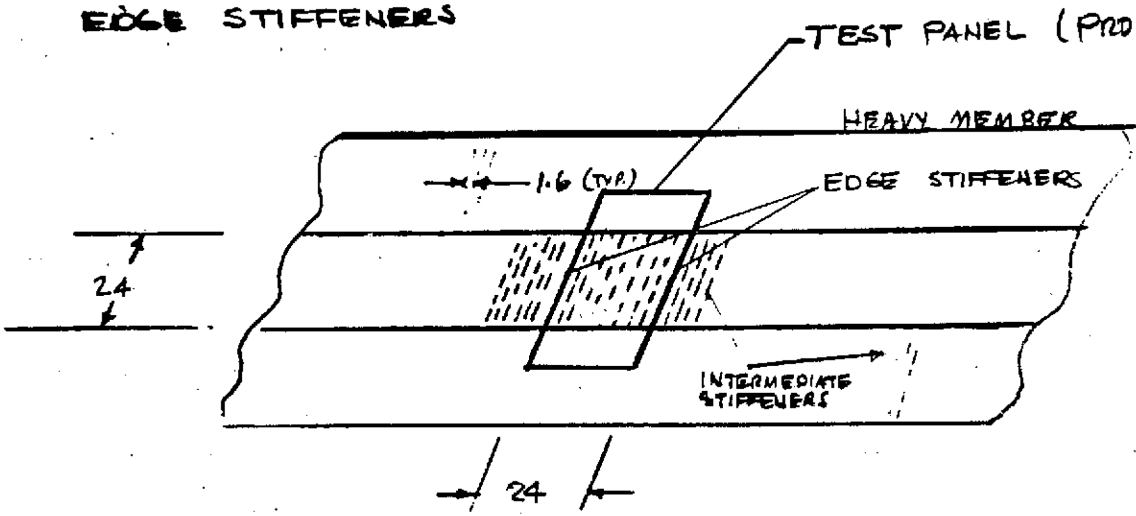

FIG.1 ASSUMED ORBITER LOWER SURFACE GEOMETRY

DETERMINE EDGE STIFFENER REQUIREMENT FOR THE PROTIPE TEST PANEL

DIFFERENTIAL STRAINS AT -250°F CONDITION CAUSE PROTOTYPE PANEL FREE EDGES TO CURL DOWN IN A FASHION THAT CANNOT OCCUR IN REAL, PROPERLY SUPPORTED PANELS. IF THIS CONDITION IS ALLOWED TO HAPPEN, THE SUBSTRUCTURE WOULD HAVE CUSPS.

ASSUMING THAT THE PROTOTYPE PANEL IS A SECTION OF THE ORBITER BOTTOM SURFACE AS SHOWN IN FIG.1, THE PANEL EDGES ARE SUPPORTED BY THE CONTINUOUS STRUCTURE AGAINST ROTATION AND EXCESSIVE LOCAL (VERTICAL DEFLECTIONS). IT IS THEREFORE NECESSARY TO IMPOSE EDGE RESTRICTIONS TO THE PROTOTYPE PANEL TO SIMULATE THESE CONDITIONS.

IN THE FOLLOWING ANALYSIS, THE QUESTION OF HOW MUCH SUPPORT THE CONTINUOUS STRUCTURE IS PROVIDING WILL BE ANSWERED.

DEFLECTION OF A SEMI-INFINITE BEAM ON ELASTIC FOUNDATION

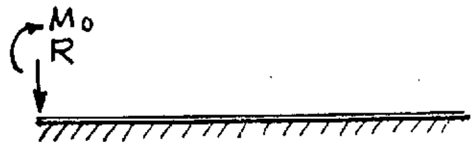

$$\delta_R = \frac{(R - \beta M_0)}{2\beta^3 EI_{BEAM}}$$

(REF. TIMOSHENKO, STR. OF MATERIALS)

ROTATION AT THE EDGE

$$\theta = -\frac{1}{2\beta^2 EI_{BEAM}}\left(R - 2\beta M_0\right)$$ (REF. ")

WHERE

$$\beta = \left[\frac{k}{4EI_{BEAM}}\right]^{1/4}$$

k = MODULUS OF THE FOUNDATION

IF WE CONSIDER THAT THE SLOPE OF THE EDGE IS EQUAL TO ZERO (REPRESENTING CONTINUOUS PANEL) THEN (FROM THE ROTATION EQUATION)

$$M_{0_{\theta=0}} = \frac{R}{2\beta}$$ MOMENT REQUIRED FOR ZERO ROTATION

SUBSTITUTING M_{0_0} INTO DEFLECTION EQUATION,

$$\delta_{\theta=0} = \frac{R - \left(\beta \frac{R}{2\beta}\right)}{2\beta^3 EI_{BEAM}} = \frac{1}{4}\,\frac{R}{\beta^3 EI_{BEAM}}$$

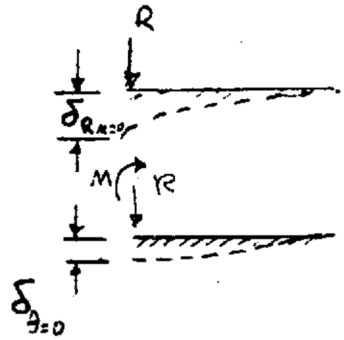

IT FOLLOWS THAT

$$\delta_{\theta=0} = \frac{1}{2}\,\delta_{R_{M=0}}$$

SINCE DEFLECTION IS INVERSELY PROPORTIONAL TO STIFFNESS EI, THE STIFFNESS REQUIRED TO MAINTAIN ZERO SLOPE IS TWICE THE ORIGINAL STIFFNESS OF THE PANEL. THIS HAS BEEN APPROXIMATED BY PLACING HEAVY EDGE MEMBERS TO THE PROTOTYPE PANEL (AS SHOWN BELOW):

	A_{STIF} in^2	I_{STIF} in^4
PANEL CENTER	0.200	0.04911
EDGE STIFFENER	0.420	0.1188

$$\text{STIFFNESS RATIO} = \frac{0.1188}{0.04911} = 2.42$$

INCREASE OF AREA (TOTAL CROSS SECTION OF PANEL)

BASIC PATTERN = 1.0
WITH ORIGINAL STIFFENER = 1.02
NEW STIFFENER = 1.12

NET AREA INCREASE = 10 %

IN ACTUAL PRACTICE, ALL PANELS WILL BE SUPPORTED AT THE EDGES AGAINST NORMAL DEFLECTION AS WELL AS ROTATIONS, THEREFORE THE EDGE STIFFNESS REQUIREMENTS SHOULD BE CONSIDERABLY HIGHER THAN THE PRESENT CONFIGURATION. HOWEVER DUE TO TEST FIXURE LIMITATIONS, THE LOWER BOUND STIFFNESS FOR THE EDGE MEMBERS IS USED. IN THIS WAY THE INCREASE IN TOTAL AREA IS ABOUT 10%.

NEW EDGE STIFFENER

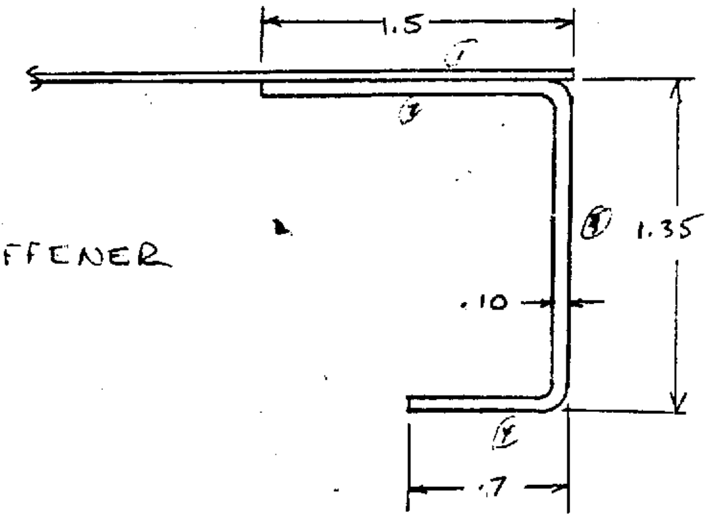

ORIGINAL STIFFENER

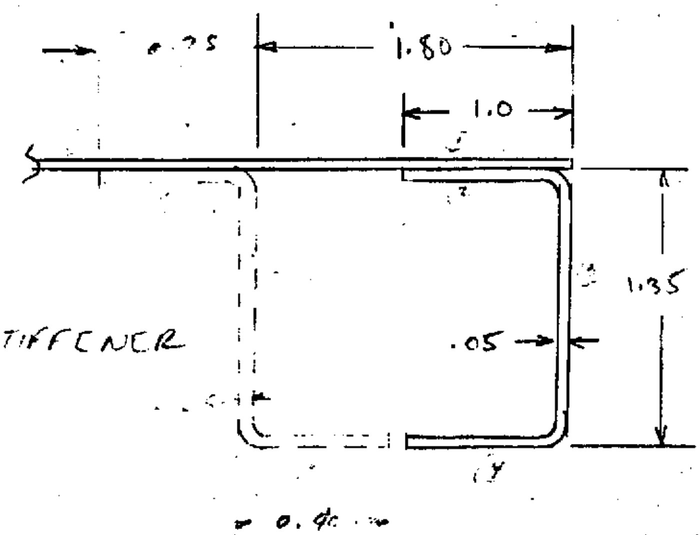

Stiffeners @ 1.6" spacing

Section Properties

	A (in²)	$\bar{r}$ (in)	I_r (in⁴)
Panel Center	0.2000	0.3888	0.04911
Orig. Stiffener	0.2375	0.502	0.07516
New Stiffener	0.420	0.483	0.1189

Relative values

Panel Center	1.0	0.0	1.0
Orig. Stiffener	1.19	+0.113	1.53
New Stiffener	2.10	+0.094	2.42

Gross Areas

	Area (in²)	Relative Areas
Basic Pattern	$= 3.20 + 2 \times 0.200 = 3.60$	1.0
Orig. Stiffener	$= 3.20 + 2 \times 0.2375 = 3.675$	1.02
New Stiffener	$= 3.20 + 2 \times 0.420 = 4.04$	1.12

STIFFENER SIMULATION

FOR POINT LOADING AT BEAM CENTER, SPRING RATE WAS PREVIOUSLY FOUND TO BE (IN TERMS OF MODULUS):

$$\boxed{E_c = 48 \frac{L}{A} \frac{I_s}{\ell^3} E_s}$$

E_c = column modulus
E_s = stiffener "
L = column length
ℓ = stiffener "
A = column width

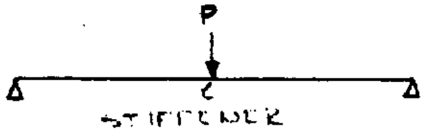

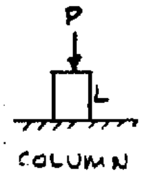

FOR PRESSURE LOADING:

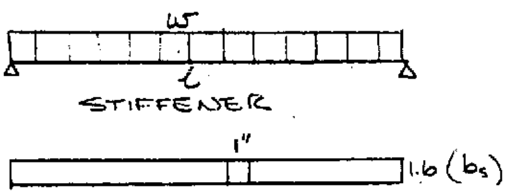

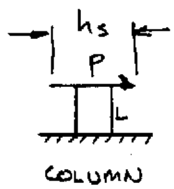

$w = (1.6)p$ Load $= (1.6)p$

$$\delta_{max} = \frac{5}{384} \frac{w\ell^4}{E_s I_s} \qquad \delta_{max} = \frac{(1.6)pL}{AE_c}$$

Setting δ's equal.

$$\frac{5}{384} \frac{(1.6)p\ell^4}{E_s I_s} = \frac{(1.6)pL}{AE_c}$$

$$\therefore E_c = .00046296\ IE_s \quad \begin{bmatrix} L=1, A=.5, \ell=24 \\ E_s=10.5(10^6) \end{bmatrix}$$

In more general form:

$$\frac{5}{384} \frac{(b_s)p\ell^4}{E_s I_s} = \frac{(h_s)pL}{AE_c}$$

$$\boxed{E_c = \left(\frac{384}{5}\right) \frac{h_s}{b_s} \frac{L}{A} \frac{I_s}{\ell^4} E_s}$$

Appendix B 1

RESULTS OF 20-CYCLE ENVIRONMENTAL CONDITIONING OF LI-900 MATERIAL FOR USE UNDER TASK B CONTRACT NAS 9-12856

ENGINEERING MEMORANDUM

TITLE: RESULTS OF 20-CYCLE ENVIRONMENTAL CONDITIONING OF LI-900 MATERIAL FOR USE UNDER TASK B CONTRACT NAS 9-12856	EM NO: L8-1.3.1.3-M1-7 REF: DATE: 27 November 1972
AUTHORS: D. R. Bright *Donald R. Bright*	APPROVAL: ENGINEERING *[signature]* SYSTEM ENGRG

PROBLEM STATEMENT

This EM documents the procedures utilized and the data generated during the cyclic environmental conditioning of the LI-900 material.

TEST REQUIREMENTS

The test parameters specified in the program plan (Ref. 1) were:

1. Reduce the cold plate and tile base temperature to $-320^{\circ}F$ with LN_2.
2. Shut off flow of LN_2 to cold plate.
3. Immediately apply Area 2P heat pulse to top surface of LI-900 tiles.
4. Wait one hour after lamp shut off; then begin flow of LN_2 through cold plate.
5. Repeat above procedures 1 through 4 - 19 times.

The above test requirements were later amended by the customer (Ref. 2), with inclusion of a requirement to perform the test in a pressure environment of air at .147 psia, the pressure to be held constant throughout the test.

The test parameters are shown in Figure 1.

TEST SPECIMEN CONFIGURATION

The test specimens were (4) LI-900 tiles having dimensions of approximately 12.00-inches by 12.00-inches by 3.00-inches. The tiles were coated with 0042 material on the outboard surface and on the outboard half of the sides.

Test tile identification designations were:

TT-1261
TT-1262
TT-1263
TT-1264

Test tile TT-1264 was instrumented with a .75-inch diameter plug thermocouple installation containing (2) platinum-platinum 13% rhodium and (3) chromel-alumel thermocouples as shown in Figure 2. The other tiles were uninstrumented.

Because of the necessity of later bonding this material to test fixtures for the accomplishment of mechanical properties tests, the test tiles were not waterproofed until after test cycle 12, when it bacame obvious that the bonding convenience was outweighed by the water leak hazard of the RADVAC facility.

TEST INSTALLATION

This test program was performed using the RADVAC facility to generate the required test environments. The RADVAC facility is a small vacuum chamber with provisions for the simulation of pressure and heating environments that would be experienced by the space shuttle orbiter during launch, orbit and entry operations. The facility has the capability of simultaneously establishing a controlled chamber pressure and a radiant energy flux field within the space shuttle service envelope. In addition, the chamber is fitted with a cold plate which provides a capability for establishment of orbital temperatures in the test item prior to subjecting the test item to the simulated entry environment. The cold plate is designed for use with water or liquid nitrogen working fluids. At present, the chamber must be open to cool down the test item. Physically, the RADVAC facility consists of the chamber, a support structure for the chamber that incorporates provisions for test item loading, a vacuum control, a water distribution system for chamber cooling, an air blower and ducting for cooling the radiant heater, a vacuum pump and lines, a heating power electrical system and control console, and data sensors and recorders.

Detailed specification of RADVAC are tabulated below:

PRESSURE RANGE: Surface Ambient to 0.15-in. Hg
MAXIMUM HEAT RATE: 50 BTU/FT^2 SEC
MAXIMUM CONTINUOUS HEAT RATE: 25 BTU/FT^2 SEC
COLD PLATE MINIMUM TEMPERATURE: -300°F
COLD PLATE SURFACE DIMENSIONS: 25-in. by 25-in.
MAXIMUM TEST ITEM ENVELOPE: 24-in. by 24-in. by 3-in.

INTRUMENTATION FEEDTHROUGHS IN PRESSURE SHELL:

Thermocouple, Type K, Chromel-Alumel: 16 pr.

Thermocouple, Type R, Pt-Pt 13% Rh 12 pr.

Thermocouple, Type T, Iron-Constantan: 4 pr.

RADIANT HEATER ARRAY: 88 each 5000 watt/500 volt quartz/tungsten heat lamps

The chamber section of RADVAC consists of two sub-assemblies, a top box and a bottom box. The fixed top box contains the heat power system, water system, radiant heater, cooling air system, and viewports. The removable bottom box contains the cold plate, the instrumentation feedthroughs and terminals, and the test volume for test item installation. All testing in RADVAC must be performed with the test item horizontal and the surface to be heated facing up. The installation of the test tiles in the facility is shown in Figure 3. Test heating control was effected by monitoring the surface temperature of the control surface thermocouple (T/C) blocks.

TEST PROCEDURE

The test procedures followed in performance of these material conditioning operations were:

1. Connect LN_2 cooling lines.
2. Cool copper plate to -320°F (approx. time of 20 to 40 minutes).
3. Disconnect LN_2 lines, move specimen array into chamber, seal chamber, and start vacuum pump. (Approx. 6 to 8 minutes)
4. Initiate heat pulse when chamber pressure drops to 0.5 in. Hg during pump down to 0.3 in. Hg. (Approx. 3 minutes)
5. Apply Area 2P heat pulse. (44 minutes)
6. Bleed chamber pressure to 1 ATM, move spec. array to LN_2 lines, connect LN_2 lines to cold plate. (Approx. 7 to 9 minutes)

   NOTE: The total time delay from end of LN_2 cool down to start of heat pulse was between 9 and 11 minutes.

TEST RESULTS

The test program was started on October 19, 1972, and progressed without significant anomaly until cycle 10. During the last five minutes of the cycle 10 test, the water jacket end seals of the RADVAC facility failed, allowing water to be ingested into the vacuum chamber. The water leak affected cold plate temperature and chamber pressure, and was visible through the chamber viewports.

After completing cycle 10, the test tiles were immediately removed, weighed, and returned to the composite materials laboratory for drying. The test tiles were dried and returned to the test laboratory. The leaking seals of the RADVAC facility were repaired.

A non-destructive examination for coating cracks was also performed after cycle 10, with the result that TT-1264 was found to have one crack across the surface. Inspection showed that the crack had originated at the edge of the tile adjacent to the LN_2 connection. As these connections are made and broken during each test cycle, it is likely that the crack was caused by tool damage. The crack is sketched in Figure 3.

At completion of facility repairs, test cycle 11 was performed without anomaly. The specimen array was removed from the vacuum chamber, cooled down to test temperature, then reinstalled in the chamber for test. During the pump-down for cycle 12 the water jacket seal which was repaired after the cycle 10 failure again failed, with the resulting ingestion of water. The chamber was opened and inspected. The amount of water ingested into the chamber did not appear to be excessive compared to the water usually present in the chamber after venting to atmosphere. The tiles were examined and did not appear to be wet, nor were they noticeably heavier than normal. The test tiles were removed and set aside and the RADVAC seals were removed and replaced with new seals. The test tiles were not weighed or dried.

At completion of facility repairs, test cycle 12 was performed, resulting in damage to the coating of tiles TT-1262 and TT-1263, probably caused by rapid generation of steam inside the tile by the applied heat. Cycle 12 was completed and the damaged tiles were removed and returned to the composite materials lab for repair to the coating, inspection, drying and waterproofing.

The repaired and reworked tiles were returned to the test lab, and testing was re-iniated. Test cycle 13 was performed, resulting in a darkening of the coating and in the appearance of the cracks shown in Figure 4. These darkening effects were due to the application of an excess of waterproofing material by the Composite

Materials Laboratory. Photographs were taken and testing continued. Test cycle 14 through test cycle 20 were performed without anomaly and the test tiles were photographed after 20 cycles of environmental conditioning, then removed from the facility and returned to the composite materials lab.

A summary of the significant test data is presented in Table I. Included are temperature maximums and time of maximum for each specimen thermocouple installed, cold plate temperatures, chamber pressures, and control thermocouple temperature maximums and time of maximum for each control thermocouple block. These data are tabulated for each test cycle.

A plot of the ranges of maximum temperatures at each thermocouple versus distance from the heated surface of the tile to the thermocouple is shown in Figure 5.

A comparison of an early nominal test cycle (Cycle 4) and a late nominal test cycle (Cycle 18) temperature responses versus test time is presented in Figure 6.

DISCUSSION

Several deviations from the test requirements occurred due to the marginality of the RADVAC test facility in establishing the test environments. These deviations were:

1. Cold plate minimum temperatures obtainable ranged from -300°F to -265°F. These temperatures were measured with thermocouples installed at edge and center of the cold plate, in areas away from the LN_2 cooling coils, resulting in higher temperature readings than were probably present at the tile/cold plate interface areas.
2. Nominal chamber pressure varied between .40 psia and .08 psia during this test program. The maximum test pressure experienced was 1.25 psia; which occurred during cycle 10, when a large amount of water was ingested into the chamber. This condition was not typical of the test program, but is indicative of a facility failure. These variations were due to the inability of the pumping system to maintain the pressure levels when material outgassing, frost, or water was present in the chamber. Some pressure increases are attributable to leaks at the sealing gaskets and outgassing of the sealing gaskets from heating effects.

The vacuum system is capable of reducing the chamber pressure to 0.20 in Hg in approximately three minutes when the chamber is empty and clean. The minimum pressure obtainable with the present pumping system is approximately 0.15 in. Hg.

3. Cycle 1 temperature program was erratic due to defective control thermocouples.

4. Cycle 20 temperature response was slightly low due to degradation of the control thermocouple.

In general the test data indicates that the required test environments were nominally achieved. The data is in agreement with the analytical predictions and is consistent from cycle to cycle throughout the test program.

The effects of heating the test material in a low pressure environment with water present, as occurred during cycle 12, on the mechanical properties of the material are not known at this time.

REFERENCES

1. LMSC/D282611, DRL-1, 20 July 1972, "Program Plan for Development and Design of Rigidized Surface Insulation Thermal Protection Systems Contract NAS 9-12856".
2. TWX, 2222032-UUUU-RUWMBNA, dated 25 August 1972, P. W. Liebhardt to R. D. Buttram, Subject: RSI Tile Conditioning Requirements on Property Generation Task NAS 9-12855.

TEST FACILITY PARAMETERS
TEMPERATURE & PRESSURE REQUIREMENTS
LI-900 MATERIAL CONDITIONING

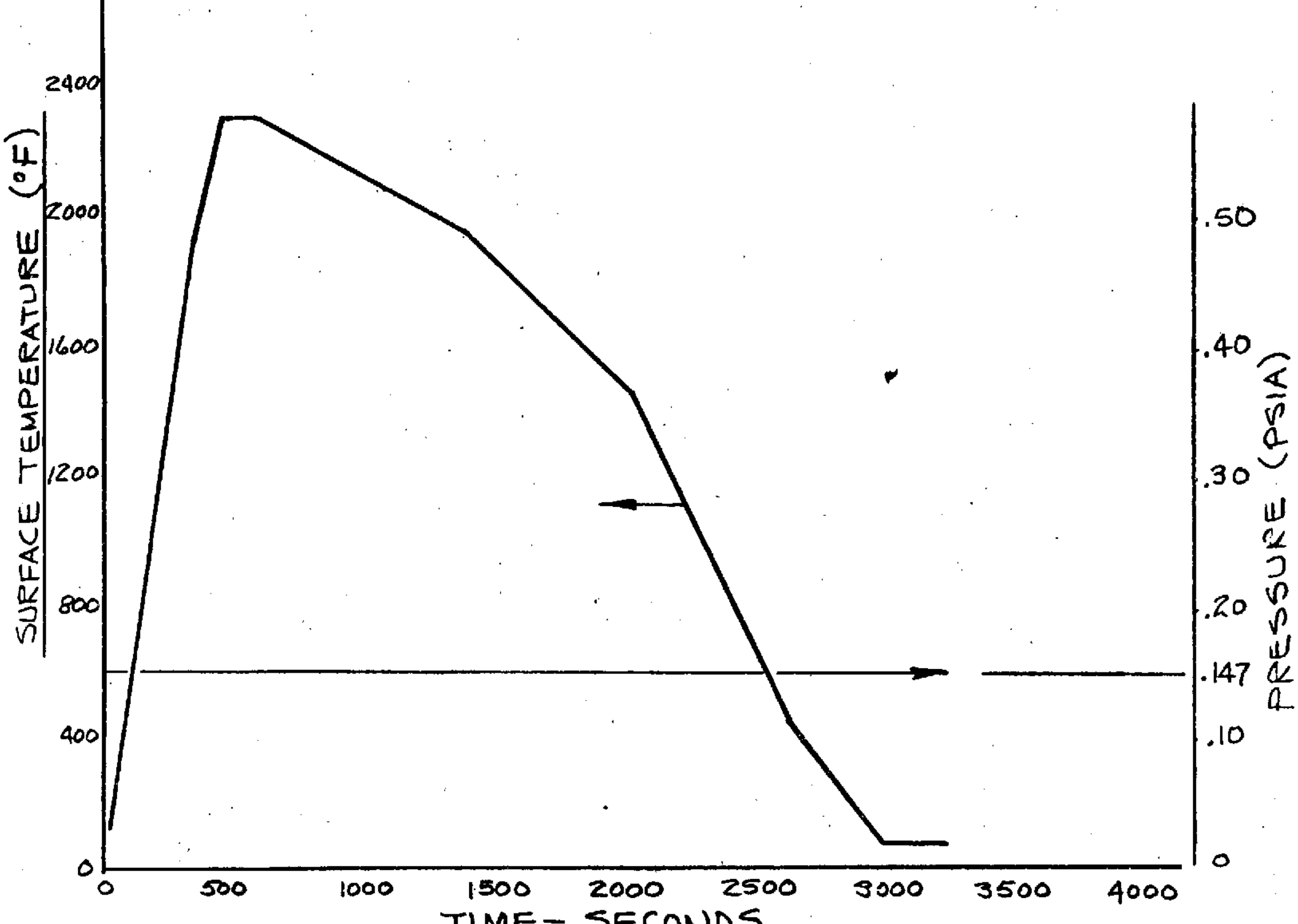

FIGURE 1

TASK B THERMAL CYCLING TESTS

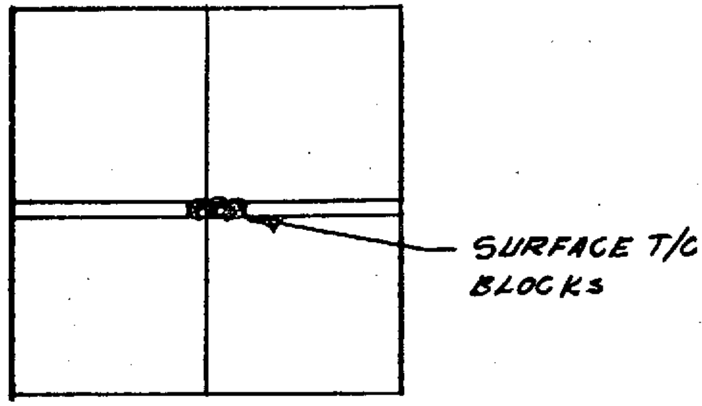

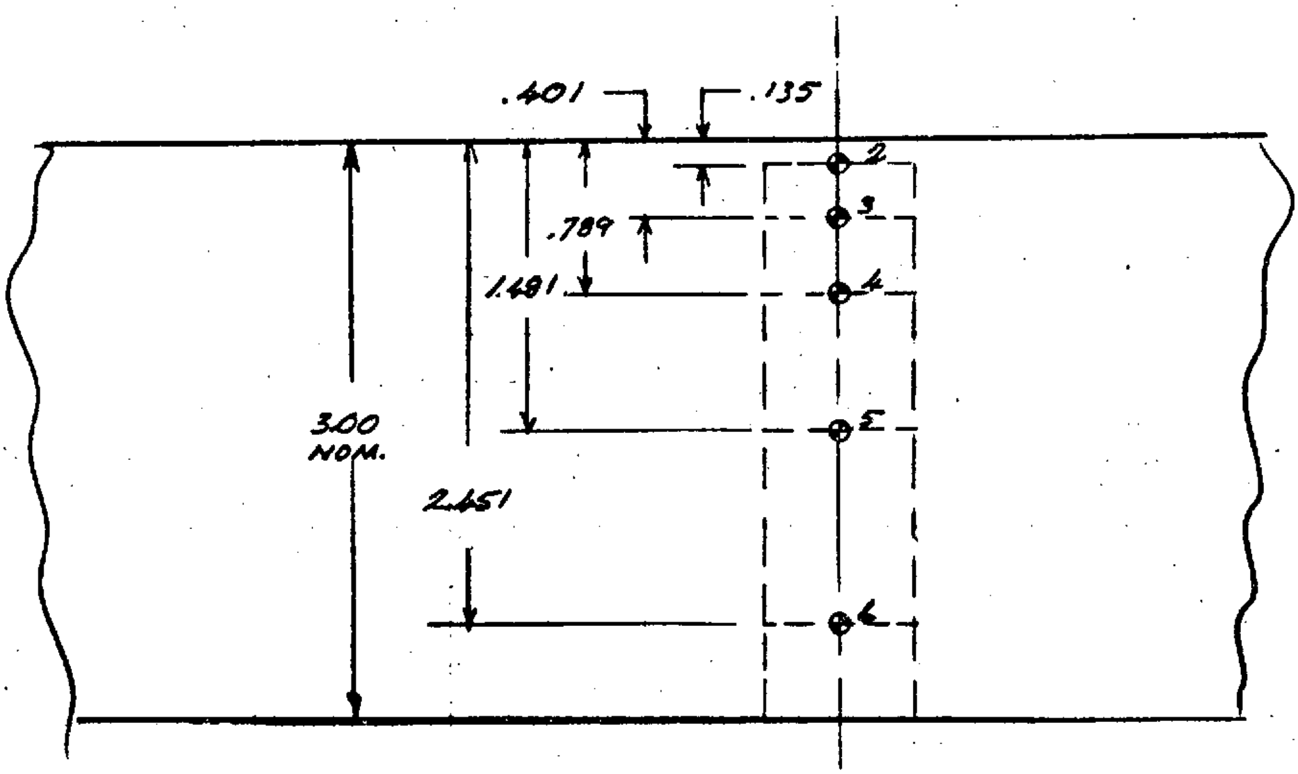

THERMOCOUPLE LOCATIONS

NOTE: T/C'S 2 AND 3 ARE Pt/Pt-13% Rh
(TYPE R); T/C'S 4,5, AND 6 ARE C/A
(TYPE K)

40<

FIGURE 2

LI-900 THERMAL/PRESSURE CYCLING TEST

TEST SETUP DIAGRAM

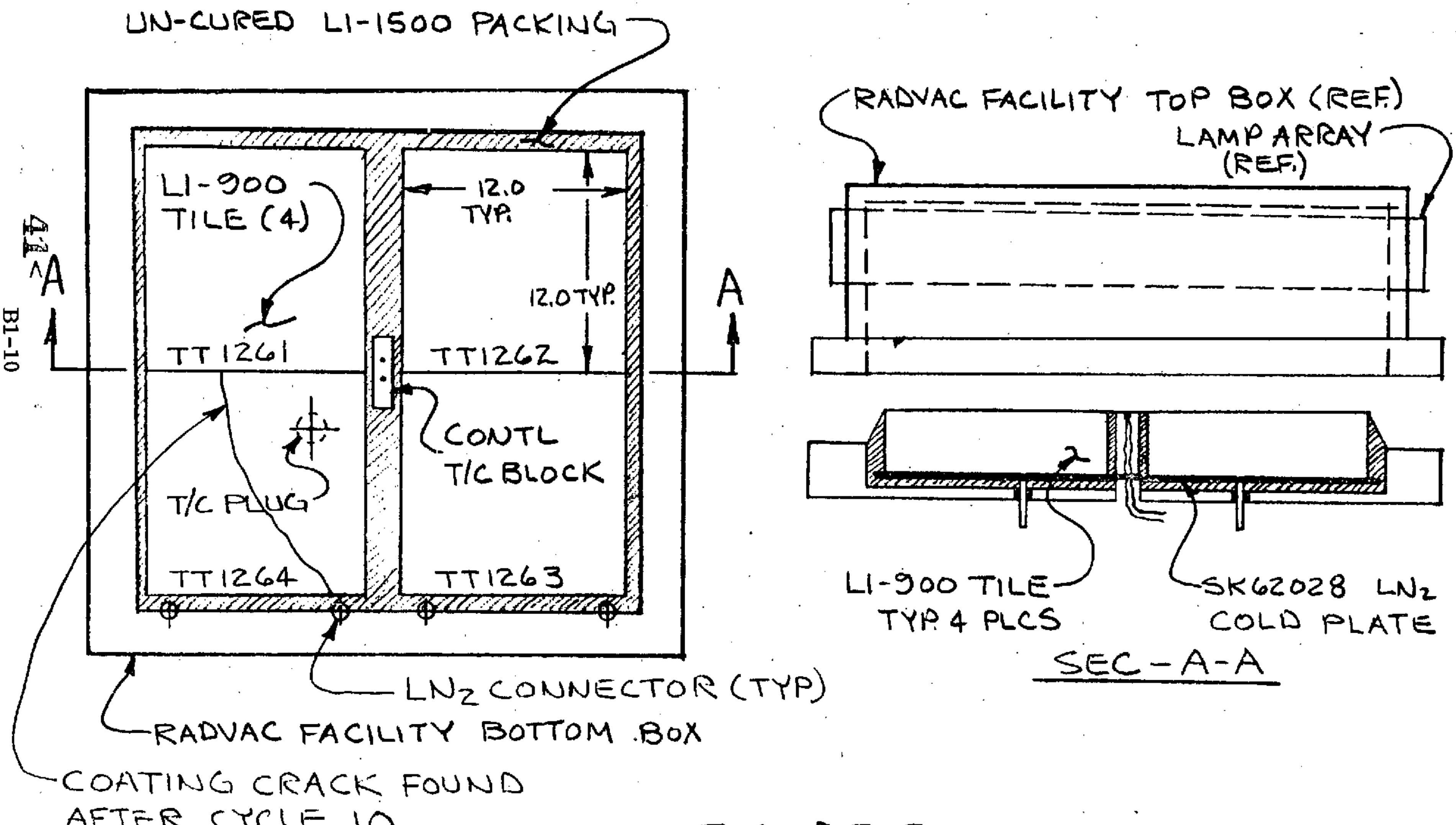

FIGURE 3

TEST TILE COATING CRACK PATTERNS APPEARING DURING TEST CYCLE 13

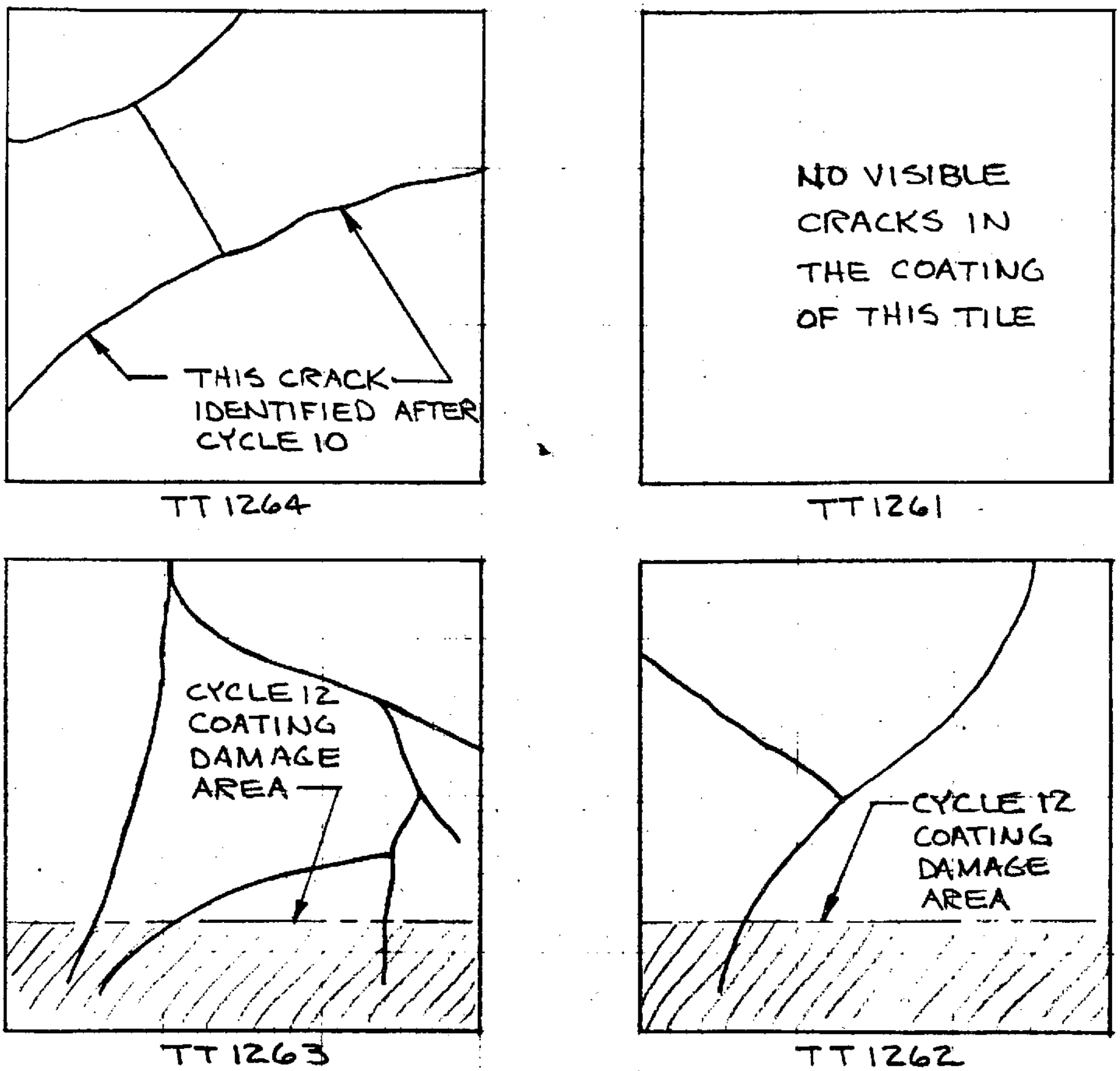

NOTE: THE ABOVE COATING CRACKS BECAME VISIBLE AFTER THE LN_2 COOL-DOWN AND THE LOW PRESSURE ENVIRONMENT HAD BEEN ESTABLISHED, BUT BEFORE THE HEAT PULSE WAS APPLIED.

FIGURE 4

TASK B MATERIAL CONDITIONING

PEAK TEMPERATURE VS. DISTANCE FROM HEATED SURFACE

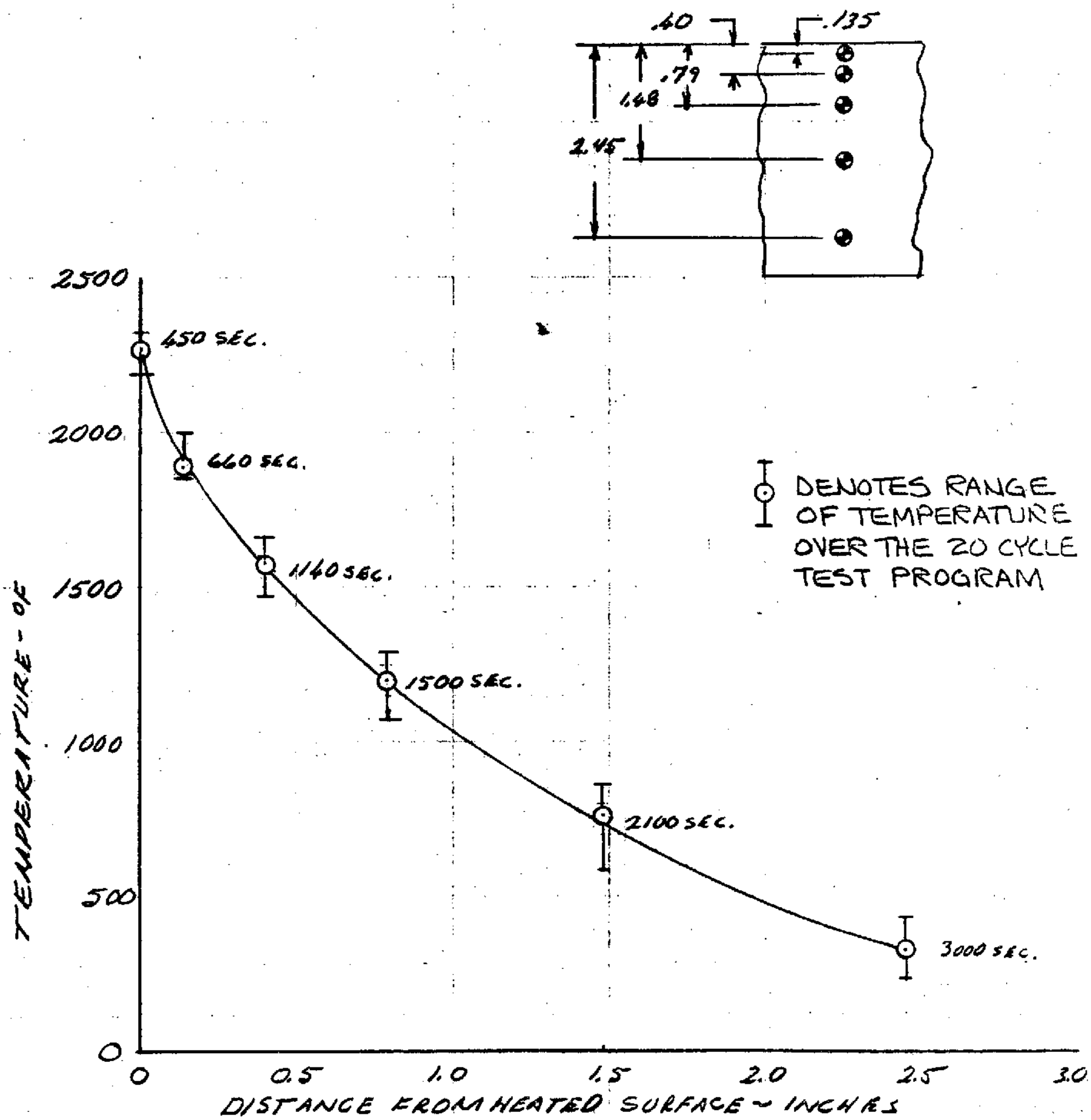

FIGURE 5

TABLE I
SUMMARY OF TEST DATA ~ TASK B MATERIAL CONDITIONING

TEST CYCLE	TEST TILE THERMOCOUPLES										CONTL T/C		COLD PLATE T/C			CHAMBER PRESS.			
	T/C 2		T/C 3		T/C 4		T/C 5		T/C 6		ACTIVE	SPARE	EAST	CENTER	WEST	INITIAL	MAX.	MIN.	FINAL
	TEMP. (°F)	TIME (SEC.)	TEMP. (°F)	TIME (SEC.)	TEMP. (°F)	TIME (SEC.)	TEMP. (°F)	TIME (SEC.)	TEMP (°F)	TIME (SEC.)	TEMP (°F)	TEMP (°F)	TEMP (°F)	TEMP (°F)	TEMP (°F)	PRESS. (PSIA)	PRESS (PSIA)	PRESS. (PSIA)	PRESS (PSIA)
1	1900	615	—	—	1220	1500	780	2100	—	—	2315	2265	-290	-297	-300	.25	.25	.10	.10
2	1950	1080	1580	1080	1250	1500	800	2100	370	2880	2315	2265	-290	-291	-296	.25	.25	.10	.10
3	1920	615	1558	1080	1175	1500	700	2100	373	2880	2315	2265	-290	-287	-290	.34	.34	.18	.18
4	2000	615	1604	1080	1220	1500	774	2100	364	3000	2315	2265	-288	-285	-285	.30	.30	.08	.08
5	1865	615	1472	1080	1072	1500	582	2100	240	3120	2315	2265	-270	-281	-287	.30	.30	.09	.09
6	1900	615	1530	1080	1180	1500	744	2100	334	2520	2315	2265	-274	-280	-285	.30	.30	.17	.30
7	1890	615	1583	1080	1200	1500	770	2100	349	2520	2315	2265	-231	-281	-292	.51	.51	.30	.30
8	1880	615	1558	1080	1182	1500	747	2100	310	2520	2315	2265	-274	-277	-280	.42	.42	.17	.34
9	1910	615	1570	1080	1175	1500	735	2100	290	2640	2315	2265	-278	-274	-285	.38	.38	.25	.25
10	1935	615	1588	1080	1180	1500	738	2100	330	2880	2315	2265	-278	-280	-290	.30	1.25	.13	1.25
11	1870	615	1600	1080	—	—	770	2100	250	3150	2315	2185	-265	-275	-286	.28	.34	.10	.10
12	1870	615	1638	1080	1215	1500	800	2100	435	2880	2315	2185	-266	-285	-282	.24	.40	.15	.25
13	1920	615	1660	1080	1280	1500	860	2100	—	—	2315	2185	-273	-278	-290	.18	.26	.08	.08
14	1885	615	1609	1080	1245	1500	815	2100	332	2880	2315	2185	-282	-282	-287	.25	.33	.08	.08
15	1870	615	1584	1080	1210	1500	785	2100	320	2880	2315	2185	-273	-278	-285	.27	.40	.08	.08
16	1870	615	1600	1080	1220	1500	785	2100	320	2880	2315	2185	-273	-280	-284	.23	.38	.08	.08
17	1855	615	1588	1080	1210	1500	770	2100	310	2880	2315	2185	-271	-280	-285	.28	.36	.08	.08
18	1855	615	1600	1080	1225	1500	800	2100	330	2880	2315	2185	-269	-290	-283	.29	.36	.08	.08
19	1890	615	1578	1080	1200	1500	770	2100	312	2880	2315	2185	-273	-280	-285	.41	.51	.10	.10
20	1850	615	1530	1080	1145	1500	700	2100	275	2880	2315	2185	-266	-275	-285	.36	.47	.10	.10

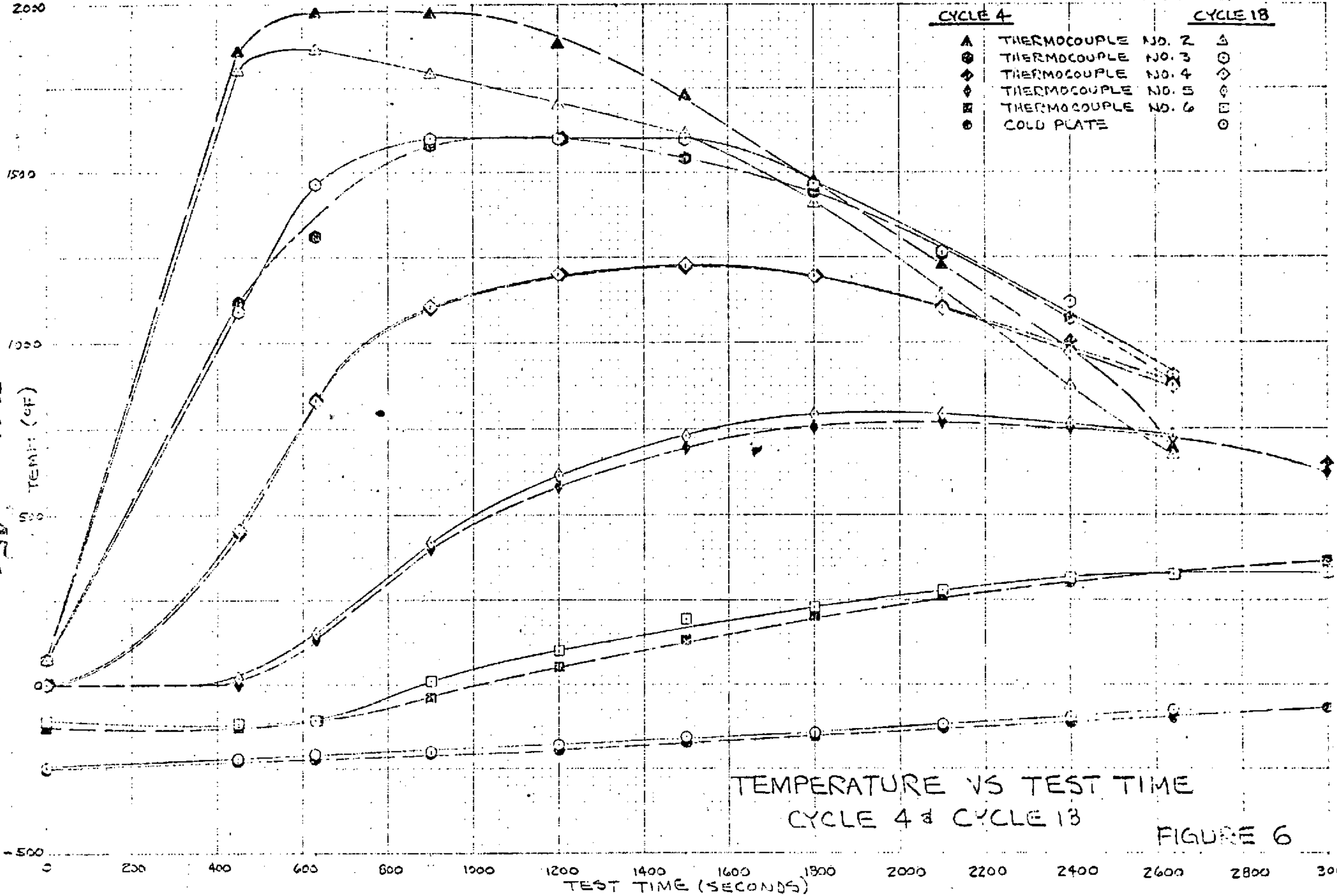

TEMPERATURE VS TEST TIME
CYCLE 4 & CYCLE 18
FIGURE 6

B1-14

45<

Appendix B2

TASK B TEST DATA

Appendix B2
TASK B TEST DATA

The raw data generated to complete the test matrix of Table 3.1-1 are presented in the following tables. With NASA concurrence, English units have been used throughout. At least ten data points for the mechanical tests required by the contract are shown for each test condition, with specimen numbers followed by at least one of the following for each specimen:

- Ultimate Strength
- Modulus
- Poisson's Ratio
- Strain to Failure

Coordinate axes to which Poisson's ratios are referred are defined in the text. Maximum, minimum, and average values are given for each test condition, as well as the standard deviation for ultimate strength, designated as $\bar{\sigma}$.

Thermophysical test data are shown first, followed by the mechanical test results. In either cateogry, 0042 coating data appear first, then that for as-fabricated LI-900, with the radiantly cycled LI-900 data next. Finally, sample load-deflection plots are shown for each mechanical test configuration at a number of temperature levels.

AS-FABRICATED

THERMAL EXPANSION DATA FOR 0042 COATING SPECIMENS

(3/8-in. dia by 3-in. long cast rods)

Temperature °F (°K)	$\Delta L/L_o \times 10^5$ Spec. No. 1	Spec. No. 2	Spec. No. 3	Maximum Uncertainty
	a Cryogenic Dilatometer			
-320 (77)	-16.2	-13.0	-15.3	1×10^{-5}
-250 (107)	-15.1	-14.2	-12.6	
-160 (167)	-13.1	-11.7	-12.0	
-60 (222)	-8.0	-6.2	-6.4	1×10^{-5}
	b Intermediate Temperature Dilatometer			
307 (426)	11.9	12.5	10.1	0.6×10^{-5}
548 (560)	26.8	26.1	23.6	
776 (687)	40.3	39.5	37.2	
999 (810)	53.7	52.7	49.4	
1222 (935)	63.4	62.5	60.1	
1447 (1059)	68.8	67.7	66.1	
1685 (1192)	76.4	75.2	74.0	0.6×10^{-5}
	c High Temperature Dilatometer			
1500 (1088)	70.2	–	–	5×10^{-5}
1510 (1094)	–	68.0	–	
1510 (1094)	–	–	66.2	
1800 (1254)	74.2	–	–	
1800 (1254)	–	72.1	–	
1822 (1270)	–	–	71.6	
1920 (1322)	70.0	–	–	
1940 (1335)	–	–	72.0	
1957 (1345)	–	67.9	–	
2032 (1383)	–	66.2	–	
2040 (1388)	–	–	62.2	
2050 (1394)	71.7	–	–	
2090 (1415)	-20.2	–	–	
2112 (1428)	–	–	-60.0	
2117 (1431)	–	-39.7	–	5×10^{-5}
% length change after c	2.6	1.9		

AS-FABRICATED

THERMAL EXPANSION DATA FOR LI-900 AS-FABRICATED SPECIMENS IN FOR IN-PLANE DIRECTION

Temperature °F (°K)	$\Delta L/L_o \times 10^5$ Spec. No. 1	Spec. No. 2	Spec. No. 3	Maximum Uncertainty
	a Cryogenic Dilatometer			
-320 (77)	+1	0	0	1.3×10^{-5}
-250 (107)	-3.1	-3.4	-2.5	–
-160 (167)	-4.0	-4.0	-3.6	1.2×10^{-5}
-60 (222)	-2.6	-3.0	-2.0	–
	b Intermediate Temperature Dilatometer			
307 (426)	6.9	7.8	7.0	0.7×10^{-5}
548 (560)	15.9	16.9	16.8	–
776 (687)	24.7	26.5	25.7	–
999 (810)	34.2	35.6	34.6	0.6×10^{-5}
1222 (935)	42.2	43.7	42.7	–
1447 (1059)	48.8	49.9	49.5	–
1685 (1192)	53.4	55.2	54.0	0.6×10^{-5}
	c High Temperature Dilatometer			
1500 (1088)	–	–	53.0	5×10^{-5}
1590 (1138)	56.0	–	–	
1610 (1150)	–	57.9	–	
1774 (1240)	58.2	–	–	
1825 (1270)	–	62.1	–	
1910 (1315)	–	–	58.2	
1920 (1321)	60.0	–	–	
1980 (1355)	–	63.9	–	
2015 (1375)	–	–	59.6	
2048 (1394)	56.2	–	–	
2080 (1411)	42.4	–	–	
2100 (1422)	–	46.8	–	
2116 (1430)	–	–	40.0	
2135 (1440)	-16.4	–	–	
2160 (1453)	–	-10.0	–	
2200 (1477)	-500	-450	-395	
% length change after c	-1.4	-1.4	-1.1	
% weight change after c	<0.2	<0.2	<0.2	

AS-FABRICATED

LI-900 THERMAL CONDUCTIVITY DATA FOR TRANSVERSE DIRECTION

Specimen No.	Mean Temperature (^oF)	Thermal Conductivity (Btu-in./hr-ft^2 ^oF)	Pressure Torr
7-1	99	0.100	10^{-4}
	102	0.142	1
	82	0.268	10
	80	0.287	50
	75	0.371	760
	-172	0.062	10^{-4}
7-2	93	0.110	10^{-4}
	-190	0.075	10^{-4}
	75	0.373	760
7-3	110	0.121	10^{-4}
	331	0.155	10^{-4}
	75	0.377	760
	356	0.459	760
8-1	504	0.154	10^{-4}
	490	0.178	0.1
	459	0.351	10
	442	0.447	760
	1002	0.833	760
	1033	0.300	10^{-4}
	1420	1.047	760
	1456	0.502	10^{-4}
	1723	0.785	10^{-4}
8-2	590	0.166	10^{-4}
	551	0.223	1
	567	0.409	10

*7 designates 7-in. dia. guarded hotplate
8 designates 8-in. dia. guarded hotplate

AS-FABRICATED

LI-900 THERMAL CONDUCTIVITY DATA FOR TRANSVERSE DIRECTION

(Continued)

Specimen No.*	Mean Temperature (^{o}F)	Thermal Conductivity (Btu-in./hr-ft^2 ^{o}F)	Pressure Torr
8-2	556	0.538	760
	1085	0.833	760
	1070	0.517	10
	1059	0.385	1
	1053	0.287	10^{-4}
	1522	0.532	10^{-4}
	1517	0.548	0.1
	1512	0.591	1
	1503	1.150	760
	1845	1.48	760
	1890	0.804	10^{-4}
8-3	453	0.168	10^{-4}
	507	0.192	0.1
	519	0.486	760
	1502	1.13	760
	1485	0.575	1.0
	1533	0.555	0.1
	1545	0.532	10^{-4}
	1860	0.807	10^{-4}
	1872	0.818	0.1
	1840	0.830	1.0
	1830	1.02	10
	1830	1.49	760

*7 designates 7-in. dia. guarded hotplate
8 designates 8-in. dia. guarded hotplate

AS-FABRICATED

LI-900 THERMAL CONDUCTIVITY FOR IN-PLANE DIRECTION

Specimen No.	Mean Temperature (^oF)	Thermal Conductivity (Btu-in./hr-ft^2 ^oF)	Pressure (Torr)
IP-1	93	0.477	760
	100	0.183	10^{-4}
	209	0.228	10^{-4}
	348	0.582	760
	389	0.278	10^{-4}

COMPOSITE COATING TENSION TESTS
-250°F (BATCH 1)

Specimen	σ_{ult} (psi)	E (psi x 10^{-6})	ϵ_{max} (%)	t_{total} (in.)
TT110-41	1140	14.40	0.008	0.020
TT110-51	1360	6.67	0.021	0.018
TT110-54	1325	4.40	0.032	0.024
TT110-55	682	4.15	0.016	0.023
TT110-56	860	7.15	0.014	0.024
TT110-59	935	4.43	0.021	0.026
TT110-60	1070	3.99	0.027	0.026
TT110-61	1760	8.38	0.021	0.023
TT110-65	1320	6.00	0.024	0.026
TT110-76	1050	2.17	0.049	0.025
Max	1760	14.40	0.049	0.026
Av	1150	6.17	0.023	0.0235
Min	682	2.17	0.008	0.018
$\bar{\sigma}$	290			

COMPOSITE COATING TENSION TESTS
ROOM TEMPERATURE (BATCH 1)

Specimen	σ_{ult} (psi)	E (psi x 10^{-6})	ϵ_{max} (%)	t_{total} (in.)
TT110-4	1550	2.27	0.068	0.021
TT110-5	775	4.18	0.018	0.020
TT110-6	1110	2.38	0.048	0.025
TT110-9	1330	3.55	0.046	0.025
TT110-10	890	4.42	0.020	0.025
TT110-11	780	5.30	0.015	0.025
TT110-12	1725	3.36	0.055	0.023
TT110-13	2190	4.58	0.047	0.025
TT110-15	1490	3.04	0.050	0.024
TT110-17	1680	2.78	0.058	0.020
TT110-20	2150	4.05	0.053	0.017
Maximum	2190	5.30	0.068	0.025
Average	1425	3.63	0.043	0.0227
Minimum	775	2.27	0.015	0.017
$\bar{\sigma}$	479			

COATING COMPRESSION TESTS
ROOM TEMPERATURE

Specimen	σ_{ult} (psi)	E (psi x 10^{-6})	ϵ_{max} (%)
1	13,500	2.62	0.52
2	12,700	2.49	0.51
3	11,700	2.63	0.42
Maximum	13,500	2.63	0.52
Average	12,633	2.58	0.48
Minimum	11,700	2.49	0.42
$\bar{\sigma}$	742		

COMPOSITE COATING TENSION TESTS
400°F (BATCH 3)

Specimen	σ_{ult} (psi)	E (psi x 10^{-6})	ϵ_{max} (%)	t_{total} (in.)
A-301	1770	1.46	0.121	0.013
A-302	510	0.50	0.103	0.017
A-303	715	0.70	0.102	0.014
A-304	1215	1.51	0.081	0.015
A-305	640	0.75	0.086	0.013
A-306	2370	0.67	0.355	0.014
A-307	1490	1.68	0.089	0.011
A-308	2680	1.85	0.145	0.013
A-309	2990	1.58	0.189	0.012
A-310	1540	1.55	0.100	0.015
Max	2990	1.85	0.355	0.017
Av	1592	1.22	0.137	0.0137
Min	510	0.50	0.081	0.011
$\bar{\sigma}$	823			

COMPOSITE COATING TENSION TESTS
$800^{o}F$ (BATCH 2)

Specimen	σ_{ult} (psi)	E (psi x 10^{-6})	ϵ_{max} (%)	t_{total} (in.)
QB-201	2450	3.94	0.062	0.020
QB-202	1585	7.24	0.022	0.011
QB-203	1500	8.20	0.018	0.019
QB-204	2970	8.97	0.033	0.017
QB-205	1810	7.38	0.025	0.013
QB-206	2420	7.04	0.034	0.016
QB-207	3390	9.32	0.036	0.016
QB-208	1555	4.07	0.038	0.011
QB-209	1280	9.63	0.013	0.015
QB-210	1420	4.65	0.031	0.018
Max	3390	9.63	0.062	0.020
Av	2038	7.04	0.031	0.0156
Min	1280	3.94	0.013	0.011
$\bar{\sigma}$	689			

COMPOSITE COATING TENSION TESTS
$1200^{\circ}F$ (BATCH 2)

Specimen	σ_{ult} (psi)	E (psi x 10^{-6})	ϵ_{max} (%)	t_{total} (in.)
QB-201	3190	4.42	0.072	0.013
QB-102	3130	8.18	0.038	0.011
QB-103	2570	5.05	0.051	0.011
QB-104	1440	4.43	0.033	0.012
QB-105	2280	6.23	0.037	0.012
QB-107	1530	6.61	0.025	0.019
QB-108	1410	4.01	0.035	0.012
QB-109	1645	2.77	0.060	0.012
QB-110	2780	3.62	0.077	0.016
QB-111	3700	3.12	0.119	0.016
Max	3700	8.18	0.119	0.019
Av	2368	4.84	0.055	0.0134
Min	1410	2.77	0.025	0.011
$\bar{\sigma}$	789			

COMPOSITE COATING TENSION TESTS

$1600^{o}F$ (BATCH 2)

Specimen	σ_{ult} (psi)	E (psi x 10^{-6})	ϵ_{max} (%)	t_{total} (in.)
QB-6	1570	2.66	0.059	0.015
QB-7	1840	4.54	0.040	0.013
QB-8	1880	2.58	0.073	0.016
QB-9	1520	3.42	0.044	0.023
QB-10	1325	3.07	0.043	0.012
QB-11	1475	2.70	0.055	0.013
QB-12	2510	2.78	0.090	0.013
QB-13	1725	3.09	0.056	0.014
QB-14	2380	3.17	0.075	0.015
QB-15	2410	1.78	0.135	0.012
Max	2510	4.54	0.135	0.023
Av	1864	2.98	0.067	0.0146
Min	1325	1.78	0.040	0.012
$\bar{\sigma}$	406			

AS-FABRICATED
WEAK TENSION TESTS
$-250^{o}F$

Specimen	σ_{ult} (psi)	E (psi)	ϵ_{max} (%)
B-17	29.8	6025	0.527
B-18	29.6	6625	0.457
B-19	36.0	6550	0.575
B-20	32.0	5300	0.625
B-21	23.5	5850	0.416
B-22	19.7	2960	0.720
B-23	23.5	3520	0.710
B-26	21.4	3640	0.645
B-27	32.4	7900	0.423
B-29	32.4	9575	0.338
Max	36.0	9575	0.720
Av	28.0	5795	0.544
Min	19.7	2960	0.338
$\bar{\sigma}$	5.3		

AS-FABRICATED
WEAK TENSION TESTS
ROOM TEMPERATURE

Specimen	σ_{ult} (psi)	E (psi)	ϵ_{max} (%)
B-2	21.0	6700	0.313
B-5	10.0	3290	0.303
B-6	10.0	3840	0.260
B-7	19.0	7150	0.265
B-8	20.0	6500	0.307
B-10	14.0	7650	0.183
B-11	18.0	6370	0.282
B-24	9.0	4425	0.203
B-25	13.5	3900	0.346
B-28	25.0	7925	0.319
Max	25.0	7925	0.346
Av	16.0	5775	0.278
Min	9.0	3290	0.183
$\bar{\sigma}$	5.2		

AS-FABRICATED
WEAK TENSION ULTIMATE
$400^{\circ}F$

Specimen	σ_{ult} (psi)
F-1	26.8
F-2	27.5
F-4	23.3
F-5	27.8
F-6	23.0
F-7	23.3
F-8	20.4
F-9	23.3
F-10	19.5
F-11	19.8
Max	27.8
Av	23.5
Min	19.5
$\bar{\sigma}$	2.7

AS-FABRICATED
WEAK TENSION MODULUS
$400^{\circ}F$

Specimen	E (psi)
D-51	6,850
D-52	7,770
D-53	4,500
D-54	5,430
D-55	7,070
D-56	7,000
D-57	6,550
D-58	7,600
D-60	6,500
D-61	8,380
Max	8,830
Av	6,765
Min	4,500

AS-FABRICATED
WEAK TENSION ULTIMATE
800°F

Specimen	σ_{ult} (psi)
F-12	19.5
F-15	17.2
F-17	26.5
F-19	19.8
F-23	24.3
F-24	21.1
F-25	23.0
F-27	22.7
F-28	29.4
F-47	18.5
Max	29.4
Av	22.2
Min	17.2
$\bar{\sigma}$	3.6

AS-FABRICATED
WEAK TENSION MODULUS
800°F

Specimen	σ_{ult} (psi)	E (psi)	ϵ_{max} (%)
D-36		8,110	
D-39		7,980	
D-40		8,540	
D-43		7,280	
D-44		8,900	
D-45		7,350	
D-46	22.4	7,640	0.319
D-47		7,675	
D-48		7,950	
D-50		7,420	
Max		8,900	
Av		7,885	
Min		7,280	

AS-FABRICATED
WEAK TENSION ULTIMATE
1200°F

Specimen	σ_{ult} (psi)
F-3	22.0
F-29	24.9
F-32	16.6
F-33	18.5
F-35	24.3
F-36	25.6
F-37	25.6
F-39	24.0
F-40	23.0
F-41	23.6
Max	25.6
Av	22.8
Min	16.6
$\bar{\sigma}$	2.9

AS-FABRICATED
WEAK TENSION MODULUS
1200°F

Specimen	σ_{ult} (psi)	E (psi)	ϵ_{max} (%)
D-20		8,550	
D-21		9,520	
D-23		7,800	
D-27	24.3	7,900	0.322
D-28		7,840	
D-31		7,700	
D-32		10,500	
D-33		8,040	
D-34		7,560	
D-35		7,880	
Max		10,500	
Av		8,329	
Min		7,560	

AS-FABRICATED
WEAK TENSION ULTIMATE
$1600^{o}F$

Specimen	σ_{ult} (psi)
F-13	19.2
F-20	23.6
F-21	23.0
F-22	20.1
F-26	20.8
F-30	20.1
F-34	22.0
F-38	24.9
F-42	31.6
F-43	41.5
Max	41.5
Av	24.7
Min	19.2
$\bar{\sigma}$	6.6

AS-FABRICATED
WEAK TENSION MODULUS
$1600^{o}F$

Specimen	σ_{ult} (psi)	E (psi)	ϵ_{max} (%)
D-3		7,725	
D-4	30.4	8,850	0.388
D-5		7,050	
D-6	29.4	9,560	0.338
D-8	31.8	8,100	0.392
D-10		8,075	
D-12		7,280	
D-13		7,550	
D-16		9,540	
D-19		7,725	
Max		9,560	
Av		8,146	
Min		7,050	

AS-FABRICATED
STRONG TENSION TESTS
$-250^{\circ}F$

Specimen	σ_{ult} (psi)	E (psi)	ϵ_{max} (%)
A-11	75.0	30,300	0.242
A-12	55.0	24,250	0.221
A-13	64.0	21,900	0.280
A-14	71.5	18,900	0.384
A-15	77.0	19,350	0.390
A-16	48.5	19,400	0.250
A-17	70.0	13,550	0.486
A-18	52.7	13,600	0.378
A-19	67.5	14,400	0.443
A-20	88.0	21,400	0.370
Max	88.0	30,300	0.486
Av	66.9	19,705	0.344
Min	48.5	13,550	0.221
$\bar{\sigma}$	11.6		

AS-FABRICATED
STRONG TENSION TESTS
ROOM TEMPERATURE

Specimen	σ_{ult} (psi)	E (psi)	ϵ_{max} (%)
A-1	48.0	23,650	0.202
A-2	48.0	21,300	0.225
A-3	49.0	23,200	0.211
A-4	48.0	19,800	0.242
A-5	51.0	23,300	0.218
A-6	48.0	22,600	0.212
A-7	50.0	22,600	0.241
A-8	47.0	20,200	0.232
A-9	68.0	33,600	0.202
A-10	50.0	25,200	0.198
Max	68.0	33,600	0.242
Av	50.7	23,545	0.218
Min	47.0	19,800	0.198
$\bar{\sigma}$	5.9		

AS-FABRICATED
STRONG TENSION ULTIMATE
400°F (BATCH 1)

Specimen	σ_{ult} (psi)
E-4	69.6
E-9	63.9
E-10	62.3
E-11	76.6
E-14	68.4
E-28	63.2
E-29	67.1
E-44	77.4
E-45	70.9
E-46	68.1
E-47	76.7
Max	77.4
Av	69.5
Min	62.3
$\bar{\sigma}$	5.2

AS-FABRICATED
STRONG TENSION MODULUS
400°F

Specimen	E (psi)
C-27	29,300
C-28	29,600
C-29	34,600
C-30	36,450
C-63*	39,700
C-64	42,600
C-65	34,900
C-66	34,400
C-67	32,750
C-68	40,100
Max	42,600
Av	35,440
Min	29,300

*New batch of specimens started here

AS-FABRICATED
STRONG TENSION ULTIMATE
$800^{o}F$ (BATCH 1)

Specimen	σ_{ult} (psi)
E-48	61.9
E-49	80.7
E-52	72.9
E-53	72.5
E-55	74.7
E-56	85.0
E-57	86.3
E-58	85.0
E-59	65.2
E-61	63.3
Max	86.3
Av	74.8
Min	61.9
$\bar{\sigma}$	8.8

AS-FABRICATED
STRONG TENSION MODULUS
$800^{o}F$

Specimen	E (psi)
C-48	45,900
C-49	38,100
C-50	33,700
C-51	26,700
C-52	32,500
C-53	30,600
C-55	43,700
C-56	42,900
C-61*	37,000
C-62	25,150
Max	45,900
Av	35,625
Min	25,150

*New batch of specimens started here

AS-FABRICATED
STRONG TENSION ULTIMATE
$1200^{\circ}F$ (BATCH 2)

Specimen	σ_{ult} (psi)
EE-1	52.8
EE-2	47.8
EE-3	50.7
EE-8	62.8
EE-10	67.8
EE-11	88.6
EE-12	53.0
EE-13	50.7
EE-14	56.2
EE-15	55.5
Max	88.6
Av	58.6
Min	47.8
$\bar{\sigma}$	11.5

AS-FABRICATED
STRONG TENSION MODULUS
$1200^{\circ}F$

Specimen	E (psi)
C-33	32,900
C-35	45,200
C-36	38,600
C-37	42,300
C-38	40,300
C-39	32,900
C-40	34,200
C-41	34,200
C-42	34,200
C-47	55,500
Max	55,500
Av	39,030
Min	32,900

AS-FABRICATED
STRONG TENSION ULTIMATE
$1600^{o}F$ (BATCH 2)

Specimen	σ_{ult} (psi)
EE-16	47.8
EE-17	81.4
EE-18	59.3
EE-19	100.0
EE-20	69.3
EE-21	65.0
EE-22	62.8
EE-23	55.0
EE-40	63.6
EE-41	61.4
Max	100.0
Av	66.6
Min	47.8
$\bar{\sigma}$	13.9

AS-FABRICATED
STRONG TENSION MODULUS
$1600^{o}F$

Specimen	σ_{ult} (psi)	E (psi)	ϵ (%)
C-7		38,450	
C-9		40,250	
C-10		34,700	
C-11		44,000	
C-12		38,800	
C-13		39,400	
C-15		40,300	
C-20		33,800	
C-23		33,500	
C-24		24,800	
C-25		29,300	
Max		44,000	
Av		36,118	
Min		24,800	

AS-FABRICATED
WEAK TENSION POISSON RATIO TESTS

ROOM TEMPERATURE

Specimen	ν_{zx}	E_z (psi)	$S_{xz} = \nu_{zx}/E_z$ ($psi^{-1} \times 10^6$)
B-2	0.055	6,700	8.21
B-7	0.031	7,150	4.34
B-8	0.027	6,500	4.15
B-11	0.040	6,370	6.28
Max	0.055	7,150	8.21
Av	0.038	6,680	5.75
Min	0.027	6,370	4.15

AS-FABRICATED
STRONG TENSION POISSON RATIO TESTS

ROOM TEMPERATURE

Specimen	ν_{xy}	E_x (psi)	$G_{xy} = E_x/2\ (1+\nu_{xy})$ (psi)
A-3	0.118	23,200	10,376
A-4	0.117	19,800	8,863
A-5	0.115	23,300	10,448
A-7	0.198	22,600	9,432
A-8	0.238	20,200	8,158
A-9	0.281	33,600	13,115
A-10	0.188	25,200	10,606
Max	0.281	33,600	13,115
Av	0.179	23,986	10,142
Min	0.115	19,800	8,158

AS-FABRICATED
STRONG RENSION POISSON RATIO TESTS

ROOM TEMPERATURE

Specimen	ν_{xz}	E_x (psi)	$S_{xz} = \nu_{xz}/E_x$ ($psi^{-1} \times 10^6$)
A-3	0.127	23,200	5.47
A-4	0.188	19,800	9.49
A-5	0.159	23,300	6.82
A-7	0.133	22,600	5.88
A-8	0.197	20,200	9.75
A-9	0.191	33,600	5.68
A-10	0.101	25,200	4.01
Max	0.197	33,600	9.75
Av	0.157	23,986	6.73
Min	0.101	19,800	4.01

AS-FABRICATED
WEAK SHEAR TESTS
TORSION FIXTURE–3/8 IN. THICK BARS

ROOM TEMPERATURE

Specimen	τ_{ult} (psi)	G (psi)	γ_{max} (%)
G1, G2	35.8	3,190	0.83
G3, G4	32.6	3,350	0.90
G5, G6	34.9	3,830	1.07
G7, G8	35.2	3,570	0.86
G9, G10	27.1	3,920	0.62
G11, G12	31.9	3,770	0.68
G13, G14	27.1	3,530	0.68
G15, G16	30.8	3,690	0.68
G17, G18	28.3	3,530	0.78
Max	35.8	3,920	1.07
Av	31.5	3,598	0.79
Min	27.1	3,190	0.62
$\bar{\sigma}$	3.5		

AS-FABRICATED
WEAK SHEAR TESTS
TORSION FIXTURE–2 IN. THICK BARS

ROOM TEMPERATURE

Specimen	τ_{ult} (psi)	G (psi)	γ_{max} (%)
G23, G24	26.1	4,670	0.89
G25*, G26	32.1	4,580	1.02
G27, G28	31.4	4,780	0.89
Max	32.1	4,780	1.02
Av	29.9	4,677	0.93
Min	26.1	4,580	0.89
$\bar{\sigma}$	2.3		

*Batch change at this point

AS-FABRICATED
WEAK SHEAR TESTS

"Snake Skin" Grip, 0.125-In. Gage Length

$-250^{o}F$

Specimen	τ_{ult} (psi)	G (psi)	γ_{max} (%)
H-54	36.8	1156	6.5
H-55	39.3	839	7.7
H-56	39.0	1019	7.0
H-59	38.1	885	7.0
Max	39.3	1156	7.7
Ave	38.3	975	3.9
Min	36.8	839	6.5
$\bar{\sigma}$	1.0		

AS-FABRICATED
WEAK SHEAR TESTS

"Snake Skin" Grip, 0.250-In. Gage Length

$-250^{\circ}F$

Specimen	τ_{ult} (psi)	G (psi)	γ_{max} (%)
H-36	42.7	1,852	3.4
H-37	41.3	1,869	3.2
H-38	40.4	1,626	3.7
H-39	35.0	1,619	4.0
H-40	37.9	1,465	3.4
H-51	38.7	1,120	5.1
H-52	40.0	1,466	4.5
H-53	38.4	1,683	3.9
H-61	39.2	1,840	3.7
H-67	40.0	1,658	3.1
Max	42.7	1,869	5.1
Ave	39.4	1,620	3.8
Min	35.0	1,120	3.1
$\bar{\sigma}$	0.9		

AS-FABRICATED
WEAK SHEAR TESTS

"Snake Skin" Grip, 0.345-In. Gage Length

$-250^{\circ}F$

Specimen	τ_{ult} (psi)	G (psi)	γ_{max} (%)
H-57	34.4	1677	3.4
H-63	36.9	1931	2.9
H-64	34.9	1831	3.0
H-65	38.1	1969	2.8
Max	38.1	1969	3.4
Ave	36.1	1852	3.0
Min	34.4	1677	2.8
$\bar{\sigma}$	0.7		

AS-FABRICATED
WEAK SHEAR TESTS

"Snake Skin" Grip, 0.125-In. Gage Length

ROOM TEMPERATURE

Specimen	τ_{ult} (psi)	G (psi)	γ_{max} (%)
H-21	23.5	1200	4.2
H-22	24.8	1300	3.5
H-23	27.5	1420	5.1
H-34	27.7	1760	3.2
H-42	21.6	1710	4.1
H-43	22.7	1320	4.2
H-44	22.4	1620	3.3
Max	27.7	1760	5.1
Ave	24.3	1476	2.9
Min	21.6	1200	3.2
$\bar{\sigma}$	2.4		-

AS-FABRICATED WEAK SHEAR TESTS

"Snake Skin" Grip, 0.250-In. Gage Length

ROOM TEMPERATURE

Specimen	τ_{ult} (psi)	G (psi)	γ (%)
H-30	21.3	2,490	1.5
H-31	24.0	2,220	1.6
H-32	24.0	2,390	1.8
H-48	23.1	1,915	2.2
H-49	21.9	1,570	2.2
H-66	27.3	2,500	2.2
H-69	26.9	2,500	2.3
$\bar{\sigma}$	2.6		

AS-FABRICATED
WEAK SHEAR TESTS

"Snake Skin" Grip, 0.345-In. Gage Length

ROOM TEMPERATURE

Specimen	τ_{ult} (psi)	G (psi)	γ_{max} (%)
H-27	17.9	2080	1.1
H-28	20.8	2340	1.3
H-29	19.7	2300	1.3
H-35	27.2	2780	–
H-45	15.2	1740	1.2
H-46	16.6	1860	1.1
H-47	19.2	1970	1.5
Max	27.2	2780	1.5
Ave	19.5	2153	1.3
Min	15.2	1740	1.1
$\bar{\sigma}$	3.7		

AS-FABRICATED
WEAK SHEAR TESTS

"Snow-Tire Tread" Grip, 0.250-In. Gage Length

Specimen	τ_{ult} (psi)	G (psi)	γ_{max} (%)
H-71	26.7	2750	2.4
H-73	23.7	1820	3.2
H-74	26.0	2730	2.0
H-107*	24.7	3500	1.4
H-108	27.6	3810	1.8
H-109	26.5	3760	1.4
H-111	36.3	3335	2.9
H-112	32.5	4460	1.6
H-113	31.2	3290	3.5
H-129	35.4	3490	1.7
Max	36.3	4460	3.5
Ave	29.1	3295	2.1
Min	23.7	1820	1.4
σ	4.0		

*Batch Change at this Point

AS-FABRICATED WEAK SHEAR TESTS

"Snow-Tire Tread" Grip, 0.250-in. Gage Length, 400°F

Specimen	τ_{ult} (psi)	G (psi)	γ_{max} (%)
H-76	20.8	1990	2.5
H-77	22.6	1700	2.5
H-78	16.3	2250	3.0
H-79	18.4	1475	2.5
H-80	21.3	1722	4.0
H-81	19.8	1435	4.8
H-82	23.5	1980	6.5
H-83	23.7	1870	6.7
H-84	25.0	1840	4.2
H-85	24.5	1640	3.6
Maximum	25.0	2250	6.7
Average	21.6	1790	4.0
Minimum	16.3	1435	2.5
$\bar{\sigma}$	2.6		

AS-FABRICATED WEAK SHEAR TESTS

"Snow-Tire Tread" Grip, 0.250-in. Gage Length, 800°F

Specimen	τ_{ult} (psi)	G (psi)	γ_{max} (%)
H-86	24.5	1410	-
H-87	21.5	1200	5.3
H-88	22.6	1460	8.7
H-89	20.2	1685	3.7
H-90	23.0	1565	3.3
H-91	22.7	1280	7.0
H-92	24.8	1980	5.1
H-93	22.0	1710	8.1
H-94	22.5	1990	5.3
H-95	18.4	1660	7.1
Maximum	24.8	1990	8.7
Average	22.2	1594	6.0
Minimum	18.4	1200	3.3
$\bar{\sigma}$	2.0		

AS-FABRICATED WEAK SHEAR TESTS

"Snow-Tire Tread" Grip, 0.250-in. Gage Length, 1200°F

Specimen	τ_{ult} (psi)	G (psi)	γ_{max} (%)
H-96	15.7	1770	10.2
H-97	18.9	1800	5.0
H-98	19.9	1885	3.1
H-99	22.8	1770	3.7
H-100	19.6	2020	2.7
H-101	17.5	1555	5.3
H-102	17.6	1510	3.1
H-103	19.5	2000	3.4
H-104	19.2	1900	3.1
H-105	22.5	1690	5.3
Maximum	22.8	2020	10.2
Average	19.3	1790	4.5
Minimum	15.7	1510	2.7
$\bar{\sigma}$	2.2		

AS-FABRICATED WEAK SHEAR TESTS

"Snow-Tire Tread" Grip, 250-in. Gage Length, $1600^{\circ}F$

Specimen	τ_{ult} (psi)	G (psi)	γ_{max} (%)
H-106	25.9	1330	2.5
H-110	19.8	1410	3.5
H-114	16.1	1015	3.9
H-115	19.8	1556	3.1
H-116	19.1	3060	1.2
H-117	25.2	2820	1.9
H-125	21.3	1310	3.9
H-126	23.5	1260	3.5
H-127	17.5	1000	5.7
H-128	14.8	1850	2.3
Maximum	25.9	3060	5.7
Average	20.3	1661	3.2
Minimum	14.8	1000	1.2
$\bar{\sigma}$	3.5		

AS-FABRICATED WEAK COMPRESSION TESTS

ROOM TEMPERATURE

Specimen	σ_{ult} (psi)	E (psi)	ϵ_{max} (%)
07	52.1	5,525	1.29
08	46.6	4,760	1.55
09	43.0	4,550	1.79
10	51.5	5,320	1.38
11	46.0	4,450	1.77
12	45.9	5,300	1.03
Maximum	52.1	5,525	1.79
Average	47.5	4,984	1.47
Minimum	43.0	4,450	1.03
$\bar{\sigma}$	3.5		

AS-FABRICATED STRONG COMPRESSION TESTS

ROOM TEMPERATURE

Specimen	σ_{ult} (psi)
01	57.3
02	48.3
03	54.2
04	74.0
05	75.0
06	67.0
Maximum	75.0
Average	62.6
Minimum	48.3
$\bar{\sigma}$	10.3

THERMAL EXPANSION DATA FOR LI-900 AFTER RADIANT CYCLING, IN-PLANE DIRECTION

Temperature (^oF)	$\Delta L/L_0$ No. 5 Spec No. 1	Spec No. 2	Spec No. 3
307	7.5	7.3	7.3
548	17.0	16.8	16.3
776	27.0	27.7	26.7
999	36.1	36.8	35.6
1222	44.0	43.4	42.4
1447	49.1	48.4	47.6
1685	53.1	53.0	52.5
1552	52.5		
1678	53.7		
1798	54.3		
1910	55.6		
2015	55.0		
2100	38.2		
1573		53.4	
1646		53.9	
1842		54.9	
1942		56.1	
2108		46.2	
1548			51.3
1690			52.7
1861			53.8
1957			55.2
2110			35.1

RADIANTLY CYCLED
LI-900 THERMAL CONDUCTIVITY
FOR TRANSVERSE DIRECTION

Specimen No.	Mean Temperature (^{o}F)	Thermal Conductivity (Btu-in./hr-ft^{2} ^{o}F)	Pressure (Torr)
RC-1	450	0.439	760
	502	0.151	10^{-4}
	1485	0.483	10^{-4}
	1456	1.06	760
	1835	0.745	10^{-4}

RADIANTLY CYCLED
WEAK TENSION

ROOM TEMPERATURE

Specimen	σ_{ult} (psi)	Fracture Location Measured From Coated End (Inches)
N-1	13.8	0.6
N-2	16.0	2.8
N-3	15.4	2.3
N-5	15.7	1.0
N-6	14.8	2.7
N-7	15.3	1.8
N-8	13.6	0.6
N-11	15.4	1.8
N-12	15.5	0.9
N-14	14.3	1.6
Max	16.0	2.8
Av	15.0	1.6
Min	13.6	0.6
$\bar{\sigma}$	0.8	

RADIANTLY CYCLED
WEAK TENSION
400°F

Specimen	σ_{ult} (psi)	Fracture Location Measured From Coated End (Inches)
N-13	14.9	1.5
N-27	13.0	1.9
N-28	14.1	1.1
N-40	15.5**	1.3
N-41	13.7	1.3
N-44	13.6	2.9
400-6*	14.2**	2.8
400-8	15.3**	0.4
400-9	14.5**	0.8
400-10	13.7**	0.6
Max	15.5	2.9
Av	14.3	1.5
Min	13.0	0.4
$\bar{\sigma}$	0.8	

RADIANTLY CYCLED
WEAK TENSION
800°F

Specimen	σ_{ult} (psi)	Fracture Location Measured From Coated End (Inches)
N-38	15.3	0.8
N-34	13.9	2.8
N-36	14.4	1.1
N-17	13.1	2.9
N-30	15.5	1.0
N-20	16.0	1.0
N-29	16.1	0.8
N-16	14.8	0.9
800-9*	15.6	1.2
800-10	15.5**	2.9
Max	16.1	2.9
Av	15.0	1.5
Min	13.1	0.8

*Specimen numbers inadvertently not recorded before bonding ends of specimen where numbers are located. Specimens were therefore renumbered.

**Result of retest. Bond failure at 3.0 inches during initial test.

RADIANTLY CYCLED
STRONG TENSION TESTS

ROOM TEMPERATURE

Specimen	σ_{ult} (psi)	E (psi)	ϵ_{max} (%)
J-1	53.0	27,400	0.202
J-2	52.5	40,100	0.154
J-3	54.5	27,900	0.237
J-4	57.8	25,900	0.233
J-5	57.5	30,500	0.194
J-6	66.0	28,400	0.255
J-10	58.2	22,390	0.276
J-11	58.2	20,950	0.282
J-13	59.0	20,970	0.286
J-14	46.1	29,500	0.145
Max	66.0	40,100	0.286
Av	56.3	27,401	0.226
Min	46.1	20,950	0.145
$\bar{\sigma}$	4.9		

RADIANTLY CYCLED
STRONG TENSION ULTIMATE
$400^{o}F$

Specimen	σ_{ult} (psi)
L-60	73.6
L-61	64.3
L-63	65.7
L-64	65.7
L-65	77.2
L-66	73.6
L-67	42.2
L-68	59.3
L-69	58.7
L-70	72.8
Max	77.2
Av	65.3
Min	42.2
$\bar{\sigma}$	9.7

RADIANTLY CYCLED
STRONG TENSION MODULUS
$400^{o}F$

Specimen	E (psi)
K-60	33,800
K-61	26,700
K-62	34,800
K-63	31,350
K-64	31,400
K-65	29,500
K-66	33,800
K-67	42,400
K-68	26,200
K-69	36,600
Max	52,400
Av	32,655
Min	26,200

RADIANTLY CYCLED
STRONG TENSION ULTIMATE
800°F

Specimen	σ_{ult} (psi)
L-40	89.3
L-41	62.1
L-42	55.0
L-43	55.0
L-44	56.4
L-45	65.6
L-46	52.8
L-47	52.8
L-48	47.2
L-49	60.6
Max	89.3
Av	59.7
Min	47.2
$\bar{\sigma}$	11.1

RADIANTLY CYCLED
STRONG TENSION MODULUS
800°F

Specimen	E (psi)
K-40	42,000
K-41	37,300
K-42	44,100
K-43	32,600
K-44	59,300
K-45	33,800
K-46	32,100
K-47	37,600
K-48	36,800
K-50	33,000
Max	59,300
Av	38,860
Min	32,100

RADIANTLY CYCLED
STRONG TENSION ULTIMATE
1200°F

Specimen	σ_{ult} (psi)
L-22	52.8
L-23	67.8
L-24	59.3
L-25	59.3
L-26	52.8
L-28	58.6
L-29	51.4
L-30	59.9
L-31	59.9
L-32	62.1
Max	67.8
Av	58.4
Min	51.4
$\bar{\sigma}$	4.7

RADIANTLY CYCLED
STRONG TENSION MODULUS
1200°F

Specimen	E (psi)
K-20	39,600
K-22	53,900
K-28	36,100
K-29	47,600
K-30	35,700
K-31	41,000
K-32	32,500
K-33	32,600
K-34	36,600
K-6	49,400
Max	53,900
Av	40,500
Min	32,500

RADIANTLY CYCLED
STRONG TENSION ULTIMATE
1600°F

Specimen	σ_{ult} (psi)
L-2	74.3
L-3	111.0
L-4	71.4
L-5	89.3
L-6	64.3
L-7	83.6
L-8	82.9
L-9	89.3
L-11	68.6
L-12	70.7
Max	111.0
Av	80.5
Min	64.0
$\bar{\sigma}$	13.1

RADIANTLY CYCLED
STRONG TENSION MODULUS
1600°F

Specimen	E (psi)
K-1	44,800
K-2	42,600
K-3	42,400
K-4	39,200
K-5	34,500
K-7	40,400
K-8	33,800
K-9	44,500
K-10	35,100
K-11	33,800
Max	44,800
Av	39,110
Min	33,800

RADIANTLY CYCLED
WEAK SHEAR TESTS

R. T.

Specimen	τ_{ult} (psi)	G (psi)	γ (%)
M-24	24.5	2,245	2.2
M-26	25.6	2,510	2.2
M-28	23.7	2,740	2.0
M-30	15.6	2,000	1.6
M-32	20.0	2,305	1.5
M-34	20.5	2,260	2.3
M-36	18.3	2,120	1.6
M-38	22.9	2,130	1.9
M-40	22.2	2,560	1.7
M-42	20.5	2,330	1.6
Max	25.6	2,740	2.3
Av	21.4	2,320	1.9
Min	15.6	2,120	1.5
$\bar{\sigma}$	2.9		

RADIANTLY CYCLED
WEAK SHEAR TESTS
400°F

Specimen	τ_{ult} (psi)	G (psi)	γ_{max} (%)
M-4	13.1	1,760	1.9
M-6	15.6	1,740	2.0
M-8	15.7	1,245	3.1
M-10	15.2	1,520	1.8
M-14	16.4	2,310	4.3
M-44	14.1	1,730	1.5
M-46	18.1	2,080	3.6
M-48	17.1	1,765	3.4
M-50	20.2	1,970	2.5
M-52	13.6	1,690	2.6
Max	20.2	2,310	4.3
Av	15.9	1,781	2.7
Min	13.1	1,245	1.5
$\bar{\sigma}$	2.0		

RADIANTLY CYCLED
WEAK SHEAR TESTS
800°F

Specimen	τ_{ult} (psi)	G (psi)	γ_{max} (%)
M-12	13.2	1,150	5.0
M-16	12.1	965	4.8
M-18	11.7	855	5.0
M-20	15.6	1,000	6.9
M-22	13.6	1,040	4.4
M-54	16.5	2,010	3.0
M-56	13.9	1,040	15.7
M-58	16.2	1,525	5.1
M-60	17.0	1,265	9.1
M-62	14.4	1,360	9.9
Max	17.0	2,010	15.7
Av	14.4	1,221	6.9
Min	11.7	855	3.0
$\bar{\sigma}$	1.8		

RADIANTLY CYCLED
WEAK SHEAR TESTS
$1200^{o}F$

Specimen	τ_{ult} (psi)	G (psi)	γ_{max} (%)
M-1	17.6	1,100	14.7
M-3	13.6	1,290	9.7
M-5	11.7	1,055	8.4
M-7	13.6	1,115	8.6
M-9	14.0	1,065	11.5
M-21	11.2	810	5.5
M-23	13.5	515	18.0
M-25	14.5	1,010	12.0
M-27	13.0	1,050	11.0
M-29	14.9	1,100	15.0
Max	17.6	1,290	18.0
Av	13.8	1,015	11.4
Min	11.2	515	5.5
$\bar{\sigma}$	1.7		

RADIANTLY CYCLED
WEAK SHEAR TESTS
$1600^{o}F$

Specimen	τ_{ult} (psi)	G (psi)	γ_{max} (%)
M-11	17.0	752	7.2
M-13	13.3	920	3.0
M-15	13.5	1,070	2.8
M-17	11.6	828	8.3
M-19	13.6	683	3.4
M-47	15.7	905	3.0
M-49	13.3	1,080	1.7
M-51	18.4	1,600	3.0
M-53	16.2	920	4.7
M-55	17.1	1,175	3.2
Max	18.4	1,600	8.3
Av	15.0	993	4.0
Min	11.6	683	1.7
$\bar{\sigma}$	2.1		

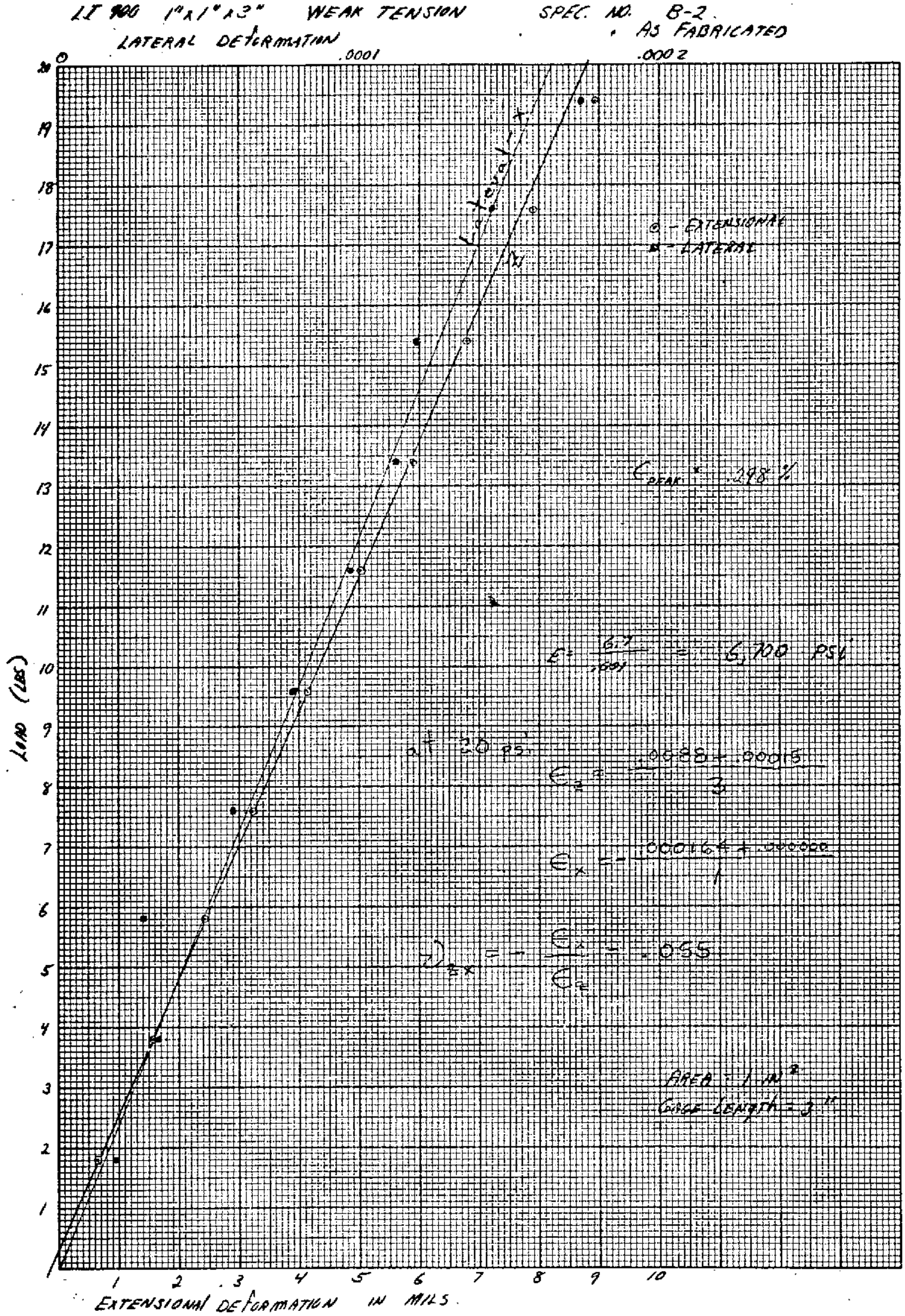
LI 900 1"x1"x3" WEAK TENSION SPEC. NO. B-2
LATERAL DEFORMATION
· AS FABRICATED
.0001
.0002
⊙ - EXTENSIONAL
■ - LATERAL
LOAD (LBS)
EXTENSIONAL DEFORMATION IN MILS
AREA = 1 IN²
GAGE LENGTH = 3"
E = 6,700 PSI
at 20 lbs
.055

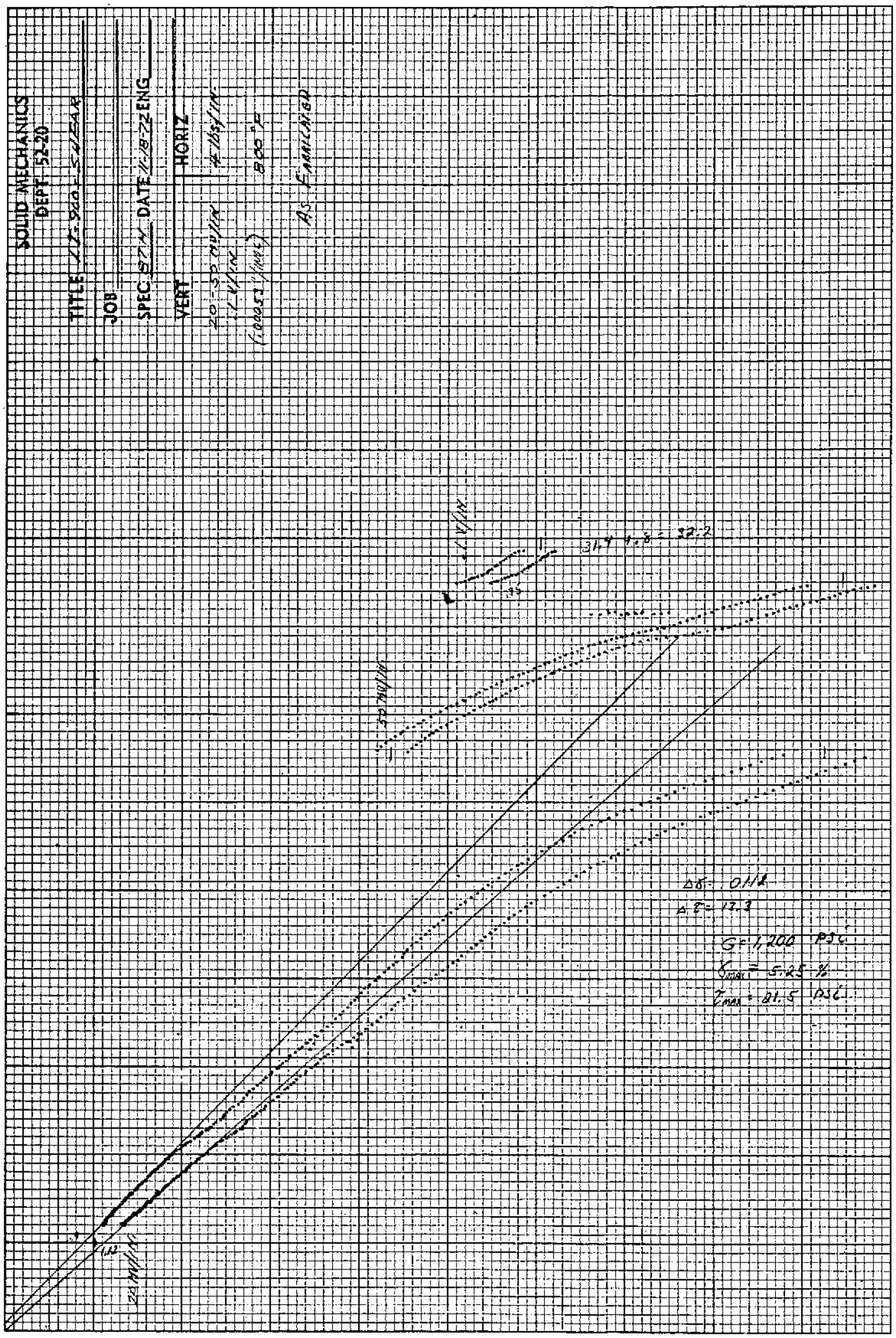
SOLID MECHANICS
DEPT 52-20
TITLE
JOB
SPEC
DATE
VERT
HORIZ
As Fabricated
G = 1,200 PSI

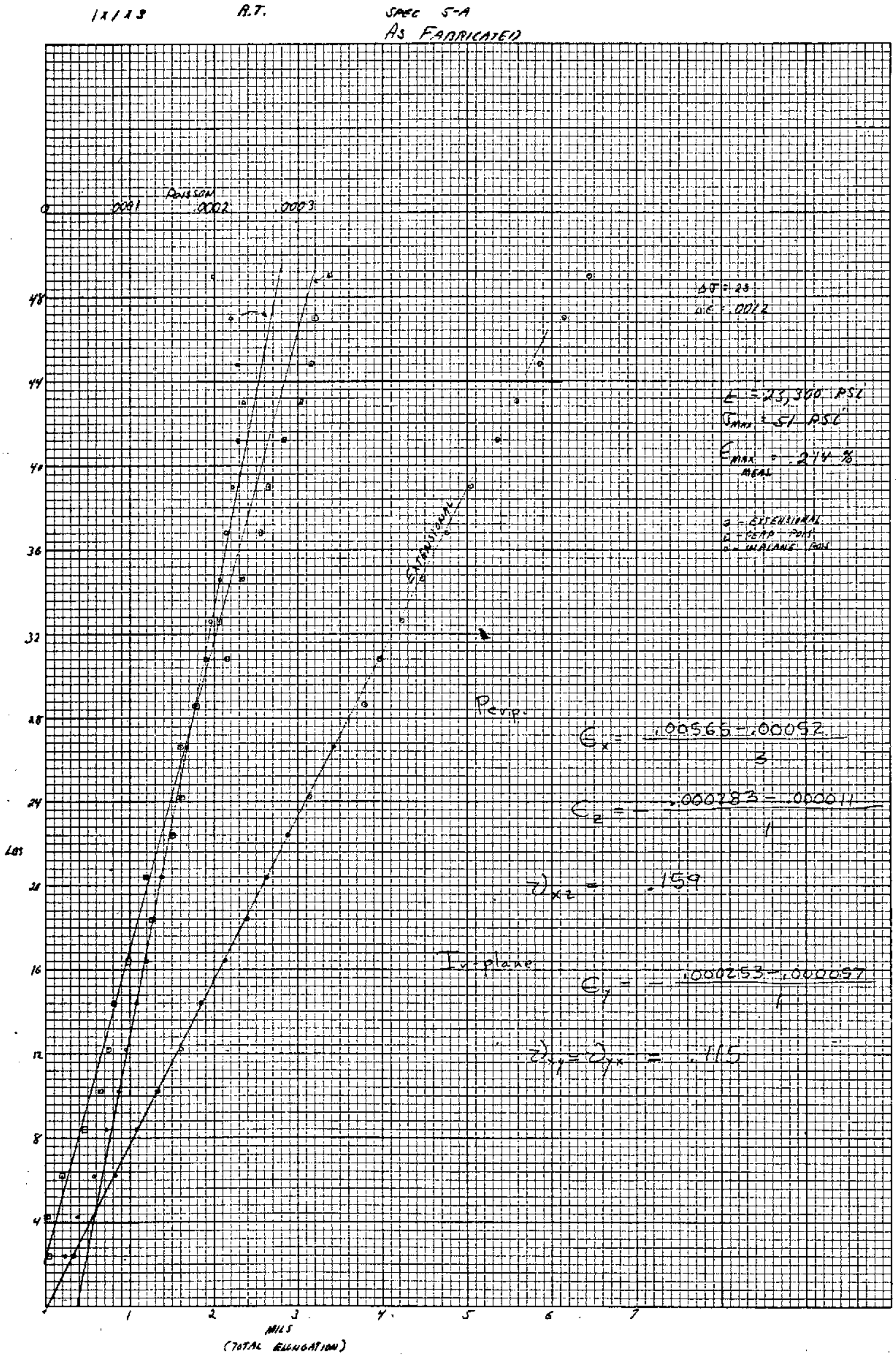

98<

LOCKHEED MISSILES & SPACE COMPANY

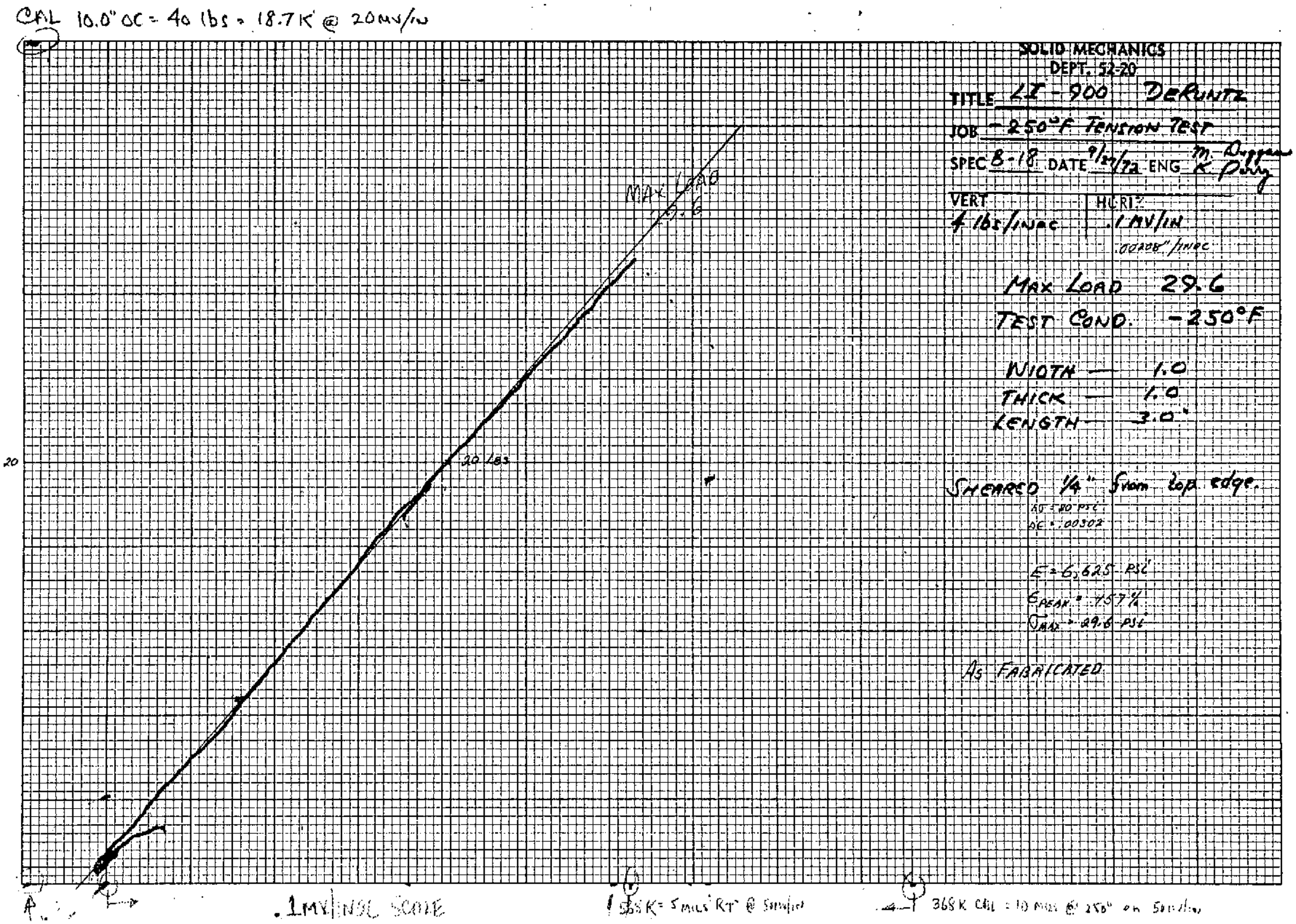

LOCKHEED MISSILES & SPACE COMPANY

B2-52

99

LMSC-D282673

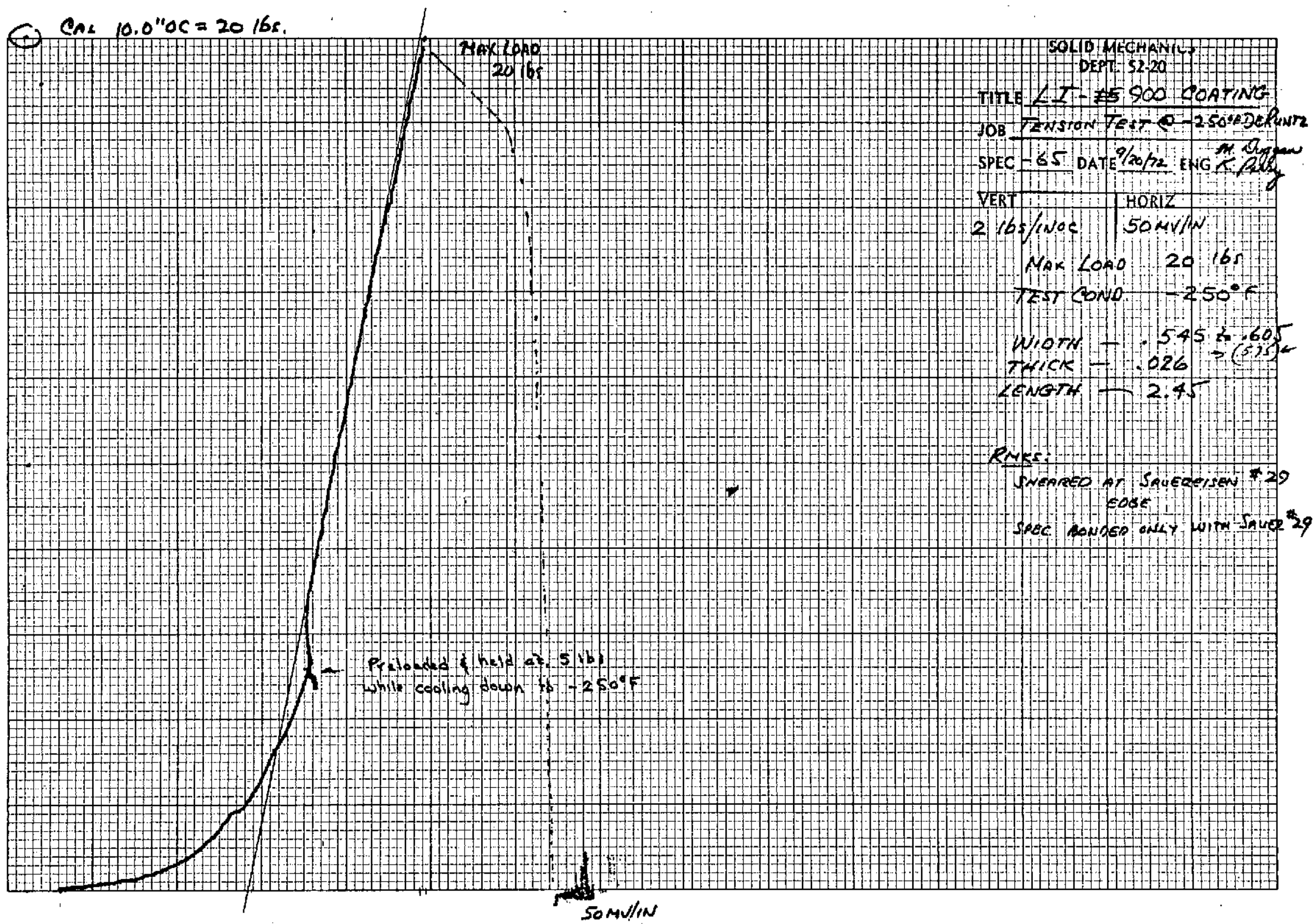

CAL 10.0"OC = 20 lbs.
MAX LOAD 20 lbs
SOLID MECHANICS
DEPT. 52-20
TITLE LI-~~15~~ 900 COATING
JOB TENSION TEST @ -250°F DeRuntz
SPEC -65 DATE 9/20/72 ENG M. Duggan K. Pulley
VERT 2 lbs/INOC
HORIZ 50 MV/IN
MAX LOAD 20 lbs
TEST COND -250°F
WIDTH — .545 to .605 → (.575)
THICK — .026
LENGTH — 2.45
RMKS:
SHEARED AT SAUEREISEN #29 EDGE
SPEC BONDED ONLY WITH SAUER #29
Preloaded & held at 5 lbs while cooling down to -250°F
50 MV/IN

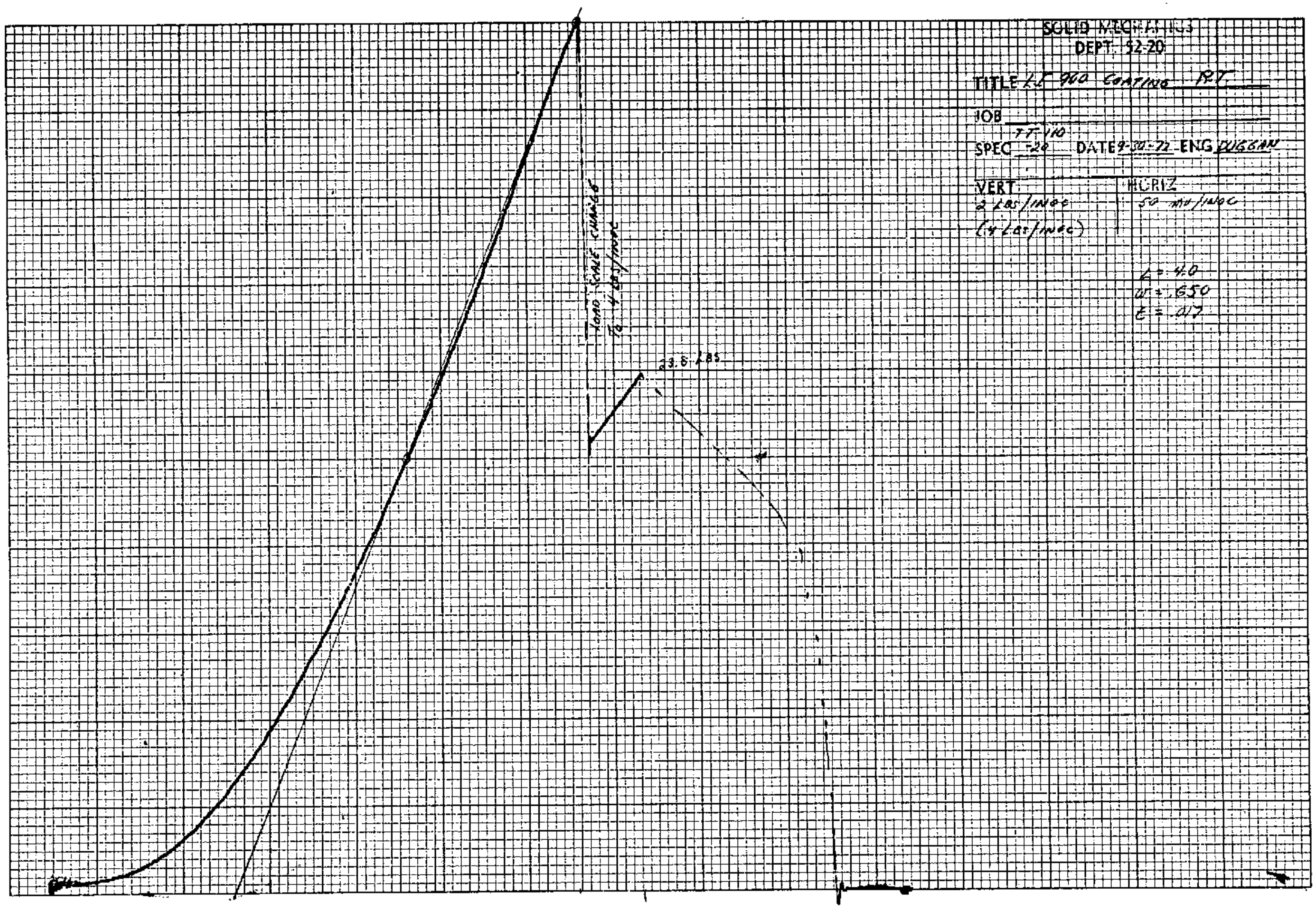

B2-54

104

LOCKHEED MISSILES & SPACE COMPANY

LMSC-D282673

LOCKHEED MISSILES & SPACE COMPANY

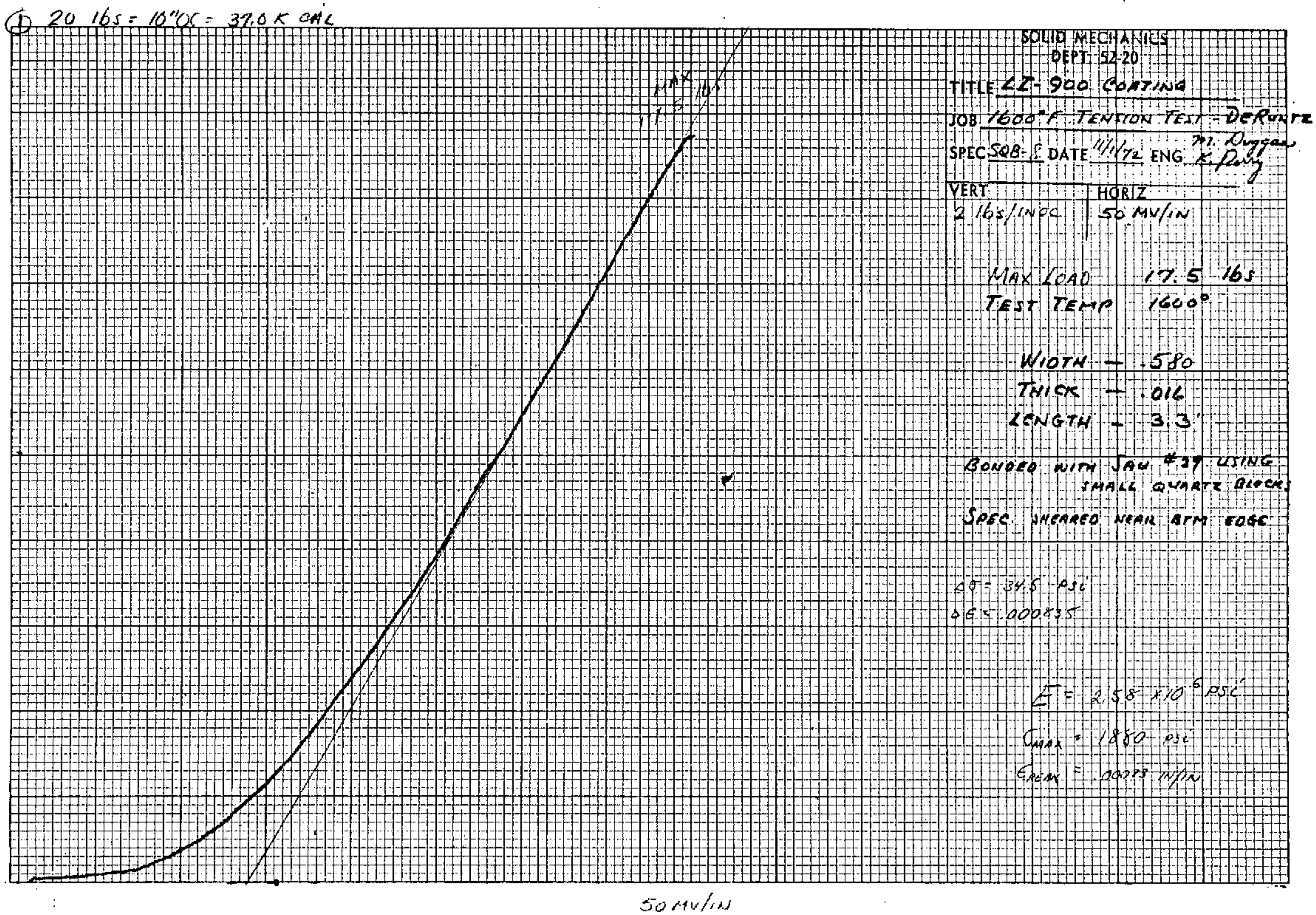

B2-55

102<

LMSC-D282673

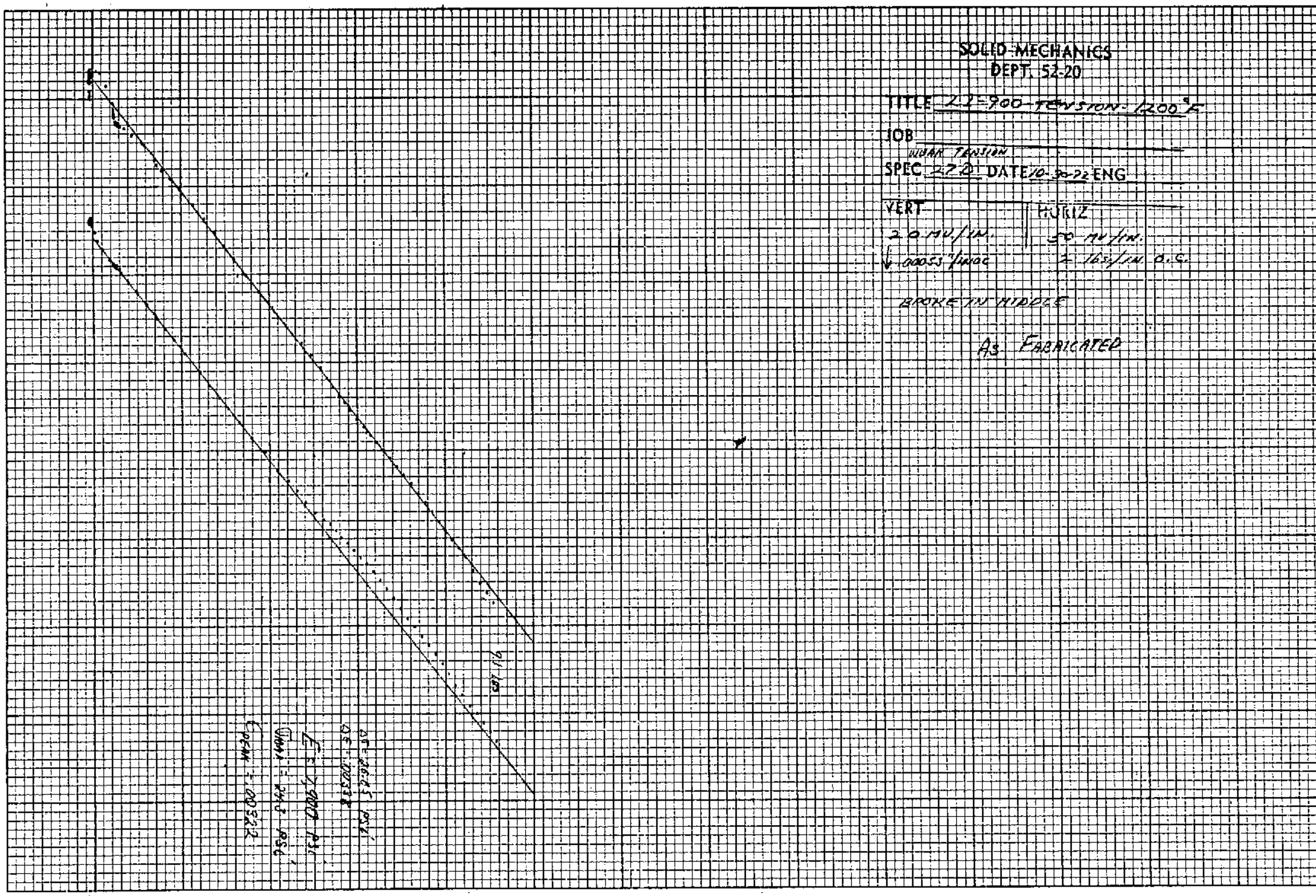
SOLID MECHANICS
DEPT. 52-20
TITLE 22-900-TENSION-1200°F
JOB
SPEC 27 DATE 10-30-72 ENG
VERT
2.0 MV/IN.
HORIZ
50 MV/IN.
BROKE IN MIDDLE
AS FABRICATED

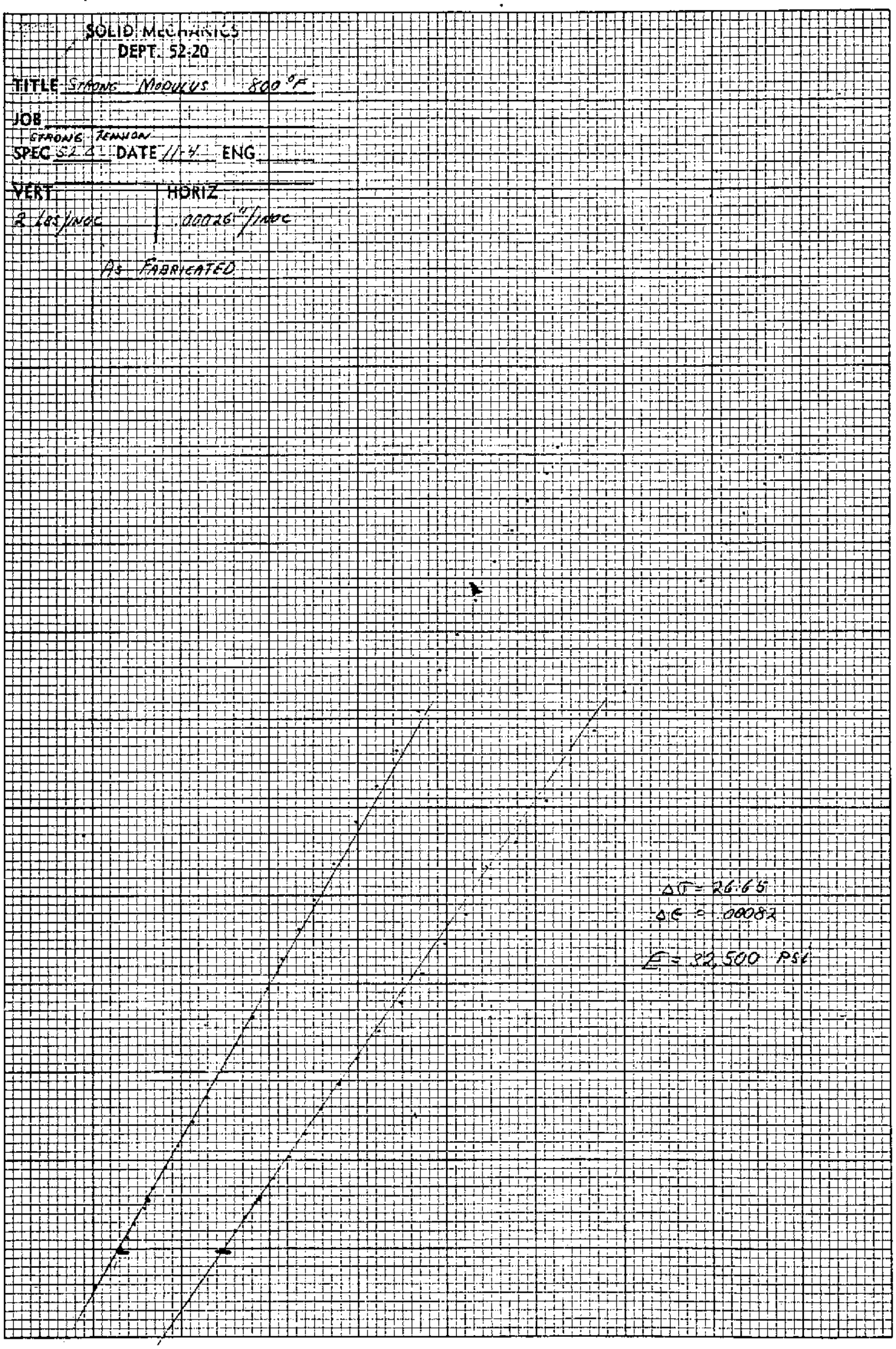
SOLID MECHANICS
DEPT. 52-20
TITLE Strong Modulus 800 °F
JOB
Strong Tension
SPEC 524 DATE 11-4 ENG
VERT
2 lbs/inc
HORIZ
.00026"/inc
As Fabricated
Δσ = 26.65
Δε = .00082
E = 32,500 PSI

B2-58

105<

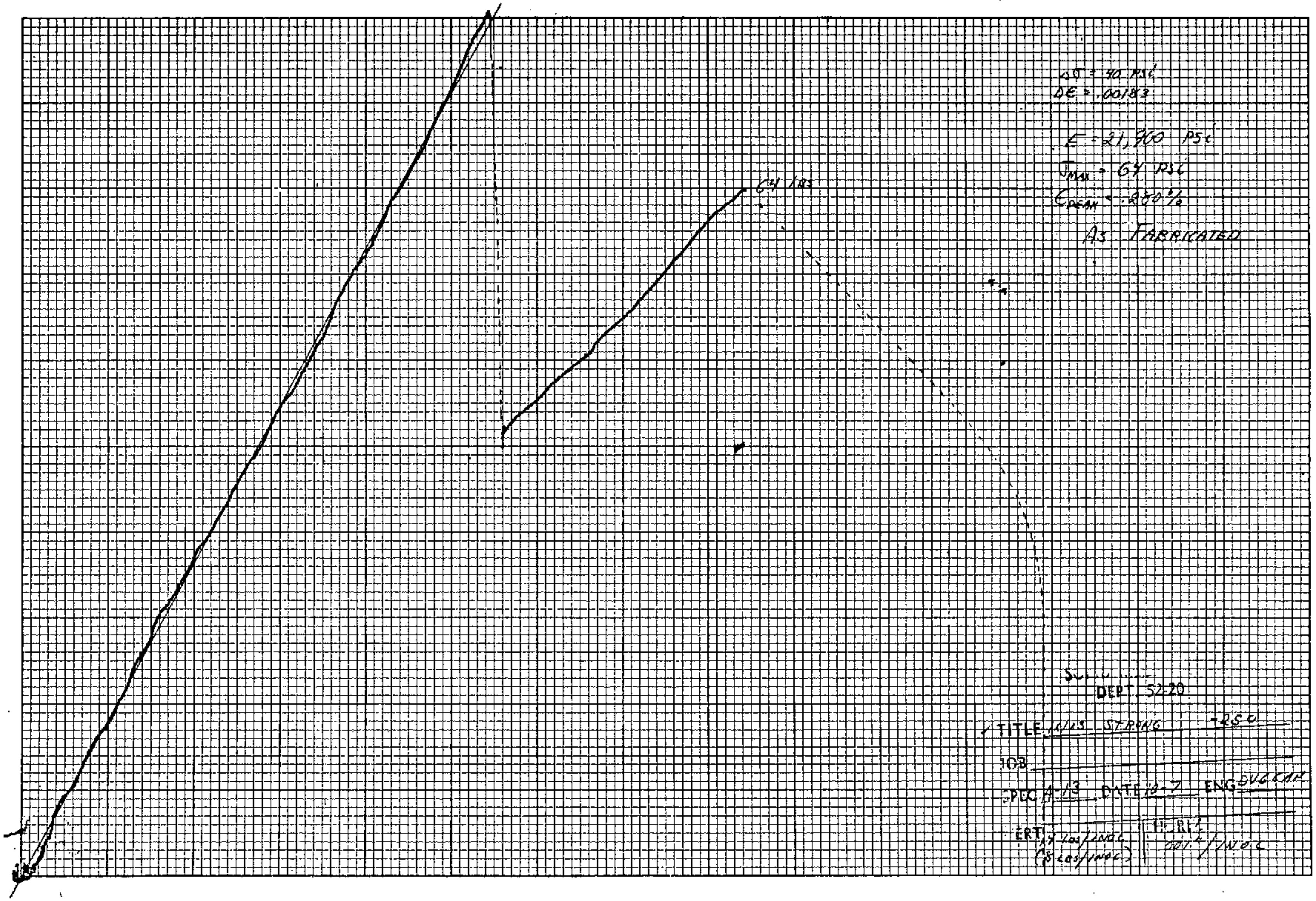

ΔE = .00183
E = 21,900 PSI
σ_MAX = 64 PSI
AS FABRICATED
64 lbs
DEPT. 5220
TITLE STRONG -250
JOB
SPEC A-13 DATE 10-7 ENG DUGGAN
VERT
HORIZ
/INCH

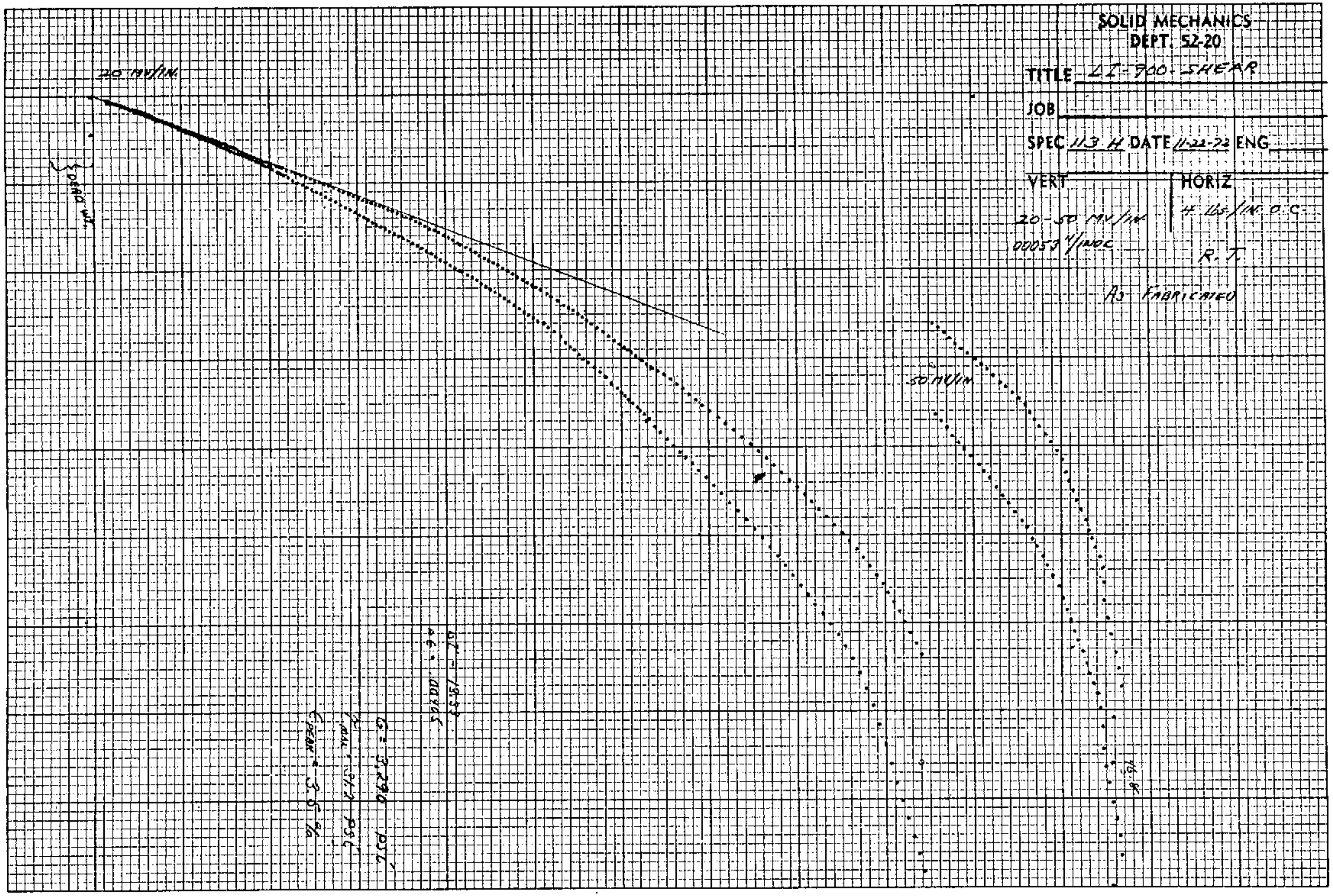
SOLID MECHANICS
DEPT. 52-20
TITLE LI-900-SHEAR
JOB
SPEC 113 H DATE 11-22-72 ENG
VERT
HORIZ
20-50 MV/IN
4 lbs/IN O.C.
R.T.
AS FABRICATED
20 MV/IN.
50 MV/IN
DEAD WT.
G = 3290 PSI

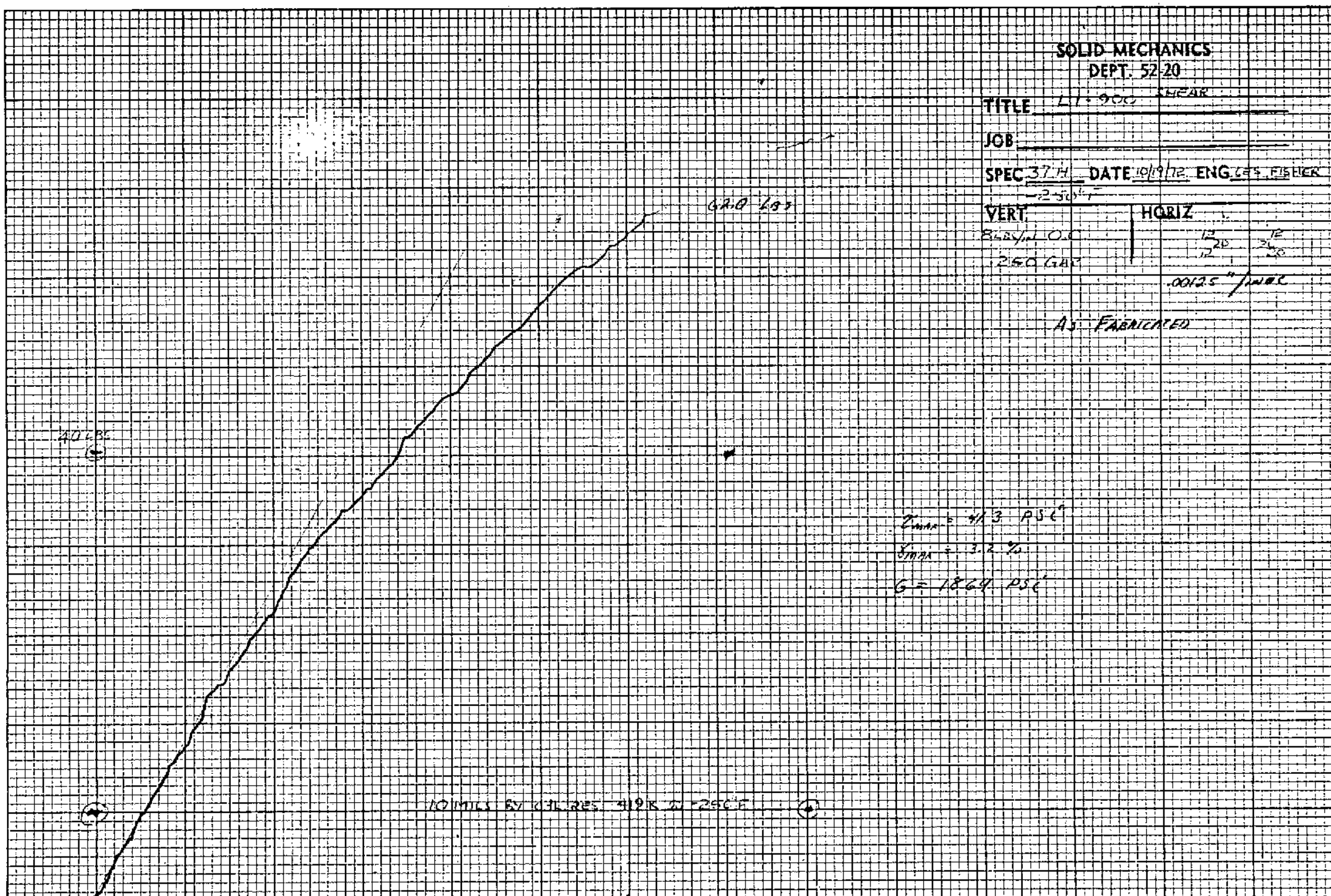

B2-60

107

LOCKHEED MISSILES & SPACE COMPANY

LMSC-D282673

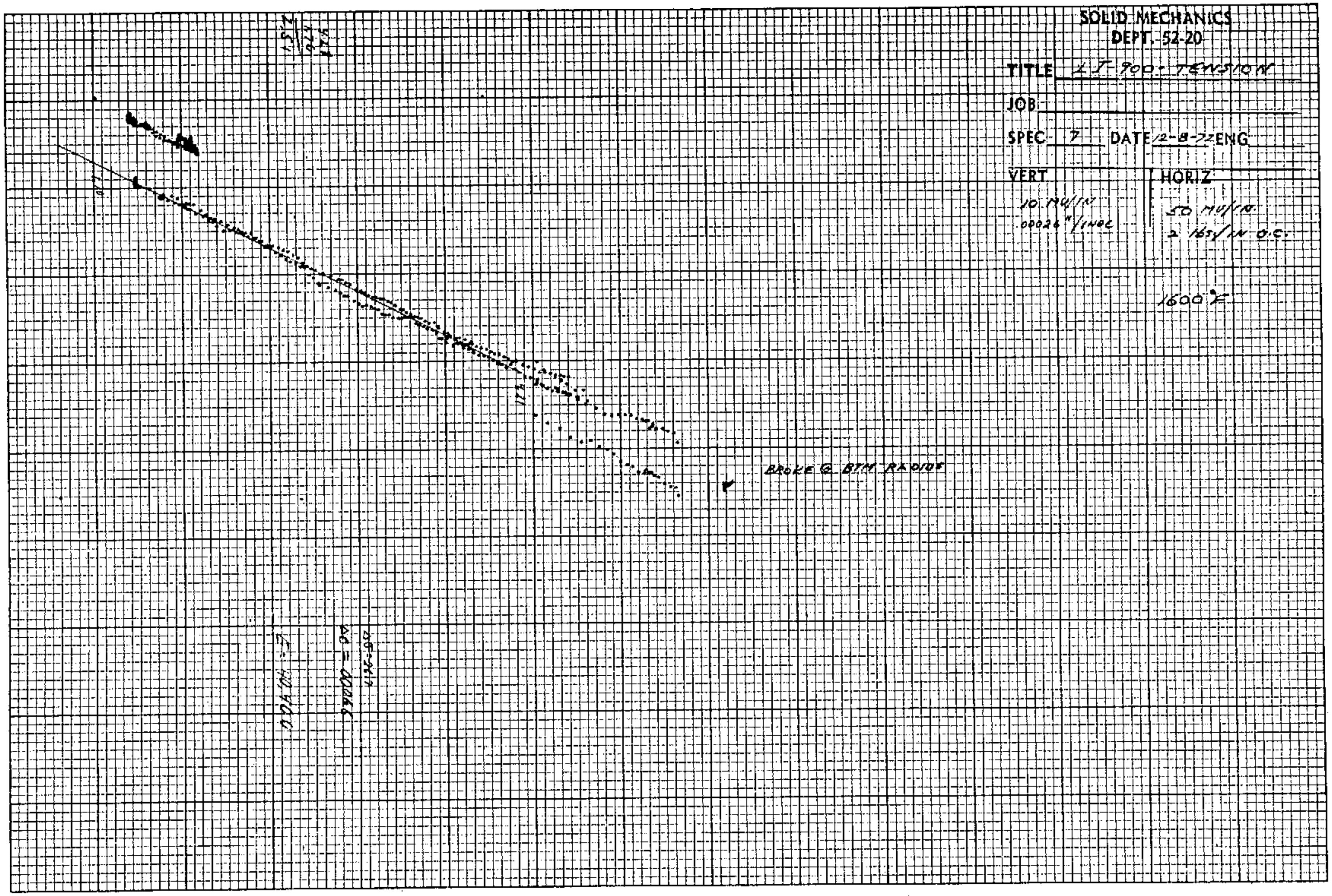

SOLID MECHANICS
DEPT. 52-20
TITLE LI 900 - TENSION
JOB
SPEC 7 DATE 12-8-72 ENG
VERT
HORIZ
1600°F
BROKE @ BTM RADIUS

B2-61

108

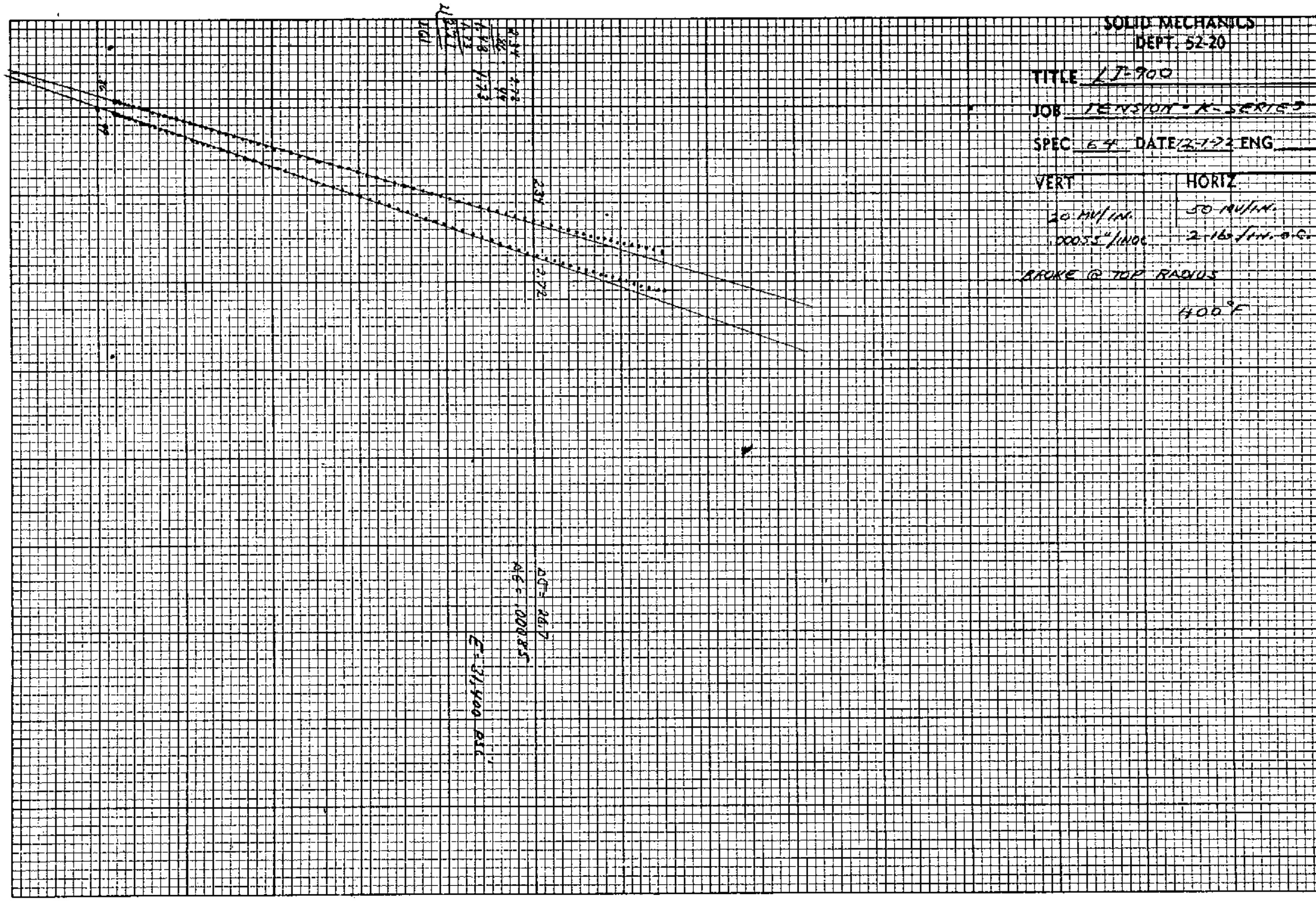
SOLID MECHANICS
DEPT. 52-20
TITLE LT-900
JOB TENSION - K-SERIES
SPEC 64 DATE 12-7-72 ENG
VERT
20 MV/IN.
.00055"/INOC
HORIZ
50 MV/IN.
2-16 /IN. O.C.
BROKE @ TOP RADIUS
400°F
Δσ = 26.7
Δε = .00085
E = 31,400 PSI

LOCKHEED MISSILES & SPACE COMPANY

110<

B2-63

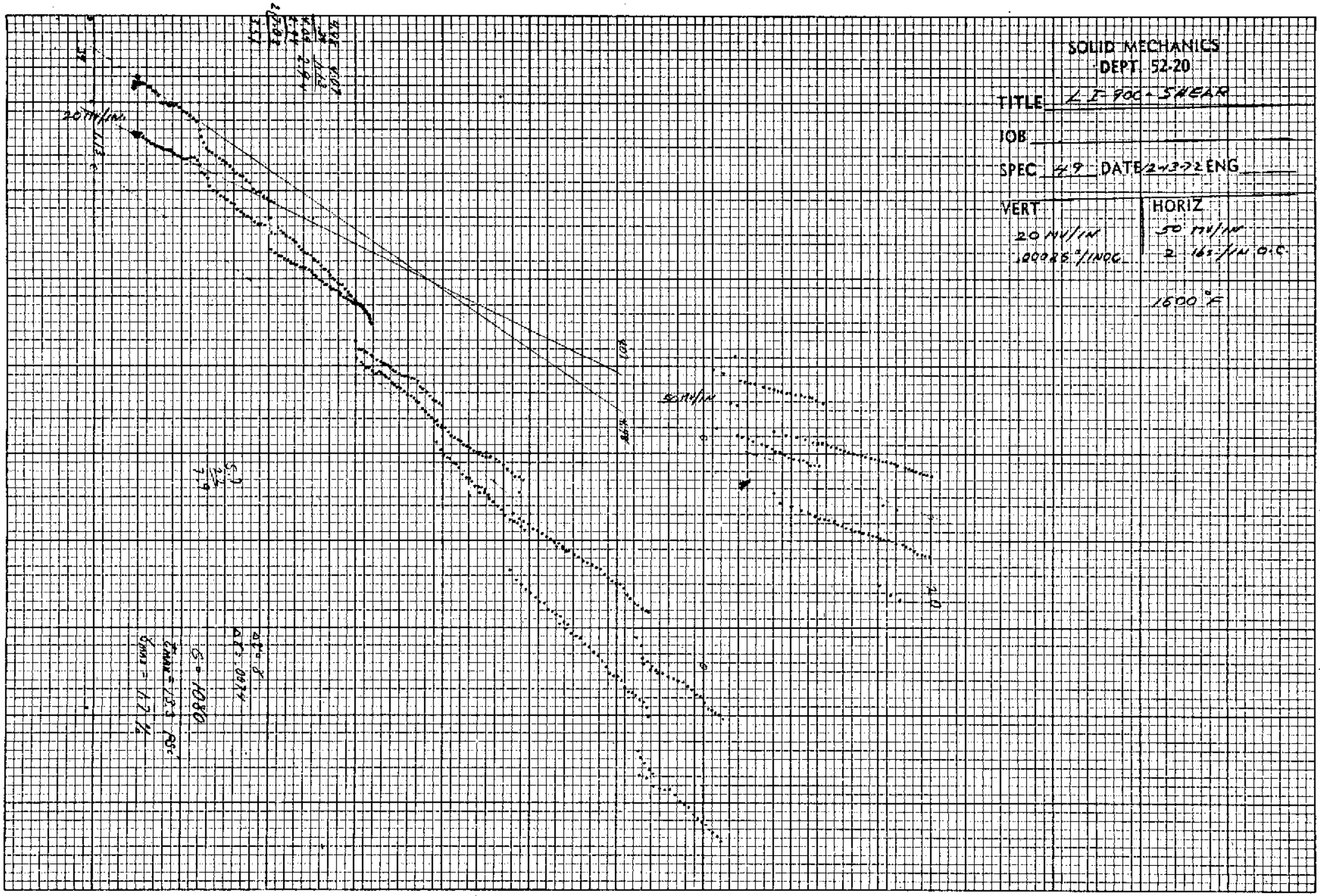

LMSC-D282673

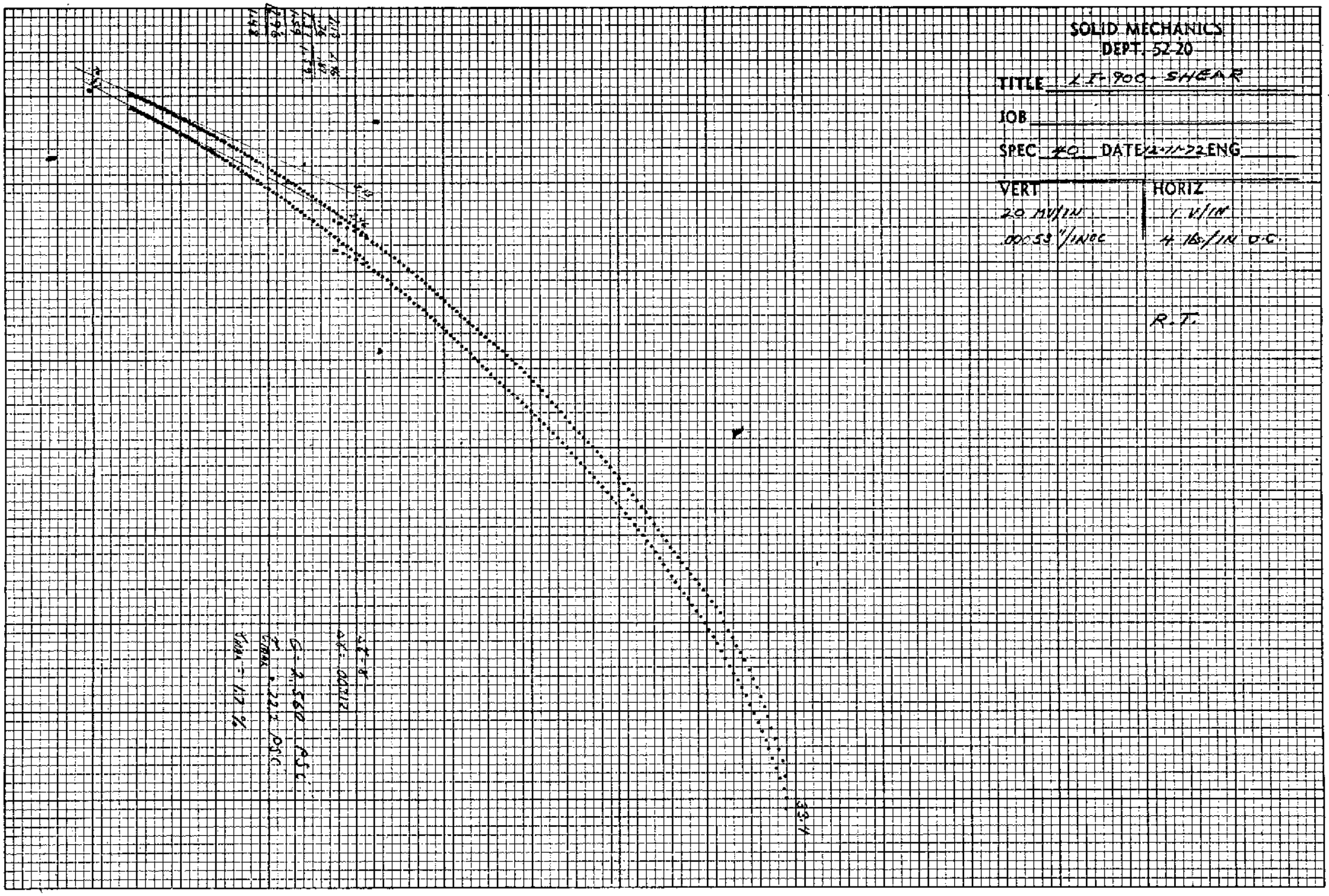

LOCKHEED MISSILES & SPACE COMPANY

111

B2-64

LMSC-D282673

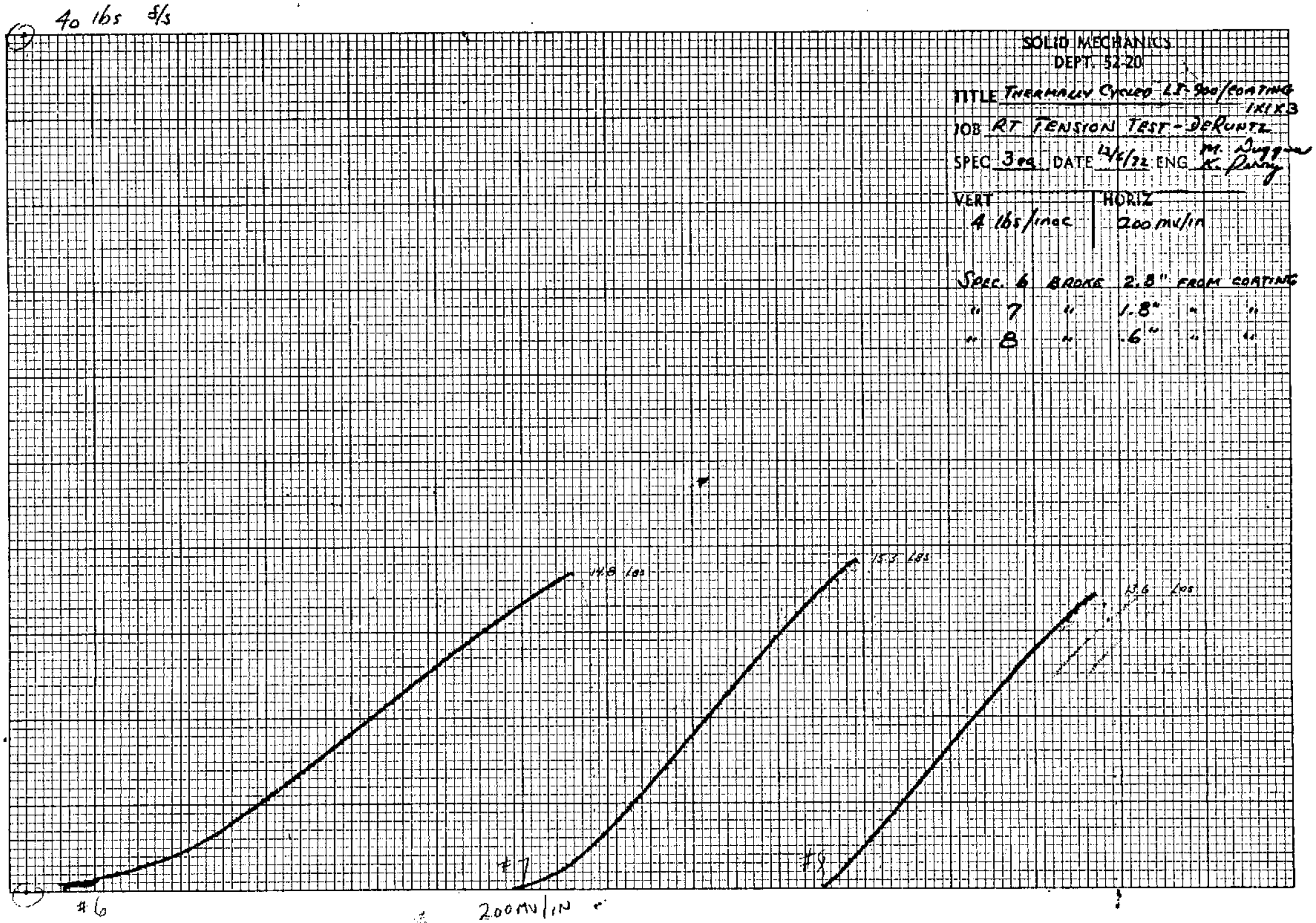

112

LMSC-D282673

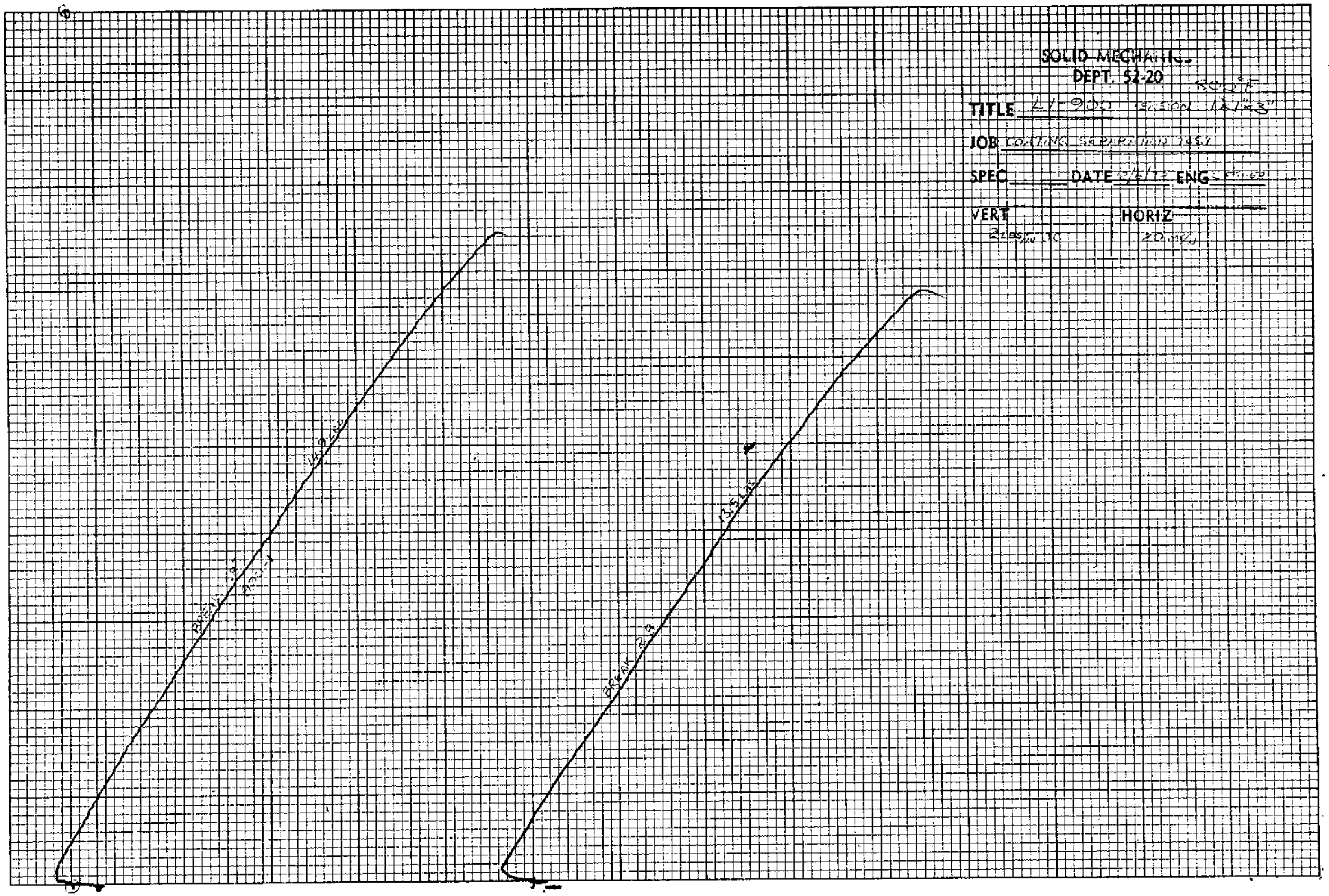

B2-66

113

LOCKHEED MISSILES & SPACE COMPANY

LMSC-D282673

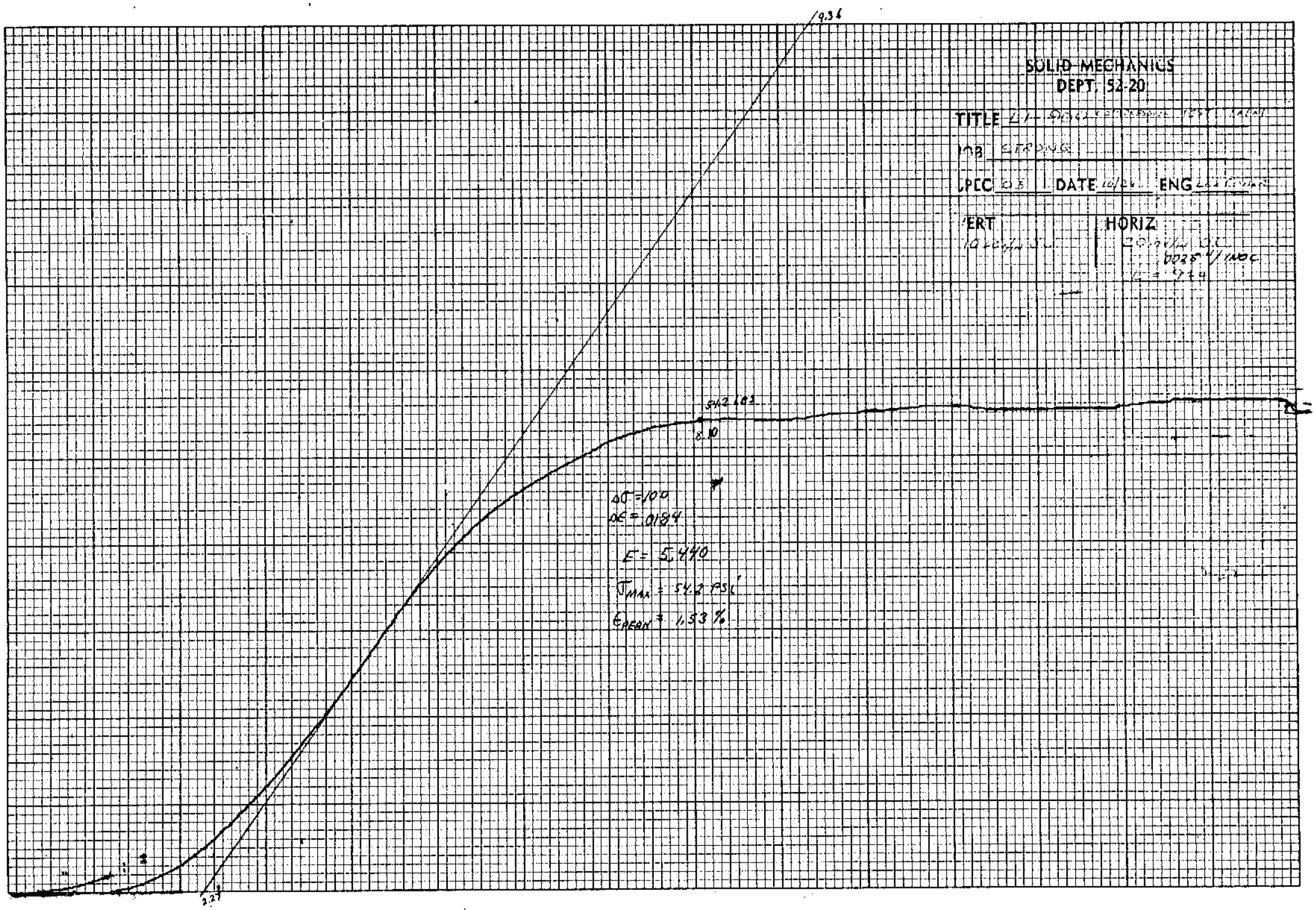

SOLID MECHANICS
DEPT. 52-20
TITLE
JOB STRONG
SPEC
DATE
ENG
VERT
HORIZ
.0025"/INCH
9.36
542 LBS
8.10
Δσ = 100
Δε = .0184
E = 5,440
σ MAX = 54.2 PSI
ε BREAK = 1.53 %
2.27

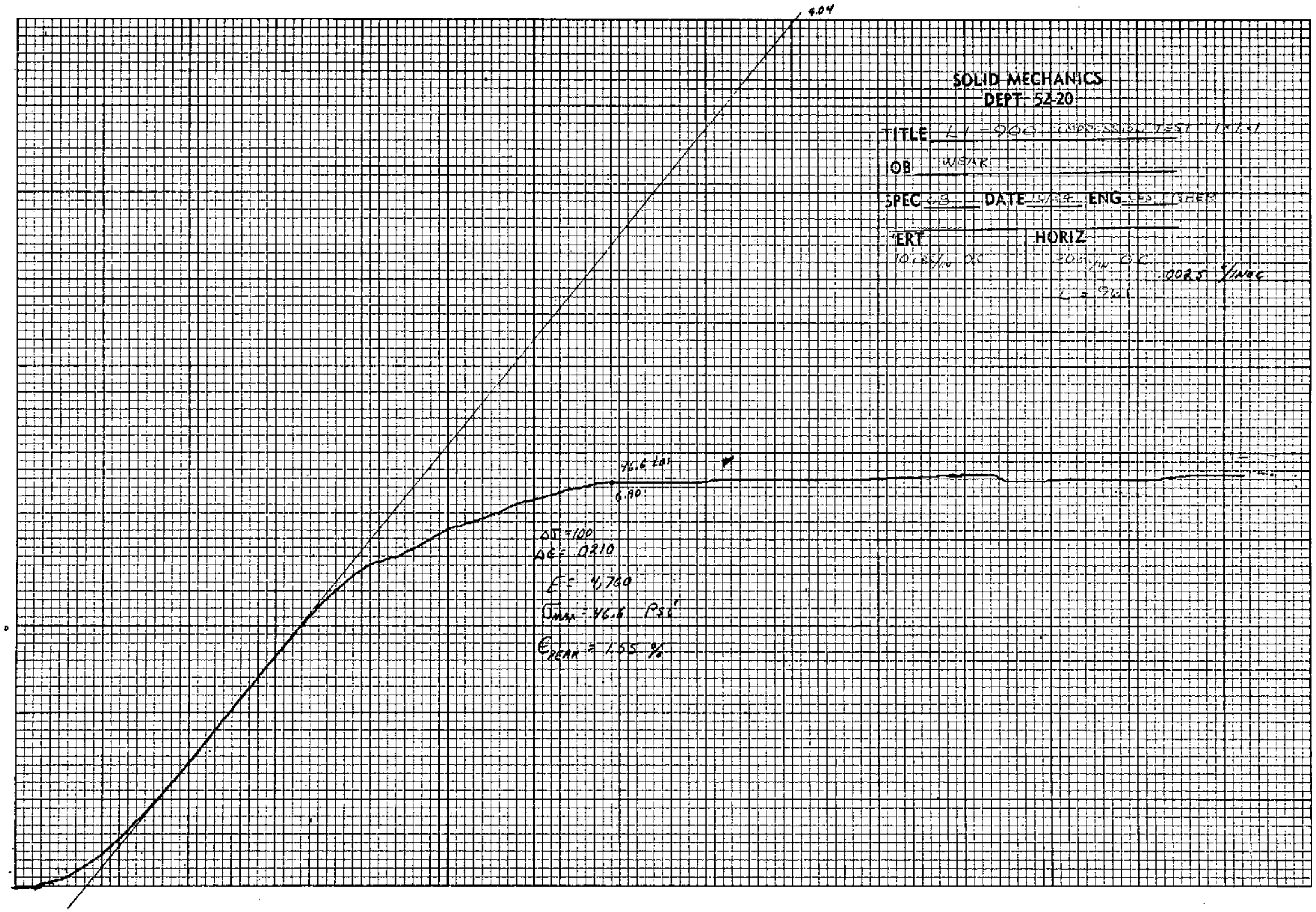

B2-68

115

LOCKHEED MISSILES & SPACE COMPANY

LMSC-D282673

Appendix B3

SHEAR TEST METHODOLOGY

Appendix B-4

SHEAR TEST METHODOLOGY

Shear test methods have always been a source of controversy. The only shear test that approaches ideal conditions requires that torsion be applied to a thin-walled cylinder, a method which was prohibitive for application to LI-900 since the diameter of the cylinder (and consequently its length) would have to be so large for the wall to be "thin" on a relative scale.

For several years, LMSC has used a modified torsion test technique in evaluating LI-1500 (during its development). The requirement for shear data at -250°F and elevated temperatures, combined with the discovery that no cement was usable at the higher temperatures, prompted the development of a new technique which did not involve cementing of the specimen (see Section 3.2.3.3 on shear testing, where both the torsion and the newer method are described in detail).

A new technique is never applied without some comparison being made between the results of the new technique and those of the previous method. Not too surprisingly, there were some discrepancies both in the peak stress obtained and in the shear modulus. The discrepancy was large enough to prompt a major reconsideration of the values obtained by the old technique. By the time a test series was run using both techniques, other tests confirmed that there is considerable variation in the shear properties from one batch of LI-900 to another, and that this factor alone could account for the discrepancies observed in the two groups of tests (using the old and new techniques). However, this did not alter the fact that unsuspected shortcomings (or sources of error) existed in the older torsion test technique.

The first and most significant source of error arises in the deformation measurement. The shear strain is obtained by measuring the tangential movement of one bar relative to the other. It assumes that when viewed in cross-section they simply translate over each other, with all the deformation occurring in the specimen (Fig. B3-1). What is easily overlooked is that the bars also deform, i.e. are twisted by the eccentric load of the specimen on them, and that in so doing, they would produce the appearance of a translation (Fig. B4-2), even if no translation (due to specimen deformation) occurred. This twisting deformation is easily and accurately calculated, and for nine specimens of LI-900, the average shear modulus was 5542 psi before correction for bar twist, and 3598 psi after the bar-twisting correction is applied.

Unfortunately, there is no way of correcting any possible effects that the twisting of the bars may have on the maximum shear strength. It is not even certain whether this twisting "favors" or penalizes the specimen's ability to carry shear stress. To ascertain this effect, three tests were conducted in which the bars had a 2.0-in. square cross-section so that twisting would be reduced by a factor of 28. The results are tabulated in Appendix B2; the average modulus was 4,677 psi while the average strength was 29.9 psi as compared with 3,598 psi (after correction) and 31.5 psi for the 3/8 inch bars. The results seem to imply that the bar-twisting correction applied to the modulus over compensates. No explanation for this can be given at this time. No definite conclusion can be drawn with regard to shear strength from the results.

It should be pointed out that the shear strength in the torsion test series was higher than the shear strengths obtained in the "snake-skin" fixtures (31.5 psi vs. 23.7 psi). On the other hand, the room temperature tests using the newer ice-tong fixture produced an average shear strength (for seven specimens) of 30.6 psi. Three specimens from the same batch as the "snake-skin" test specimens mentioned above but tested in the ice-tong fixture had an average shear strength of 25.5 psi. If we assume that the fixtures both give a fair test, it would seem that strength variation from batch to batch can account for the differences in average strengths reported.

Even within a given batch there is evidence of systematic variation in properties. Specimens H-21 through H-68 were all tested using the "snake-skin" fixture, but some were tested at room temperature and some at -250°F. In addition, the gage lengths were varied (.125, .250 and .345 inches; more about this later), so that about 8 specimens were tested in each possible configuration of gage length and temperature. If, within each group, the specimens' maximum strength is expressed as a percentage of the average <u>for that group</u>, and this percentage is plotted vs. specimen number, the result is shown in Fig. B3-3. The specimens were numbered as they were cut from a slab, so that the specimen numbering effectively represents position in the parent slab of material. It is quite evident from this figure that almost all specimens from

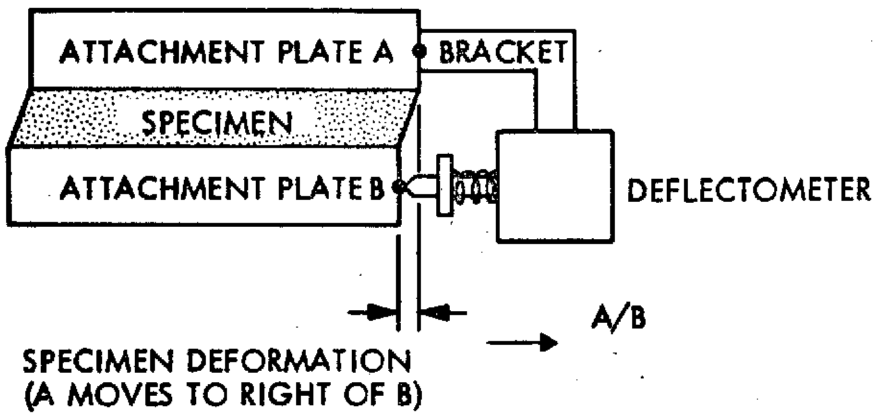

Fig. B3-1 Specimen Deformation

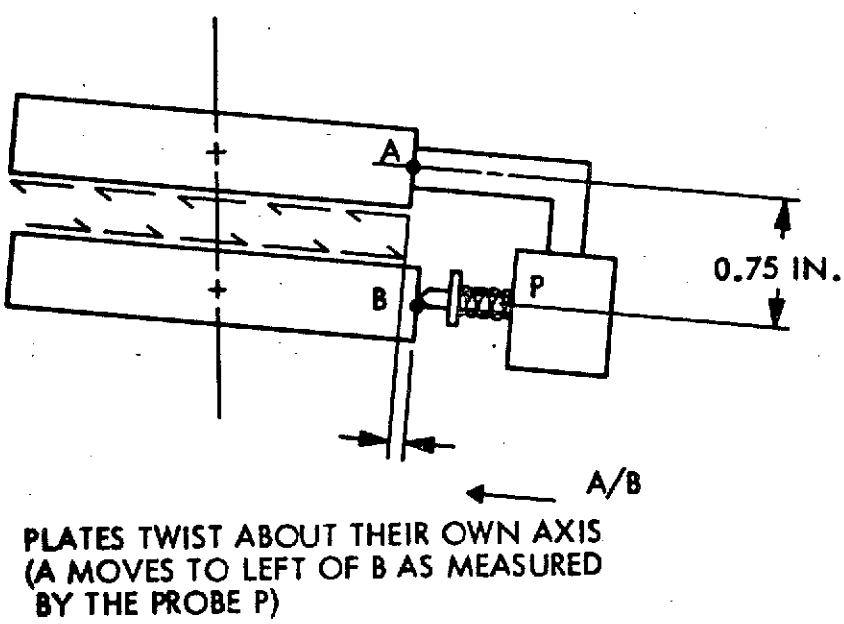

Fig. B3-2 Specimen Translation

H-39 through H-62 were below average strength, and that with only two minor exceptions (H-27 and H-30) all the specimens from H-23 through H-38 were above average strength. This clearly indicates zones of strong and weak material in the parent slab. If the material was more homogeneous in strength, the bars would be randomly distributed above and below the 100 percent line for any group of specimens as large as 16 specimens.

A similar figure has been prepared for the shear modulus in Fig. B3-4 and the same trend is apparent. Where a bar is missing for a given specimen number it is because no valid data are available on that specimen (bad test or specimen damaged prior to test). It should be added that any group of 16 consecutively numbered specimens contain a fairly random sampling when it comes to test type or test temperature (no one combination of these was bigger than eight or nine specimens, and if an entire combination was fully represented within this low-valued group of 16, there would have to have been several values above the 100 percent level.

In addition to the evidence from actual test results just presented, the experience of handling the specimens indicated a marked difference in the feel of the specimens. It was in fact this "feel" of the specimens which prompted the writer to prepare the two figures just presented. It has been mentioned that a torque wrench was used to tighten the clamping screws and that 16 inch-ounces of torque were applied at each screw. On some specimens this presented no problem. On others, the applied torque would release itself or would not hold, once applied, so that additional turning of the wrench was necessary to bring it back up to the desired level of 16 inch-ounces. In some cases, the additional tightening had to be performed several times until it was finally apparent that 16 inch-ounces would never "stay put." The specimens that displayed this characteristic were specimens numbered H-39 through H-62. Thus, all specimens that crushed easily under 16 inch-ounces or less displayed lower shear strength and shear modulus. True, it could be argued that the crushing itself caused the lower strength and modulus, but why did this group crush more easily than the rest? (The test operator was the same throughout.)

Another aspect of shear testing which was investigated with extra care was the matter of gage length (in the short beam span shear test – also known as the "tests on the

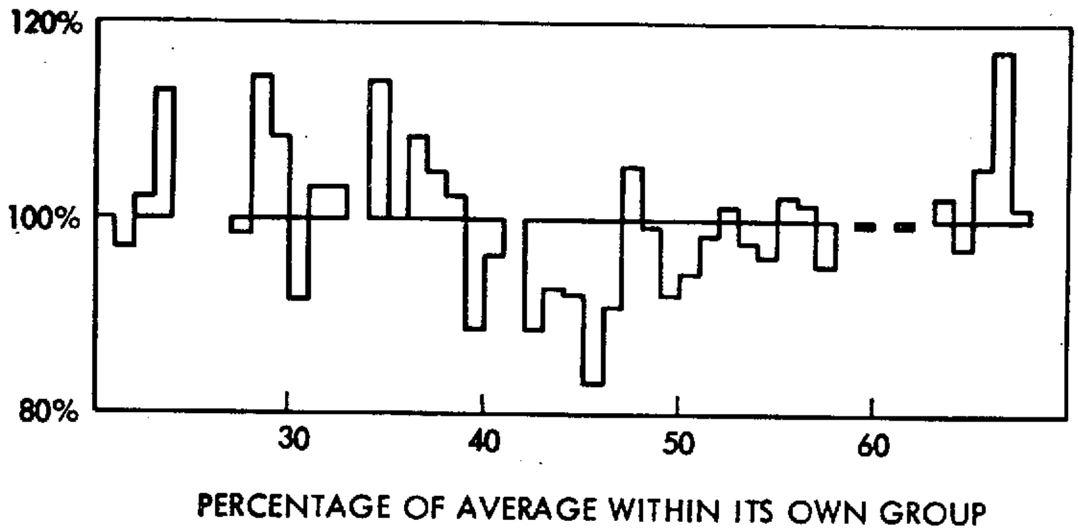

Fig. B3-3 Percentage of Shear Strength

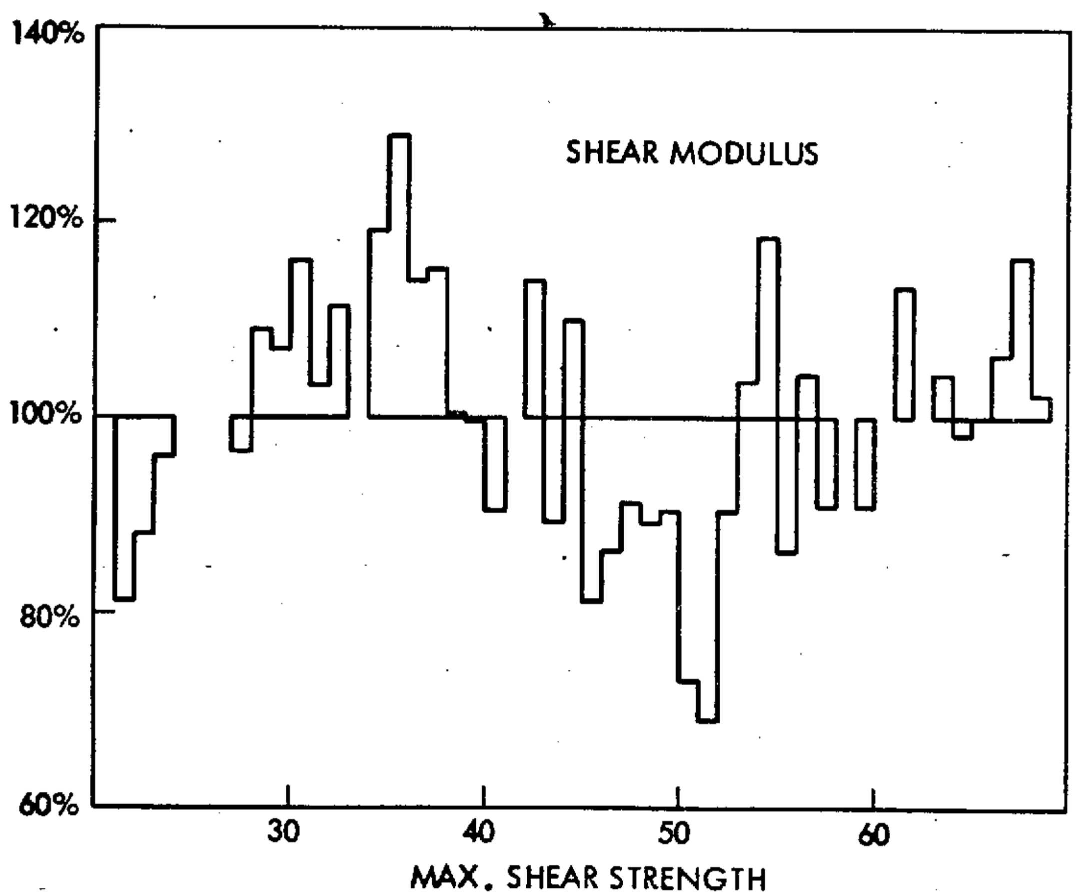

Fig. B3-4 Percentage of Shear Modulus

snake-skin fixture"). The reason for the concern is that there is no obvious or rational place for the attachment of an extensometer (or shear deformation meter) directly to the specimen. At first it was thought that the mid-points of the 2-inch edges (on either side of the clear span) would be representative points of movement, and a special set of tips was made for the extensometer so that the relative movement of these two points could be measured. On three successive tries, the load vs. deformation record looked like a staircase with steps of unequal height, so that no shear modulus could be inferred. It is felt that a shear lag condition exists, and although there is an applicable average shear stress, there are no known two points on the test section which faithfully represent the average strain that would exist if average shear stress pertained over the full two-inch length. Under these circumstances, the only compromise available is to measure the "rigid-body" movement of the two grips.

It is obvious that some shear deformation must occur within the gripped area of the specimen, especially in the case of the "snow-tire tread" pattern where the protrusions on the grip face represent only 15 to 20 percent of the grip edge. It is also probable that the shear deformation tapers off as we proceed into the grip zone (from the free edge). Is it reasonable or appropriate to approximate this condition by adding an increment to the gage length (or "span") and treating the deformation as if all of it occurred on a uniform basis across both the actual gage length and this increment of gage length? To answer this question, two extra sets of tests were run using different clear spans. The tests with the longer actual clear spans would tend to make the deformation occurring in the grips a smaller percentage of the total deformation. If it is further assumed that the deformation in the grips is the same (for any given load) regardless of the clear span, it is then possible to solve for the grip deformation and the clear span deformation if data are available from two sets of tests, each having a different clear span.

The basic equation used in the solution is

$$\frac{\Delta L}{L+x} = \gamma = \frac{\Delta \tau}{G}$$

where ΔL is the increment of deformation measured

L is the clear span

γ is the shear strain

$\Delta\tau$ is the increment of shear strain corresponding to ΔL

G is the shear modulus

x is the unknown additional span over which the deformation continues at the same uniform level as in the clear span – to be numerically equal to the integrated shear deformation which actually does occur.

The simultaneous solution of

$$L_2 + x = (\Delta L)_2 \times G/\Delta\tau \text{ and}$$

$$L_1 + x = (\Delta L)_1 \times G/\Delta\tau$$

yields $$G = \Delta\tau \ (L_2 - L_1)/(\Delta L)_2 - (\Delta L)_1$$

and $$x = \left[(\Delta L)_2 \times G/\Delta\tau\right] - L_2$$

The three clear spans or "gage lengths" tried with the "snake-skin" pattern shear fixture were .125, .250, and .345 inches. As a further refinement, the deflection due to bending in the actual clear span was subtracted from the measured deflection. Three solutions were obtained (because of the redundancy of spans). In each case the deformation increment is based on the average of at least 7 tests and the application of an 8 psi shear increment.

SIMULTANEOUS SOLUTION RESULTS

Span Lengths	G (psi)	X (inches)
.125 & .250	3940	.207
.125 & .345	2990	.128
.250 & .345	2236	.008
AVERAGES	3055	.128

The values of G obtained directly from the tests (with no slippage assumed or corrected for) were:

Span Length	G
.125	1476
.250	2146*
.345	2153

*This value may not agree with tabulation elsewhere in the report because it was based on the first eight specimens tested only.

It is evident from the slippage correction solutions that we are dealing with equations whose solutions are very sensitive to the "input" constants (i.e. the raw data). Also, in the slippage – uncorrected data, it is not surprising that the shortest gage length gives the lowest modulus since the slippage (which has to be about the same regardless of span) is distributed over a shorter gage length, making the apparent strain for any given load increment look larger.

In the slippage-corrected results it is difficult to account for variations obtained between combinations of spans. Since the shortest span now gives the highest modulus, it is possible that bending deflections (which increase as the cube of the span) play a significant role in "upsetting" the results of the solution. A further attempt was made to correct for this by pre-assuming a value for x, and including x in the bending deflection correction applied. A small computer program was written which solved for x and G after making the pre-assumed x (bending) correction. The tabulated results of x are then scanned for a solved value of x which matches the pre-assumed value. When this is done, the results are as follows:

SIMULTANEOUS SOLUTIONS WITH BENDING CORRECTIONS ADDED

Span Lengths	G (psi)	X (inches)
.125 & .250	4743	.284
.125 & .345	3291	.159
.250 & .345	2920	.102
AVERAGES	3651	.181

The weakness in this procedure is the assumption that the bending deflection behavior "parallels" the shear deflection behavior. Since one is a cube power relationship with span, and the other linear, the assumption is most likely unreasonable.

The span variation investigation was not extended to the "snow-tread tire" pattern because the latter "pattern" has a pitch (i.e. repeats itself) every 0.31 inch, which is almost the full width of the grip. The span therefore could not be increased by milling away part of the grip, as it was in the case of the snake-skin pattern (which had a pitch of 0.06 inch). To do so would be tampering with the parameter being measured. A multi-span investigation is only possible with the snow-tread grip if the grip remains the same width (and pattern) and if the specimen span itself is increased – which means varying the size of the specimen and the overall size of the grips. This procedure was not feasible within the scope of this contract. It is even possible that milling away part of the grips to increase the span in the "snake-skin" tests may have affected the results. If grips (rather than bonding) are to be adopted on a large scale, it will be necessary to conduct a more extensive investigation of the grip slippage problem.

Appendix B4

COMPOSITE COATING ANALYSIS

Appendix B4
COMPOSITE COATING ANALYSIS

Consider a two layer coating with a linear variation of Young's modulus in one layer and a constant value of Young's modulus in the other as depicted in the following sketch.

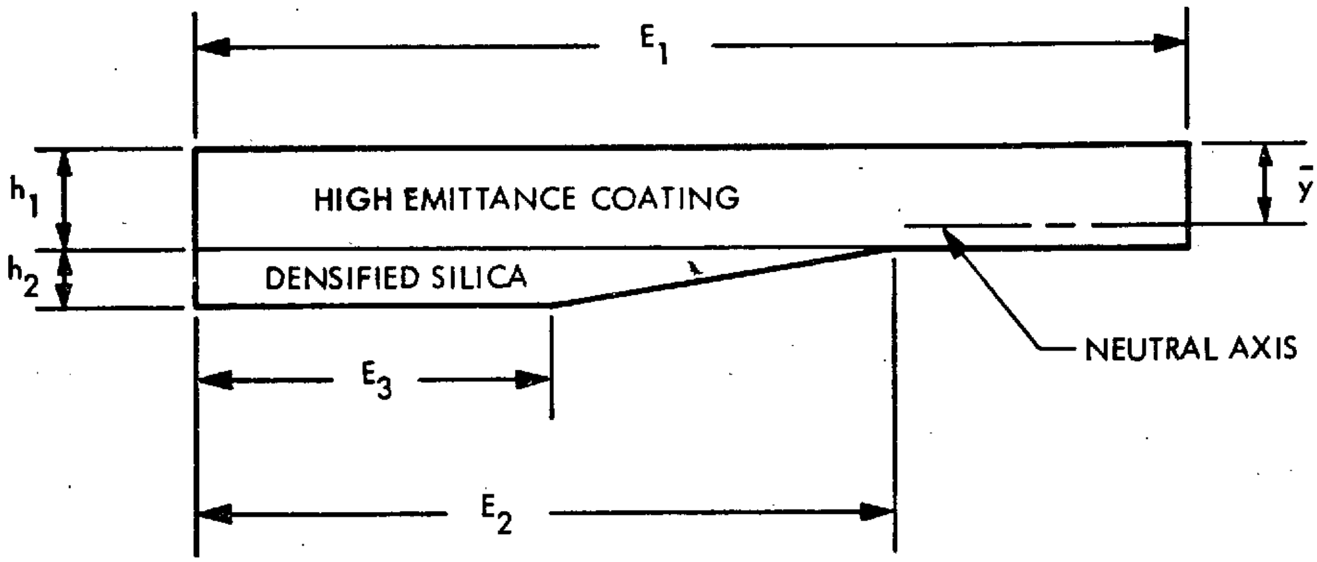

Neglecting second-order effects due to differences in Poisson's ratio in the two materials, one can express the extensional modulus E_E of the composite as

$$E_E = \frac{1}{(h_1 + h_2)} \left[h_1 E_1 + \frac{h_2}{2} (E_2 + E_3) \right] \tag{1}$$

Similarly, the flexural modulus, E_F, of the composite may be written

$$E_F = \frac{12}{(h_1 + h_2)^3} \left\{ \frac{h_1^3 E_1}{12} + h_1 E_1 \left(\frac{h_1}{2} - \bar{y} \right)^2 + \frac{E_2}{3} (h_1 + h_2 - \bar{y})^3 \right. \tag{2}$$

$$\left. - \frac{E_2}{3} (h_1 - \bar{y})^3 - \frac{(E_2 - E_3)}{3h_2} \left[h_2 (h_1 + h_2 - \bar{y})^3 - \frac{1}{4} (h_1 + h_2 - \bar{y})^4 + \frac{1}{4} (h_1 - \bar{y})^4 \right] \right\}$$

where the distance to the neutral axis $\bar{y}$ is given by

$$\bar{y} = \frac{1}{(h_1 + h_2) E_E}\left[\frac{h_1^2}{2} E_1 + \frac{h_2}{2}\left(h_1 + \frac{h_2}{3}\right) E_2 + h_2\left(\frac{h_1}{2} + \frac{h_2}{3}\right) E_3\right] \qquad (3)$$

If E_E and E_F are measured experimentally the above equations may be used to find any two of the variables appearing in the equations. In particular, if h_1, h_2 and E_3 are presumed known, then E_1 and E_2 can be determined. In general, this inversion leads to a quartic equation in E_1, which can be solved in closed form but requires a great deal of numerical manipulation. This can be facilitated by setting up an algorithm for a machine computation; however, for the case when $h_1 = h_2$ (which is the case of interest here) the solution equation degenerates after considerable algebraic manipulation to a quadratic with the solution

$$E_1 = 1.04\, E_E + .2\, E_3 + .08\sqrt{3\, E_E\,(73\, E_E - 100\, E_F + 30\, E_3)} \qquad (4)$$

the radical being taken as positive to agree with physical considerations (i.e., the add-on coating being known to have the higher modulus). E_2 is then given from equation (1) as

$$E_2 = 4\, E_E - E_3 - 2\, E_1 \qquad (5)$$

Several composite coatings from the initial batch of material were used to determine the effective flexural modulus at room temperature before destructive testing in tension. The test consisted of applying a concentrated load at the mid-point of the coating with the ends simply supported. The resulting load-deflection curve then allowed the computation of E_F. Results of five specimens are tabulated below.

Specimen	E_E (psi x 10^{-6})	E_F (psi x 10^{-6})	$h_1 + h_2$ (in.)
TT110-6	2.38	1.81	0.025
TT110-9	3.55	2.23	0.025
TT110-10	4.42	1.31	0.025
TT110-11	5.30	1.35	0.025
TT110-12	3.36	1.91	0.023
Average	3.80	1.72	0.0246

To complete the analysis, a value for E_3 must be assumed. Since the above coating specimens were fabricated on an 18-pcf RSI material, E_3 is therefore the Young's modulus of this material, which is of the order of 100,000 psi. (It is seen from equation (4) that for $E_3 << E_E$ the precise value of E_3 has little effect on the results.) Hence, using the average values for E_E and E_F and 0.1×10^6 psi for E_3, average values of E_1 and E_2 are found from equations (4) and (5) as

$$E_1 = 6.78 \times 10^6 \text{ psi}$$

$$E_2 = 1.53 \times 10^6 \text{ psi}$$

These results can then be used to interpret the composite coating data obtained over the entire range of tests from the observation that the thickness of the add-on high emittance coating remained constant at 0.012 inch from batch to batch and that only the thickness of the densified silica layer changed. The specimens used to obtain data at room temperature and at -250°F had equal thicknesses of the add-on high-emittance material and the densified silica. This fact was used in establishing equations (4) and (5). However, all other specimens had a much thinner layer of densified silica, as noted from the data tables given in Appendix B2.

In addition, it is necessary to make two assumptions, both of which appear to be plausible:

- That E_2 and E_3 from above, vary with temperature in the same manner as the experimental results for LI-900 strong direction tension
- That the modulus gradient in the densified silica, as determined from the preceeding analysis, remain constant regardless of the thickness of the densified silica layer. This effect is found to actually have only a minor influence on the results.

With these assumptions, an expression for E_1 (T) can be derived from equation (1) in which E_2 has been modified according to the second assumption. The result is

$$E_1(T) = C\,E_E(T) - \frac{C-1}{2}\left\{2\,E_3(T) + (C-1)\left[E_2(T) - E_3(T)\right]\right\} \tag{6}$$

where

$$C = \frac{h_1 + h_2}{h_1} \tag{7}$$

In the above, T is the test temperature, $h_1 + h_2$ is the total thicknesses of the composite coating and $h_1 = 0.012$ inch, the constant thickness of the high emittance layer. E_E is the modulus reported in the tables in Appendix B2. Stress allowables in those tables can also then be modified based upon the strain-to-failure data to give

$$\sigma_1 = \sigma_{composite}\left(\frac{E_1}{E_E}\right)$$

where σ_1 is the strength of the add-on high emittance layer alone.

The results of the above process, based on average values for moduli, are summarized below.

T (^oF)	Batch No.	(E_1) ave (psi x 10^{-6})	(σ_{ult}) ave (psi)	(σ_{ult}) min (psi)
-250	1	11.45	2134	1266
R.T.	1	6.21	2438	1326
400	3	1.35	1761	564
800	2	9.01	2608	1638
1200	2	5.37	2627	1564
1600	2	3.54	2215	1575

As can be seen, batch-to-batch variation has a significant effect on modulus but does not seem to impact the strength allowables. The behavior of the 400^oF data cannot be explained except to say that the material has been influenced by an unknown parameter.

Appendix C1

TEST PLAN FOR PHASE III

TURBULENT DUCT TEST MODEL

NAS 9-12856

National Aeronautics and Space Administration

Manned Spacecraft Center

Houston, Texas

Prepared By:

D. R. Elgin
Thermal Protection System

Approved By:

A. E. Trapp
Program Manager, NAS 9-12856

K. J. Forsberg, Manager
Thermal Protection System

Appendix C1
Test Plan for Phase III
TURBULENT DUCT TEST MODEL

1. INTRODUCTION

Lockheed Missiles & Space Company is delivering one test model for NASA/ARC evaluation as specified in Section 4.3.2 of the Statement of Work for Contract NAS 9-12856. This model consists of LI-900 silica rigid surface insulation (RSI) attached to an aluminum/glass honeycomb substrate with an intermediate foam pad. Thermocouple instrumentation is provided. This document outlines the LMSC recommended test program to be followed by ARC in evaluation of this test model. The objective of the test program is to perform an evaluation of the LI-900 with typical joint configurations to demonstrate the feasibility of the silica RSI for application on the Space Shuttle Orbiter Vehicle in regions of turbulent heating. A secondary objective is to evaluate the performance of a speciman that has experienced surface damage.

2. DESIGN CRITERIA/CONDITIONS

The LI-900 thickness was sized assuming the surface temperature and pressure histories corresponding to the Area 2P heat pulse (Fig. C1-1). The substrate panel is representative of the effective thickness of the primary structure in Area 2. The panel design temperature limit of 250°F occurs at touchdown, while a maximum temperature of 300°F occurs after landing. The flight pressure history and an adiabatic backface were also assumed. Since the pressures obtained in the turbulent duct are somewhat higher than flight pressures, the backface temperatures will be greater for these tests, as indicated in Fig. C1-2.

The effect of joints on the surface temperature distribution, joint temperature distributions, bondline and substrate temperatures, and in-depth temperature distributions will be determined from thermocouple measurements.

An indication of the stability of the material thermal characteristics will be determined by comparing the data obtained from duplicate test runs. It is recommended that sufficient temperature data be monitored during runs so that a rapid post-test comparison can be made. If significant variations in test data are noted on a particular test run, it is suggested that additional repeat runs be made until a stable condition is attained.

The test program consists of subjecting the model to five heating cycles in the "as received" condition. Upon completion of these tests, the panel will be removed from the fixture and the upstream tile will be purposely damaged. The damage will consist of a 0.25-in. diameter hole 0.5 in. deep. The panel will be reinstalled in the duct and subjected to two heating cycles. The damaged area will then be increased in size between two-cycle heating cycles until catastrophic failure appears imminent, or until a one-in. diameter by one-half-in. deep hole has been created. Photographs of the panel will be made after the completion of the initial five heating cycles and both before and after the double heating cycles.

3. MODEL DESCRIPTION

The test model design is shown on LMSC Drawing SK 62038 - Revision A, Fig. C1-3, (three sheets). The model consists of four LI-900 tiles that are assembled to provide one gap parallel to the flow direction and two gaps normal to the flow direction. The 3-in. thick tiles utilize the LMSC joint design employing FI-600 filler strips. The substrate consists of a 0.125-in. thick 7075-T6 aluminum plate bonded to the upper surface of a 0.375-in. thick glass/phenolid 4 lb/ft^3 perforated honeycomb. A 0.250-in. thick plate of 7075-T6 aluminum is bonded to the underside of the honeycomb. The substrate contains nut plates for fastening the model to the facility model holder. The overall model dimensions are 7.40 in. by 9.90 in. by 3.84 in. thick.

4. INSTRUMENTATION

The instrumentation is shown on Drawing SK 62038 (Fig. C1-3). The two center LI-900 tiles are instrumented with in-depth thermocouples in addition to surface thermocouples. The joints all contain thermocouples and thermocouples are installed on both sides th the substrate. The instrumentation consists of:

11 Pt - Pt 13 percent Rh thermocouples
28 Cr - Al thermocouples

The thermocouples are to be recorded continuously during all heating tests.

5. TEST PROGRAM

The model has been designed to interface with existing ARC test hardware. Since the NASA/ARC 20-nw turbulent duct arc heater facility has not previously been used to simulate an Area 2P heating pulse, it is recommended that the previously tested Area 2 LI-1500 model be used to calibrate the facility. This will help ensure against accidental over-heating of the LI-900 model.

5.1 TEST DESCRIPTION

After the Area 28 heating pulse has been established utilizing the LI-1500 model, the following series of tests are recommended for the LI-900 model:

5.1.1 Checkout Test

a. Install model in test facility with the upper surface flush with the model holder upper surface.
b. Expose model to the first 2000 seconds of simulated Area 2P heating pulse shown in Fig. C1-1. All thermocouple data shall be recorded during the test.
c. Compare measured data with predictions to determine whether the maximum bondline temperature is within acceptable limits.
d. Allow model to cool until all thermocouples indicate a temperature of less than 100, F.
e. Inspect model and record any changes.

5.1.2 Heating Cycle Tests

a. Expose model to the simulated Area 28 heating pulse shown in Fig. C1-1. All thermocouple data shall be recorded during the test.
b. Allow model to cool until all thermocouples indicate a temperature of less than 100,F.
c. Inspect model and record any changes.
d. Repeat a, b and c above an additional four times.
e. Remove model from test facility and perform NDE.
f. Photograph model.

5.1.3 Damaged Tile Tests

a. Drill a 0.25-in. diameter hole 0.5-in. deep into the center of the upstream tile upper surface.
b. Photograph model.
c. Install model in test facility with the upper surface flush with the model holder upper surface.
d. Expose model to simulated Area 2P heating pulse shown in Fig. C1-1. All thermocouple data should be recorded during the test.
   If any of the temperature readings differ from previous test readings to the extent that a catastrophic failure appears imminent, the test will be terminated. If not, proceed as follows:
e. Allow model to cool until all thermocouples indicate a temperature of less than 100°F.
f. Inspect model and record any changes
g. Repeat d, e and f above.
h. Remove model from test facility and perform NDE.
i. Photograph model
j. Enlarge drilled hole to 0.50 in. diameter to 0.5 in. depth.
k. Repeat c through i above.
l. Enlarge drilled hole to 0.75 in. diameter to 0.5 in. depth.

m. Repeat c through i above.

n. Enlarge drilled hole to 1.000 in. diameter to 0.5 in. depth.

o. Repeat b through i above.

5.2 DATA ANALYSIS

Analytical models, utilizing LMSC's THERM computer code, will be used to predict temperature distributions prior to performing the outlined tests. Test data will be compared to the analytical predictions and any discrepancies will be investigated and explained.

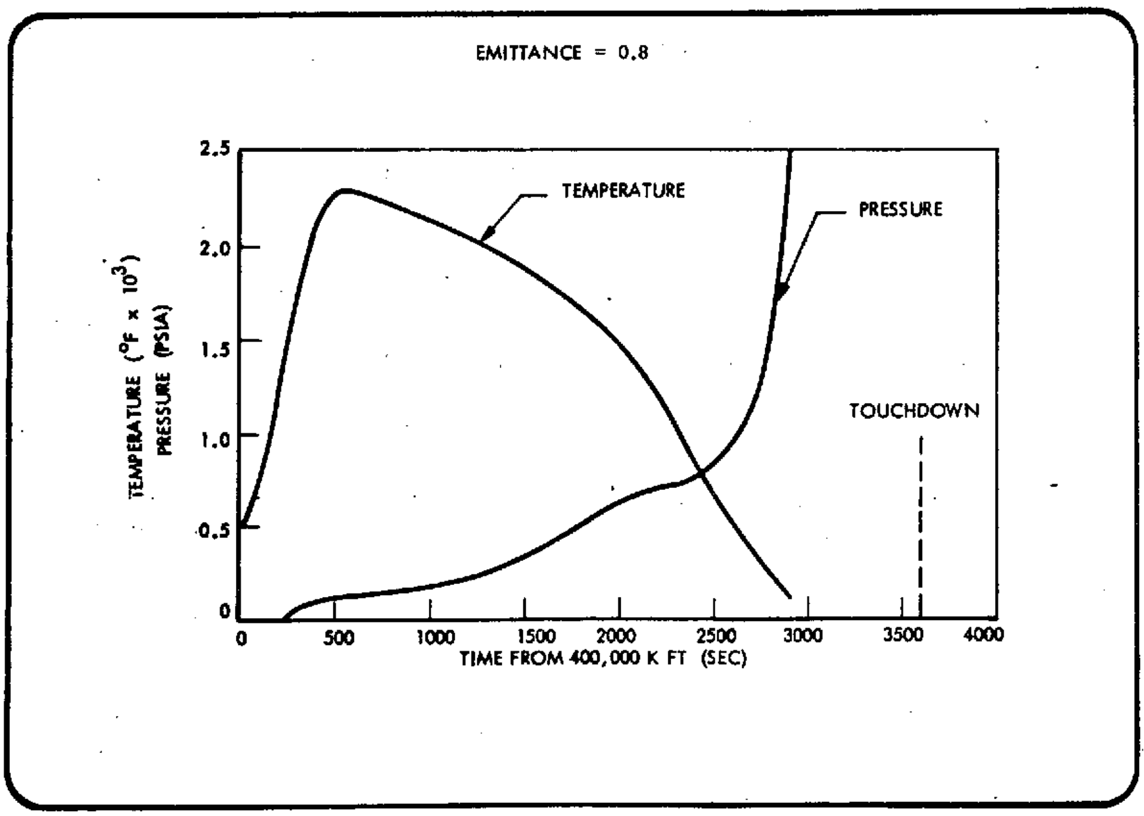

Fig. C1-1 Area 2P Temperature/Pressure History

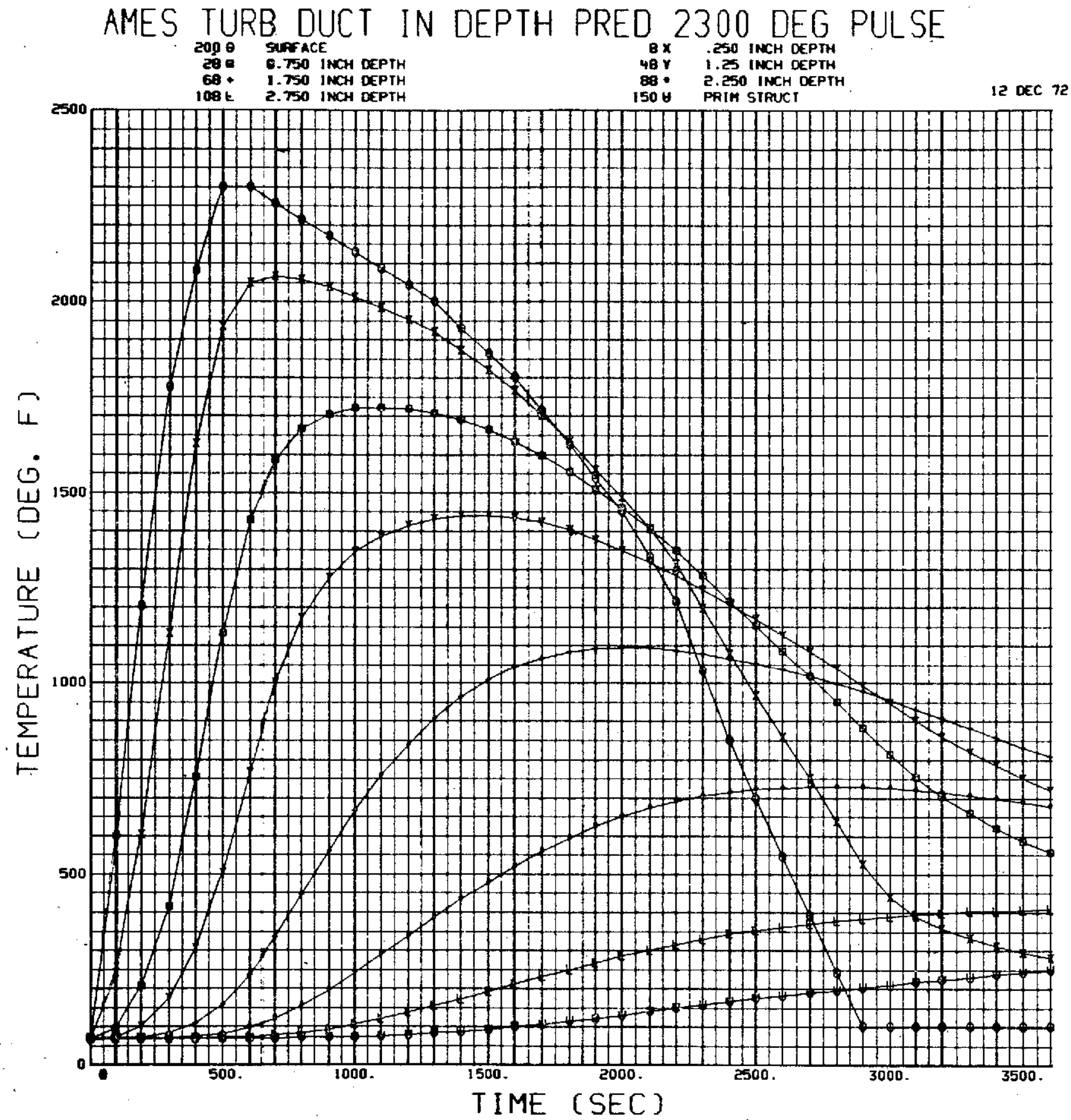

Fig. C1-2 Turbulent Duct Model Temperature Predictions

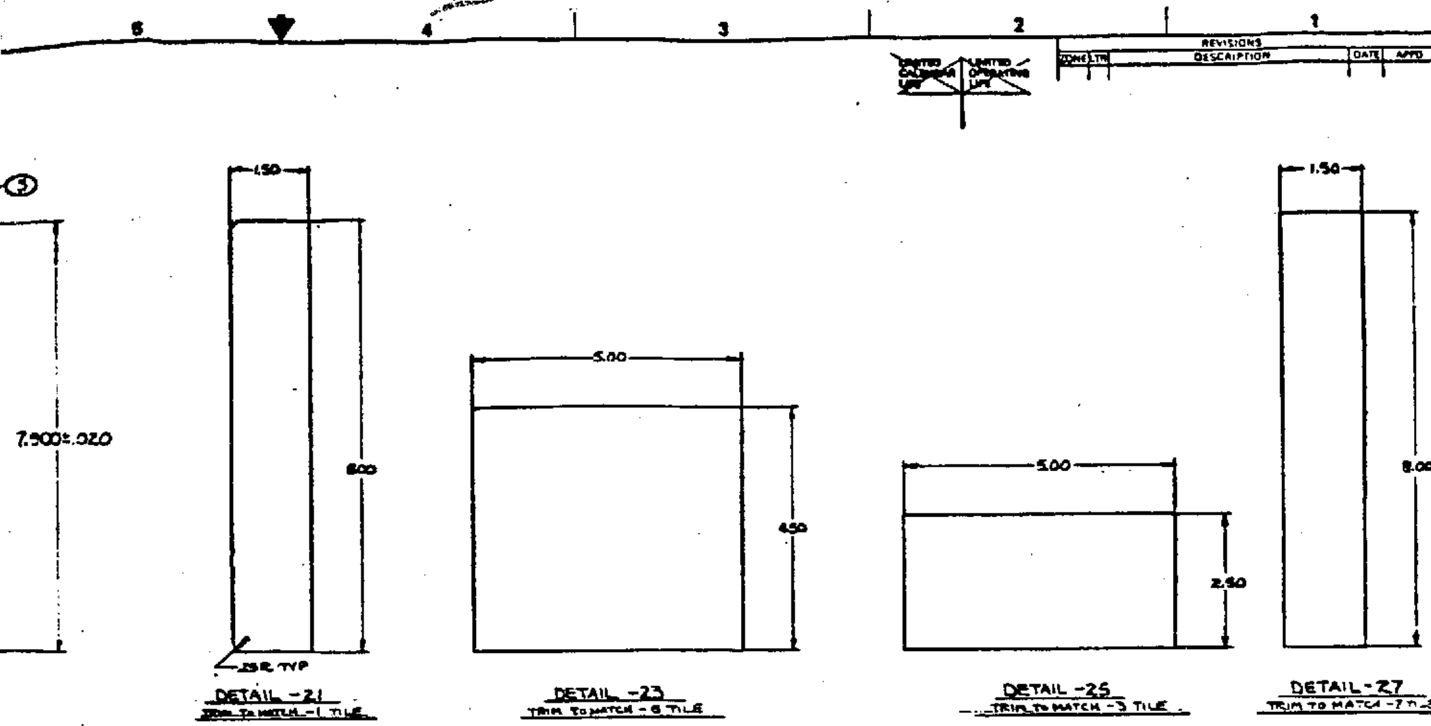

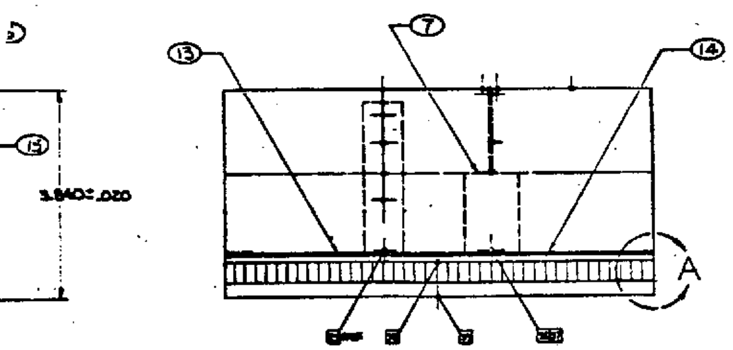

							28
							27
							26
✓		0042	COATING				25
✓		CH/AL	WIRE, T/C	10 MIL DIA			24
✓		PT/PT-13%RH	WIRE, T/C	10 MIL DIA			23
							22
✓		GE 560	RTV				21
	18	MS20426AD3-4	RIVET				20
	9	LS8830-4	NUT PLATE				19
	1	-33	BASE PLATE	.250 7075T6AL			18
	1	-31	HCMB CORE	3/8 THICK 4#/FT³ PERF	MIL-C-9073		17
	1	-29	SUBSTRATE	.125 7075T6AL			16
1		-27	FOAM	.080 THICK	PD-200		15
1		-25	FOAM	.080 THICK	PD-200		14
1		-23	FOAM	.080 THICK	PD-200		13
1		-21	FOAM	.080 THICK	PD-200		12
							11
							10
							9
							8
1		-11	FILLER	FI-600			7
2		-9	FILLER	FI-600			6
1		-7	TILE	LI-900			5
1		-5	TILE	LI-900			4
1		-3	TILE	LI-900			3
1		-1	TILE	LI-900			2
1		-301	SUBASSEMBLY				1
QTY REQD	CODE IDENT	PART OR IDENTIFYING NO.	NOMENCLATURE OR DESCRIPTION	MATERIAL DESCRIPTION OR NOTE	MATERIAL SPECIFICATION	ZONE	ITEM NO.
-501	-301		PARTS LIST				

8\. OVERALL DIMENSIONS MUST BE HELD TO TOLERANCES SHOWN. USE SELECTIVE FITTING AND SEQUENTIAL ASSEMBLY PROCEDURES AS REQUIRED TO ACHIEVE ASSEMBLY ENVELOPE DIMENSIONS.

7\. BOND LI-900 TILES TO SUBSTRATE WITH .005 INCH THICK LAYER OF G.E. RTV 560 COMPOUND ITEM 21.

7\. COAT LI-900 TILES WITH 0042 COATING, ITEM 25, PER APPLICABLE PROCEDURES PRIOR TO TILE ATTACHMENT.

6\. BOND -301 SUBASSEMBLY PER PB91 EXCEPT AS FOLLOWS:
A. USE GLASS FABRIC CORE, ITEM 17, PERFORATED.
B. DO NOT FILL EDGES OF CORE OR CUT-OUT SECTIONS OF CORE WITH ADHESIVES OR OTHER FILLERS.

5\. THERMOCOUPLES NO.12 THROUGH NO.33 ARE CH/AL MATERIAL, ITEM 24.

4\. THERMOCOUPLES NO.1 THROUGH NO.11 ARE PT/PT-13%RH MATERIAL, ITEM 23.

3\. ITEM NUMBERS ARE SHOWN THUSLY: (XX).

2\. SEE SHEET 3 FOR RSI FAB & INSTR. DETAILS.

NOTES: 1. SEE SHEET 2 FOR BASEPLATE ASSEMBLY.

UNLESS OTHERWISE SPECIFIED DIM. ARE IN INCHES. TOLERANCES ON: FRACTIONS = ± 1/16; DECIMALS: .X = ± .1, .XX = ± .03, .XXX = ± .010; ANGLES = ± 2 DEG.	DATE 3-9-72 DR D. R. BRIGHT APPD APPD ENGRG CHK APPD APPD	LOCKHEED MISSILES & SPACE COMPANY A GROUP DIVISION OF LOCKHEED AIRCRAFT CORPORATION SUNNYVALE, CALIFORNIA ENVIRON. TEST MODEL TURBULENT DUCT TESTS LI-900 MATERIAL SIZE E · CODE IDENT · DRAWING NO. SK62038 · REV A SCALE 1/1 · SHEET 1 OF 3
INTERPRET DWG PER · NEXT ASSY · USED ON · APPLICATION · CONTR · CCA/CS		

Fig. C1-1 Drawing SK62038, Sheet 1

FOLDOUT FRAME

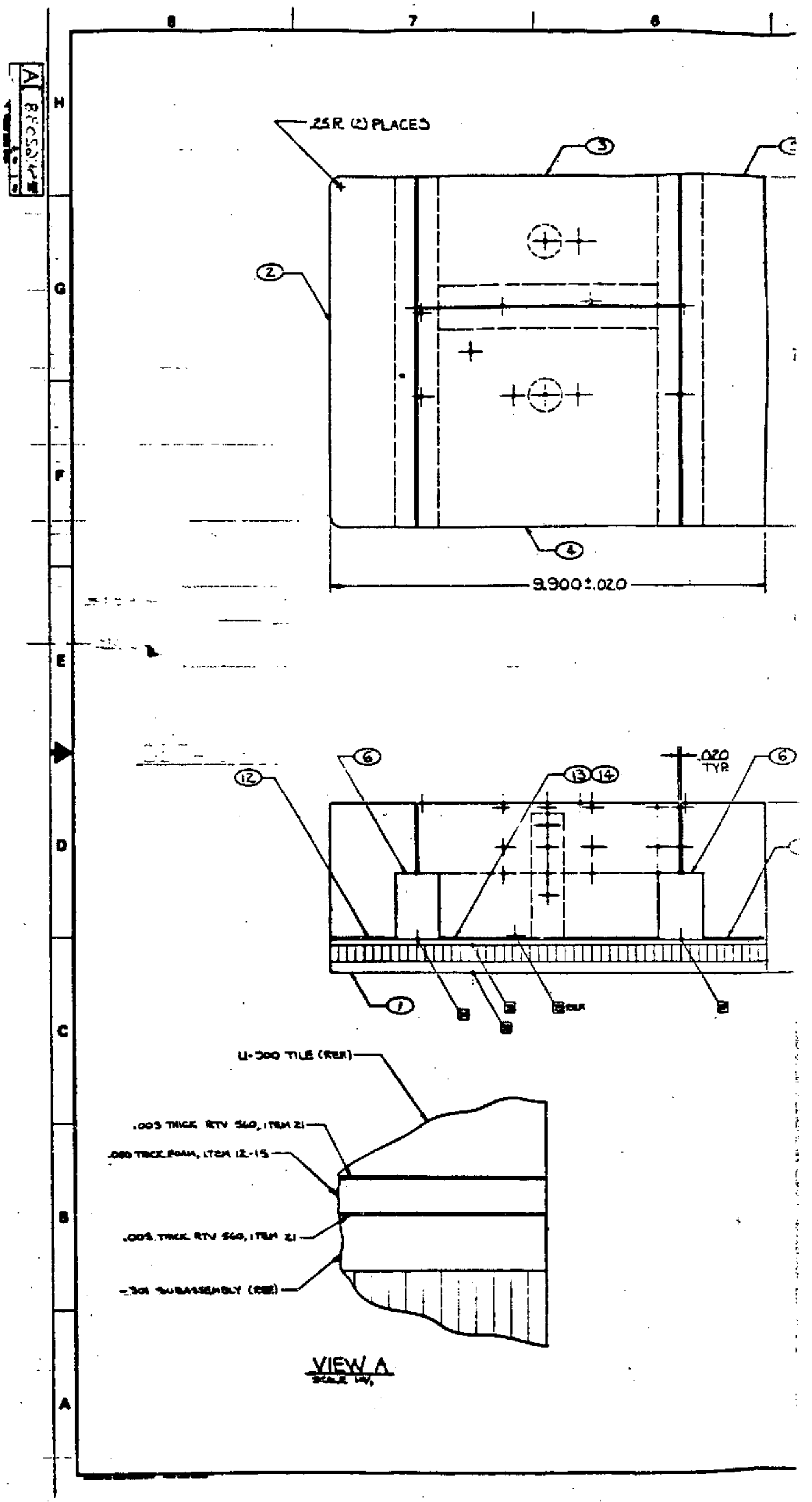

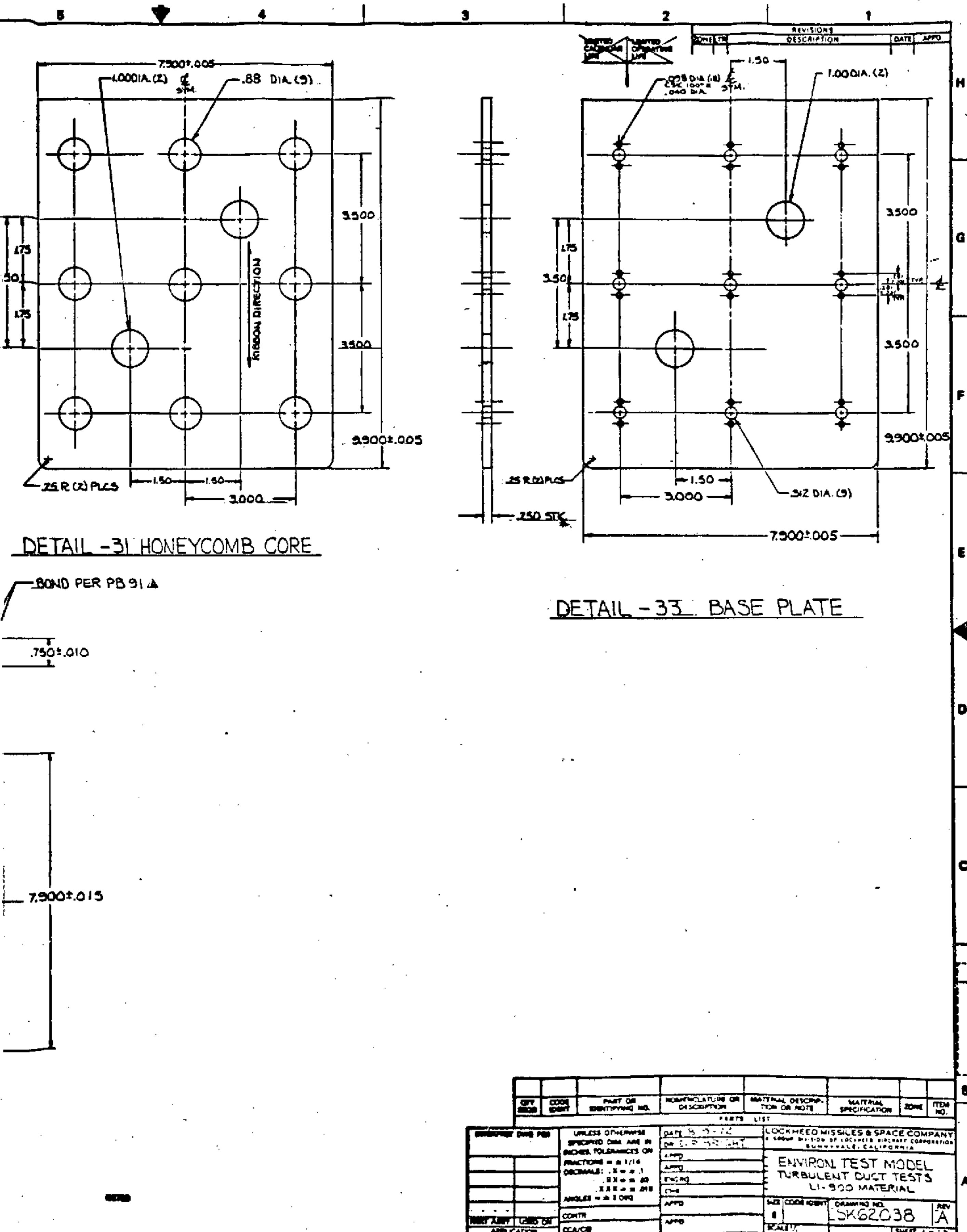

Fig. C1-2 Drawing SK62038, Sheet 2

FOLDOUT FRAME

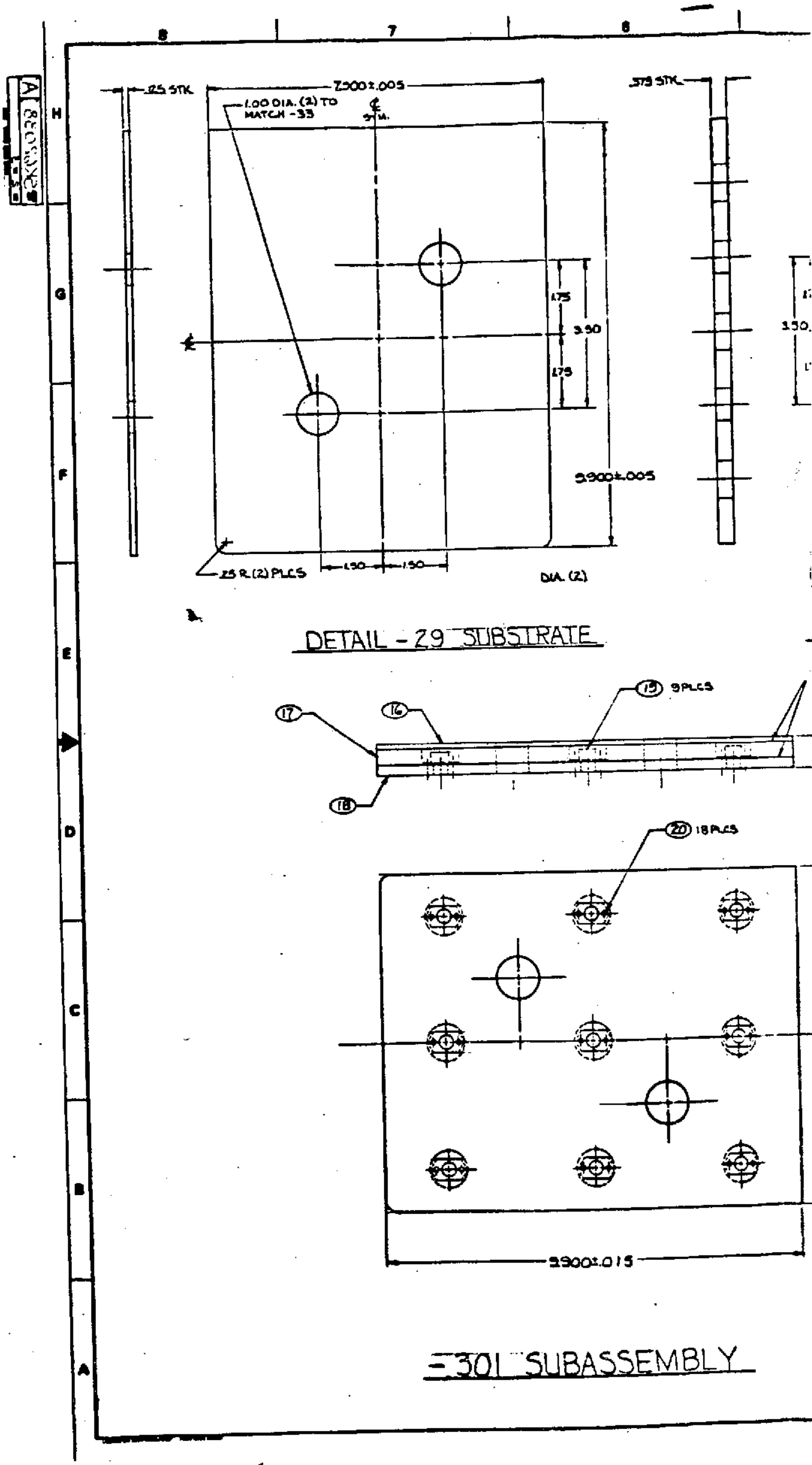

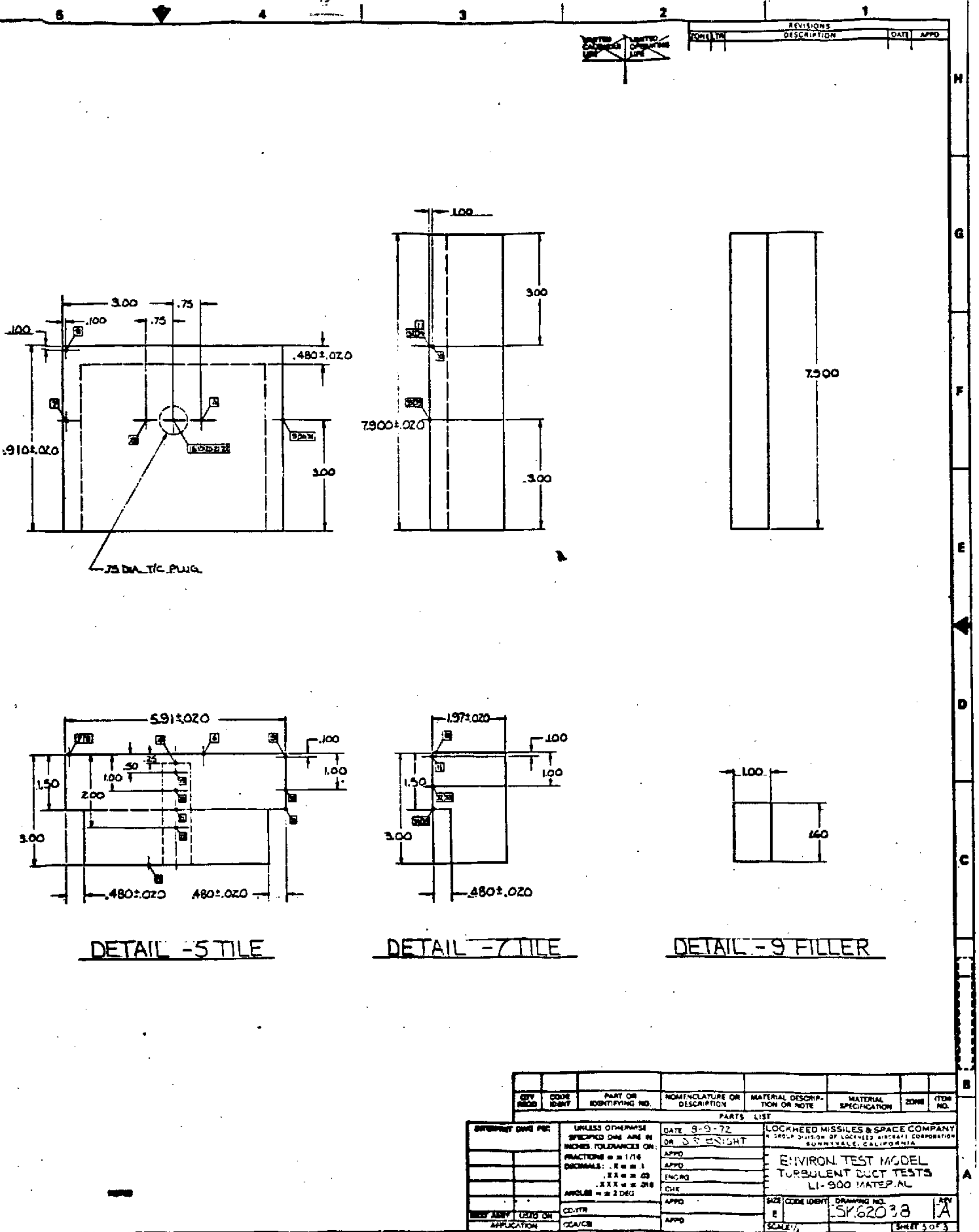

Fig. C1-3 Drawing SK62038, Sheet 3

FOLDOUT FRAME

1

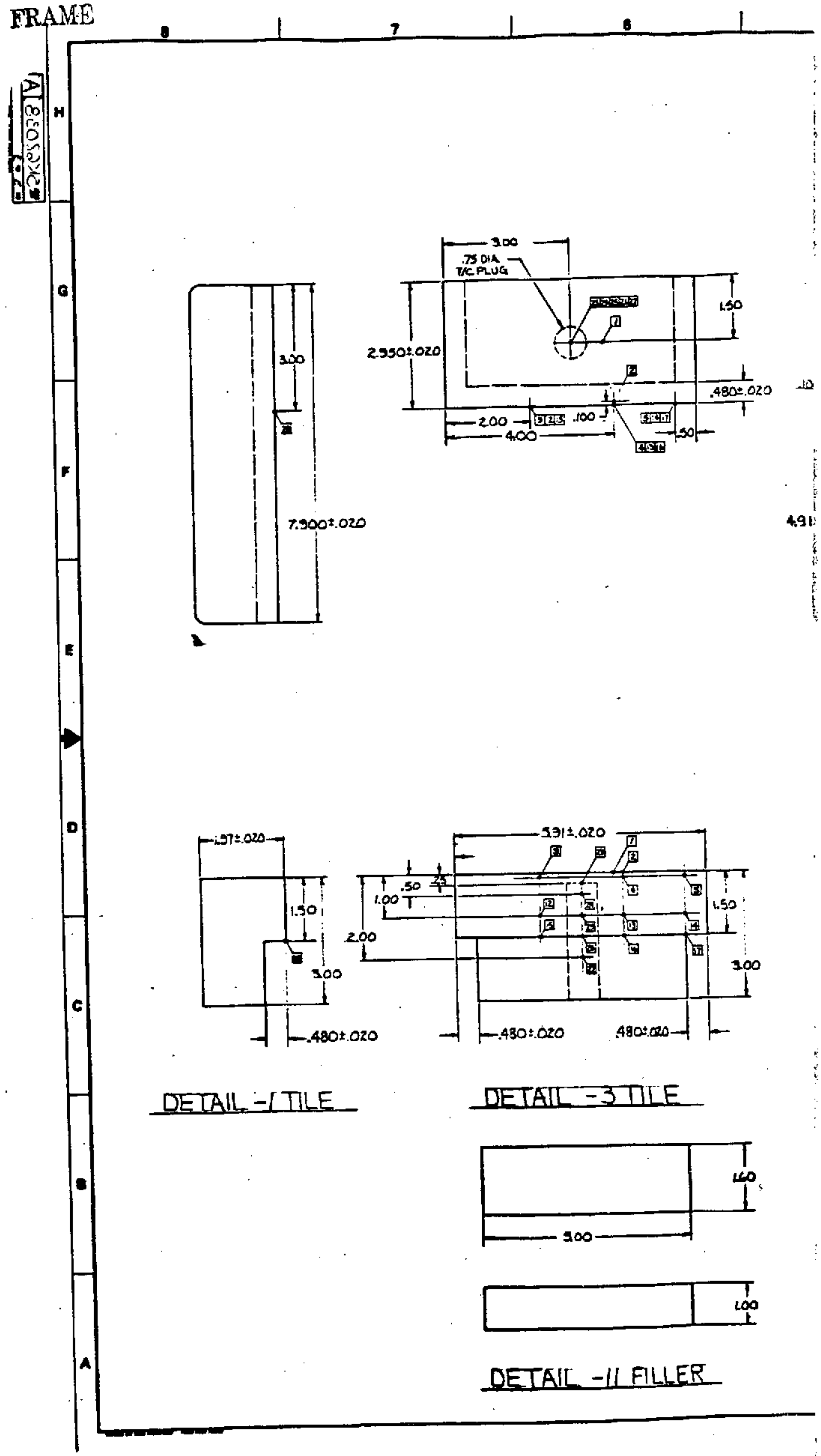

Appendix C2

TEST PLAN FOR PHASE III
100-CYCLE CONVECTION TEST MODEL
NAS 9-12856

National Aeronautics and Space Administration

Manned Spacecraft Center

Houston, Texas

Prepared By:

D. R. Elgin
Thermal Protection System

Approved By:

A. E. Trapp
Program Manager, NAS 9-12856

K. J. Forsberg, Manager
Thermal Protection System

Appendix C2
TEST PLAN FOR PHASE III
100-CYCLE CONVECTION TEST MODEL

1. INTRODUCTION

Lockheed Missiles & Space Company (LMSC) is delivering one test model for NASA/MSC evaluation, as specified in Section 4.3.3 of the Statement of Work for Contract NAS 9-12856. This model consists of LI-900 silica rigid surface insulation (RSI) attached to an aluminum substrate with an intermediate foam pad. Thermocouple instrumentation is provided. This document outlines the LMSC recommended test program to be followed by MSC in evaluation of this test model. The objective of the test program is to perform an evaluation of the LI-900, with typical joint configurations, to determine cumulative convective heating exposure effects with respect to model integrity and temperature response repeatability.

2. DESIGN CRITERIA/CONDITIONS

The model design was dictated by the following test objectives:

a. Determine the effect of heating and shear stresses on the coated surface, joint edges, and sides.

b. Determine the effect of joint orientation on surface, in-depth and backface temperatures.

c. Determine temperature response repeatability.

d. Determine cumulative convective heating exposure effects on material integrity.

The Area 2P maximum heating conditions result in a surface temperature of 2300°F at an angle-of-attack of 34 degrees. It is recommended that these conditions be established for the 100-cycle tests.

The effect of joints on the surface temperature distribution, joint temperature distributions, bondline and substrate temperatures, and in-depth temperature distributions will be determined from thermocouple measurements.

An indication of the stability of the material thermal characteristics will be determined by comparing the data obtained from duplicate test runs. It is recommended that sufficient temperature data be monitored during runs so that a rapid post-test comparison can be made. If significant variations in test data are noted on a particular test run, it is suggested that additional repeat runs be made until a stable condition is attained.

The test program consists of subjecting the model to 100 heating cycles, with the model in two orientations with respect to the flow direction. Half of the runs will be made with the long joint parallel to the flow direction and half with it normal to the flow direction. It is recommended that the tests be performed in sets of 10, with an NDE performed and photographs taken after each set.

3. MODEL DESCRIPTION

The test model design is shown on LMSC Drawing SK 62030, Revision B (Fig. C2-1, three sheets). The model consists of three full-size 6 by 6-in. tiles and two half-size 6 by 3-in. tiles. The tiles are assembled to form one joint in one direction and three joints in the 90-degree rotation direction. The 1.865 in. thick tiles utilize the current LMSC joint design employing filler strips. The tiles are bonded to a 0.062-in. thick 7075-T6 aluminum baseplate with a 0.060 in. thick RMRL 1973 foam pad intermediary. The baseplate contains two one-in. diameter holes to allow passage of the instrumentation leads. The overall model size is 11.95 by 11.95 by 2.00 in. thick.

4. INSTRUMENTATION

The instrumentation is shown on Drawing SK 62030 (Fig. C2-1). Two of the 6 by 6-in. tiles are instrumented with in-depth thermocouples as well as surface thermocouples.

In addition, the joints are instrumented with thermocouples. The instrumentation consists of:

11 Pt-Pt 13 percent Rh thermocouples
14 Cr-Al thermocouples

The thermocouples are to be recorded continuously during all heating tests.

5. TEST PROGRAM

The model has been designed to fit the existing test fixture shown on Avco drawing 307E3965. It is recommended that shims be used between the LI-900 and the holding screws. The tiles are coated on the edges and penetrating the coating with the screws may cause cracking, which could propagate to the upper surface.

5.1 TEST DESCRIPTION

It is recommended that a checkout test be performed to assure that the instrumentation is working properly and that the maximum allowable bondline temperature will not be exceeded.

5.1.1 Checkout Test

a. Install model in test facility with the upper surface flush with the model holder upper surface and the long joint parallel to the flow direction. Tiles 11 and 5 should be in the upstream position.

b. Expose model to flow to achieve a 2300°F model surface temperature at 34 degrees angle-of-attack. Maintain model in flow for 400 seconds or until bondline temperature reaches 400°F, whichever occurs first. All thermocouple data shall be recorded during the test and after the test until the maximum bondline temperature is reached.

c. Compare measured data with predictions to determine whether the maximum bondline temperature is within acceptable limits. If not, modify the test duration to obtain the desired conditions.

d. Allow model to cool until all thermocouples indicate a temperature less than 100°F.

e. Inspect model and record any changes.

5.1.2 Heating Cycle Tests

a. Expose model to heat pulse established during the checkout test. All thermocouple data shall be recorded during the test.

b. Allow model to cool until all thermocouples indicate a temperature of less than 100°F.

c. Inspect model and record any changes.

d. Repeat a, b, and c an additional nine times.

e. Perform NDE.

f. Photograph model.

g. Repeat a through f above an additional four times.

h. Rotate model 90 degrees so that the long joint is normal to the flow direction. Tiles 11 and 13 should be in the upstream position.

i. Perform a through g above five times.

5.2 DATA ANALYSIS

Analytical models, utilizing LMSC's THERM computer code, will be used to predict temperature distributions prior to performing the outlined tests. Test data will be compared to the analytical predictions and any discrepancies will be investigated and explained.

4 3 2 1

REVISIONS				
ZONE	LTR	DESCRIPTION	DATE	APPD

LIMITED CALENDAR LIFE

LIMITED OPERATING LIFE

D

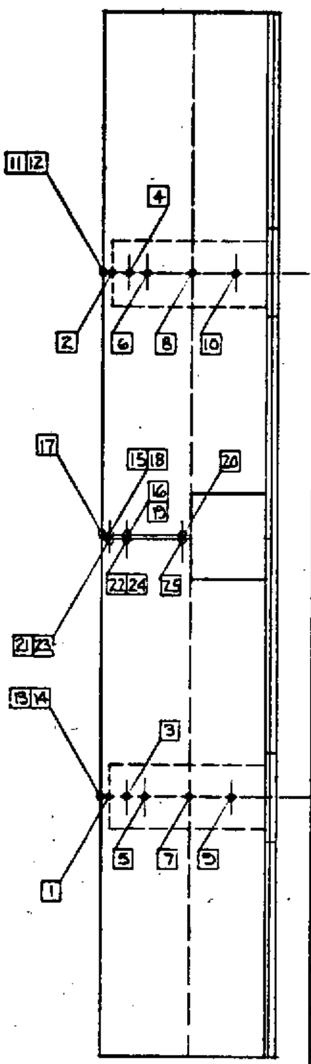

.030±.010 GAP TYP

C

B

-3

QTY REQD	CODE IDENT	PART OR IDENTIFYING NO.	NOMENCLATURE OR DESCRIPTION	MATERIAL DESCRIPTION OR NOTE	MATERIAL SPECIFICATION	ZONE	ITEM NO.
✓			WIRE, T/C, 10 MIL	CH/AL			13
✓			WIRE, T/C, 10 MIL	PT/PT-13%RH			12
✓		0042	COATING				11
✓		RTV 560	COMPOUND	RTV			10
1		-17	1.00x1.00x12.00 FILLER	FI-600 FSI			9
3		-15	1.00x1.00x5.50 FILLER	FI-600 FSI			8
1		-13	2.00x6.00x6.00 TILE	LI-900 RSI			7
1		-11	2.00x6.00x6.00 TILE	LI-900 RSI			6
1		-9	2.00x3.00x6.00 TILE	LI-900 RSI			5
1		-7	2.00x6.00x6.00 TILE	LI-900 RSI			4
1		-5	2.00x3.00x6.00 TILE	LI-900 RSI			3
1		-3	.060x12.00x12.00 SHT	RMRL 1973 FOAM			2
1		-1	.062x12.00x12.00 PL	7075-T6 AL ALLOY			1

PARTS LIST

TILES TO HEIGHT
ING WITH 0042 COATING

HEET WITH .005 (MIN.)
POUND, AND -5, -7, -9, -11,
FILLERS TO -3 SHEET
JD.

LE INSTRUMENTATION
WITH SHEET 2.

A

INTERPRET DWG PER

NEXT ASSY | USED ON
APPLICATION

UNLESS OTHERWISE SPECIFIED DIM. ARE IN INCHES. TOLERANCES ON:
FRACTIONS = ± 1/16
DECIMALS: .X = ± .1
.XX = ± .03
.XXX = ± .020
ANGLES = ± 2 DEG

CONTR

CCA/CEI

DATE 11-6-72
DR D.R. BRIGHT
APPD
APPD
ENGRG
CHK
APPD
APPD

LOCKHEED MISSILES & SPACE COMPANY
A GROUP DIVISION OF LOCKHEED AIRCRAFT CORPORATION
SUNNYVALE, CALIFORNIA

ENVIRON TEST MODEL
100 CYCLE CONVECTION TESTS
LI-900 MATERIAL

SIZE D | CODE IDENT | DRAWING NO. SK62030 | REV B
SCALE 1/1 | SHEET 1 OF 3

149

Fig. C2-1 Drawing SK62030, Sheet 1

FOLDOUT FRAME 1

FOLDOUT FRAME 2

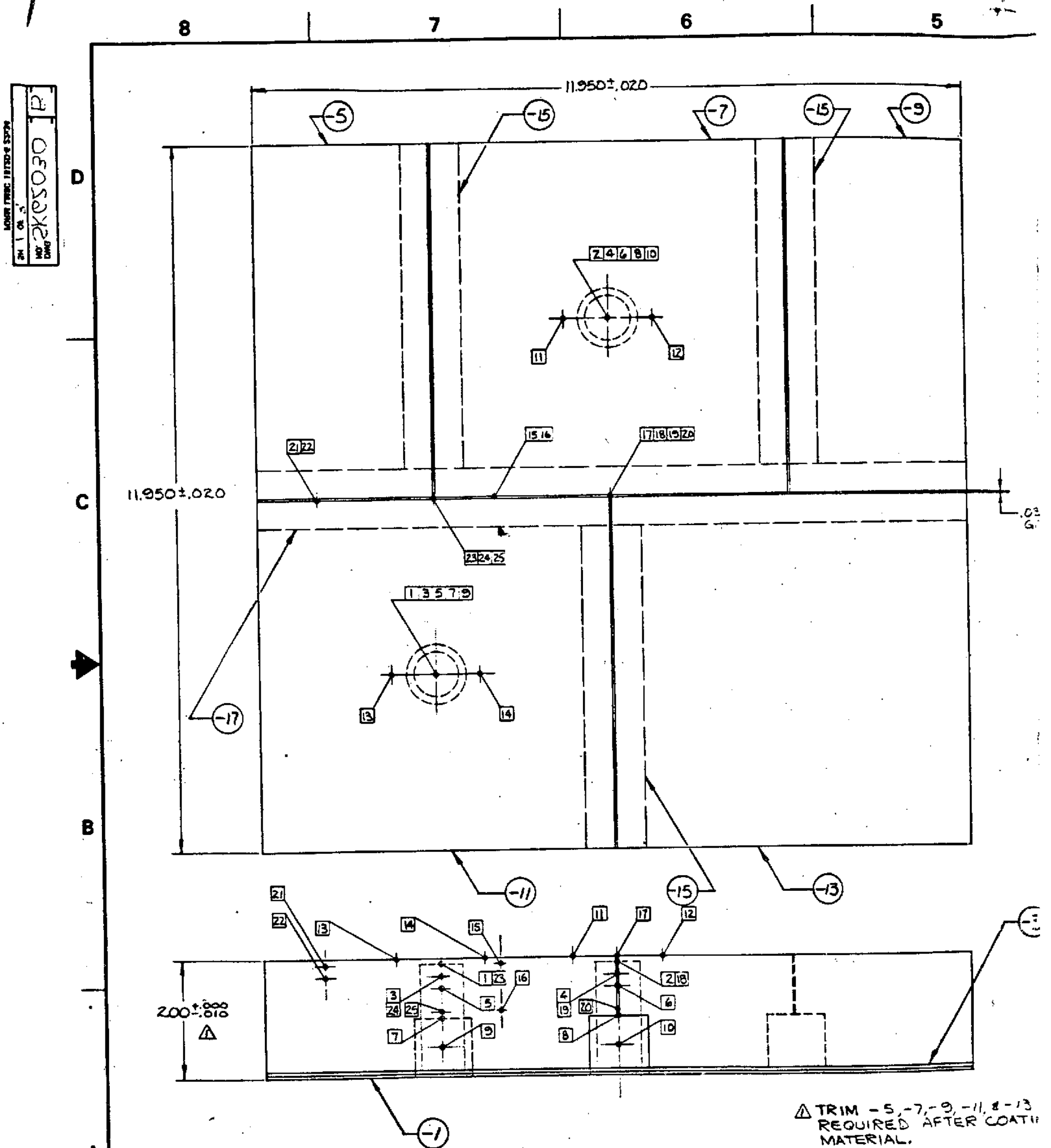

△ TRIM -5, -7, -9, -11, & -13 REQUIRED AFTER COATI[NG] MATERIAL.

2. BOND -1 PLATE TO -3 S[...] LAYER OF RTV 560 COM[...] -13 TILES AND -15 & -17 [...] WITH RTV 560 COMPOU[ND]

3. INSTALL THERMOCOUPL[ES] (T/C) IN ACCORDANCE

NOTES

FORM LMSC 1812D-6

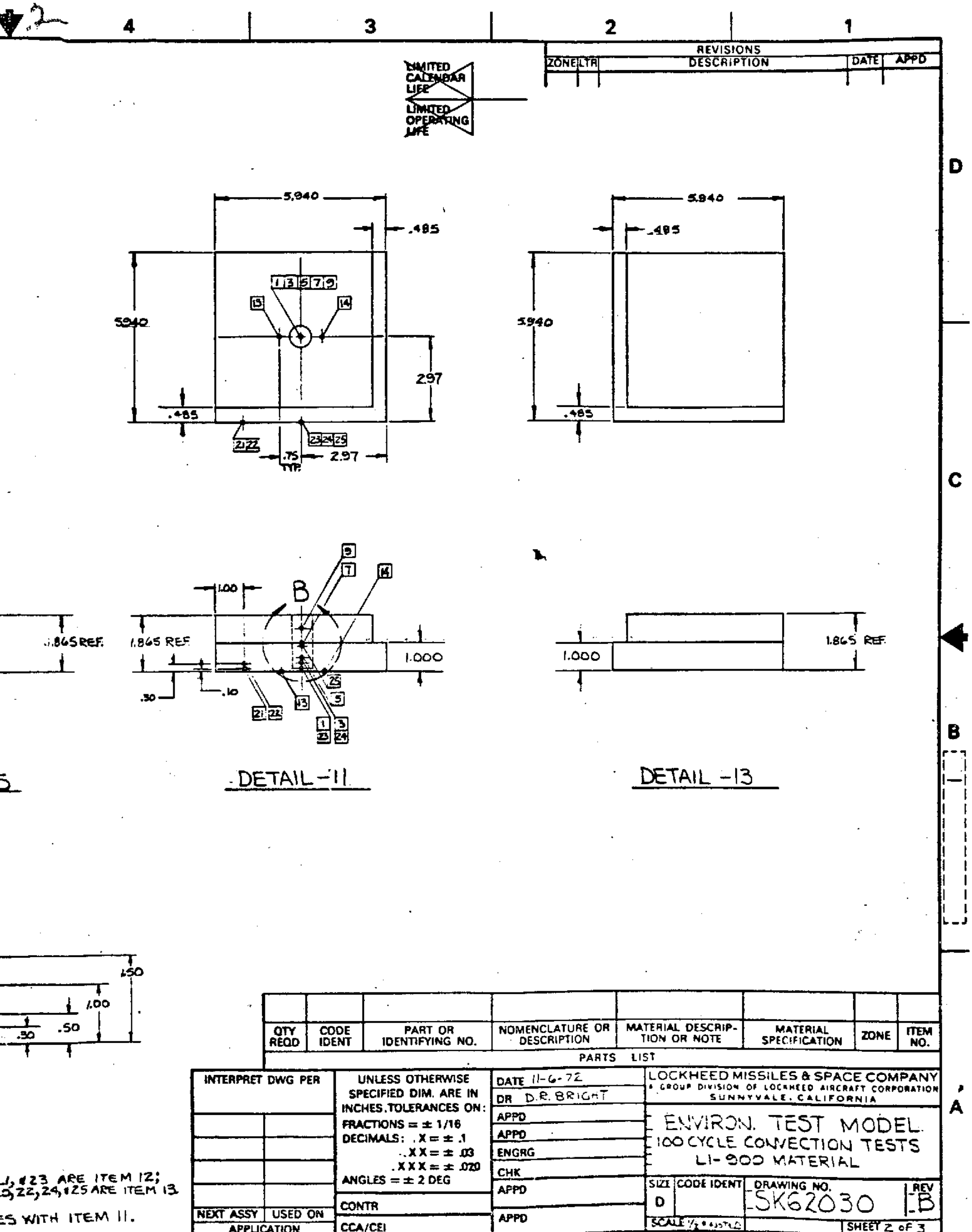

Fig. C2-2 Drawing SK62030, Sheet 2

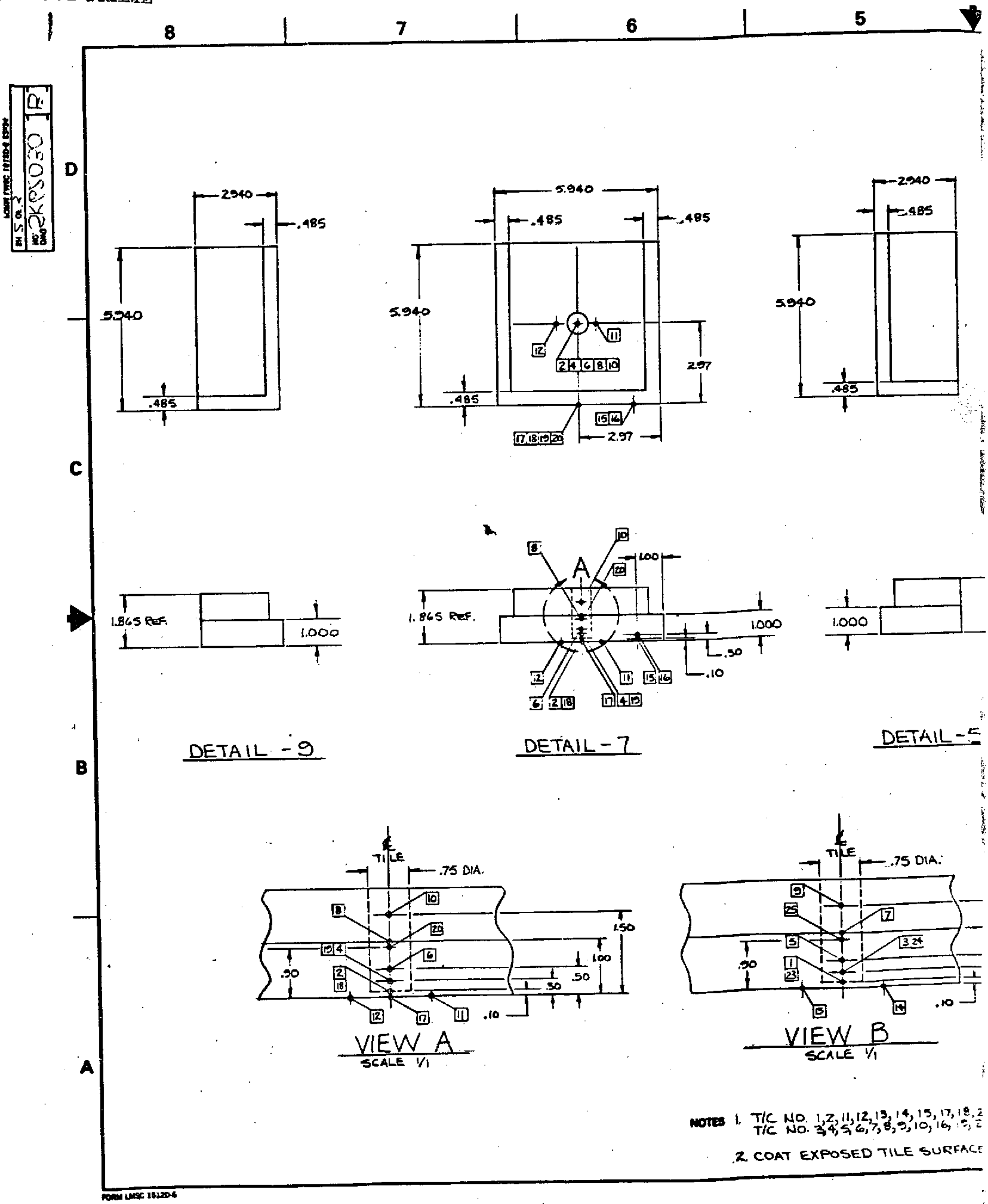

8
7
6
5
D
C
B
A
2.940
.485
5.940
2.97
DETAIL - 9
DETAIL - 7
DETAIL - 5
1.865 REF.
1.000
.50
.10
1.00
VIEW A
SCALE 1/1
VIEW B
SCALE 1/1
.75 DIA.
TILE
1.50
NOTES 1. T/C NO. 1, 2, 11, 12, 13, 14, 15, 17, 18,
T/C NO. 3, 4, 5, 6, 7, 8, 9, 10, 16,
2. COAT EXPOSED TILE SURFACE
FORM LMSC 1512D-6

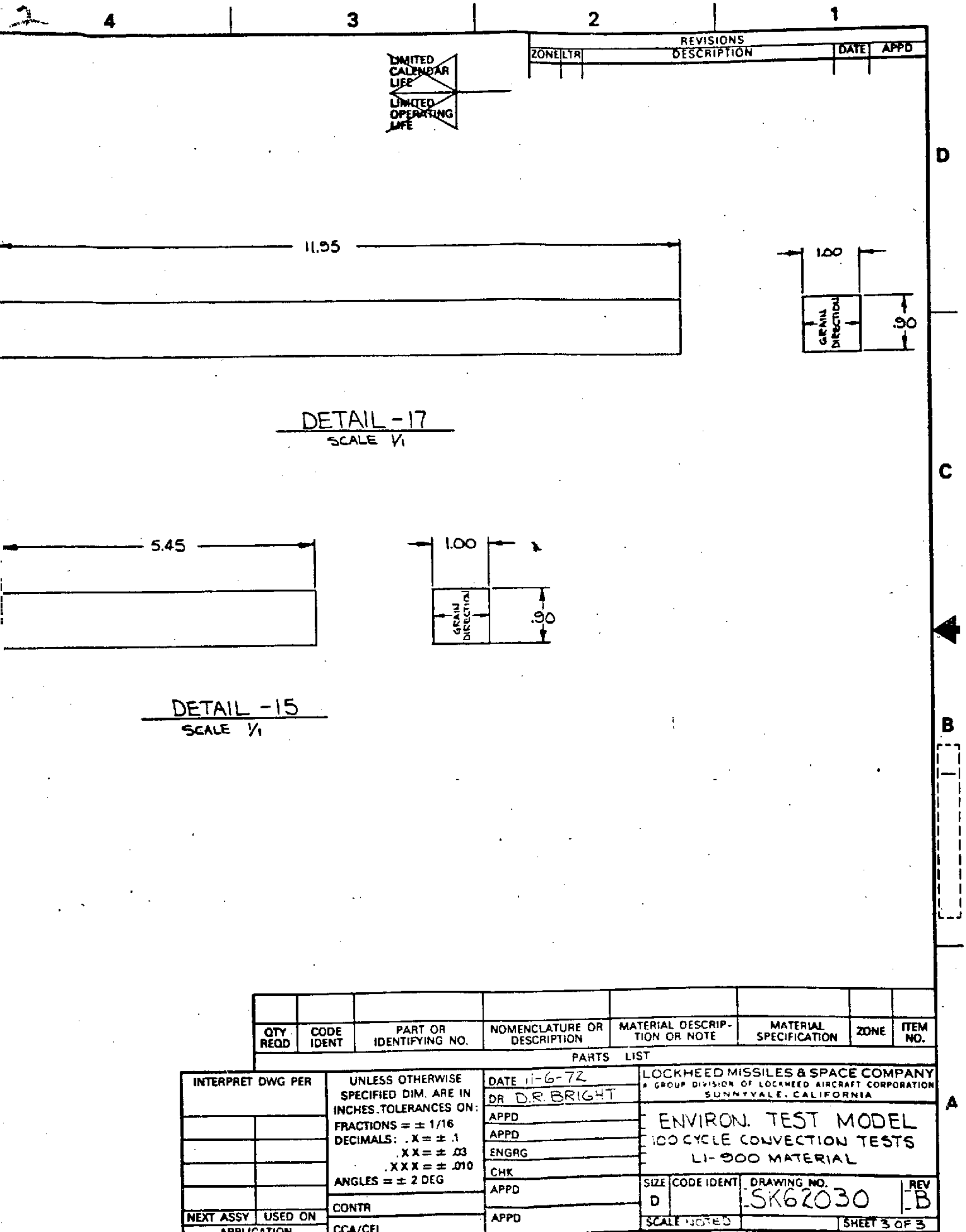

Fig. C2-3 Drawing SK62030, Sheet 2

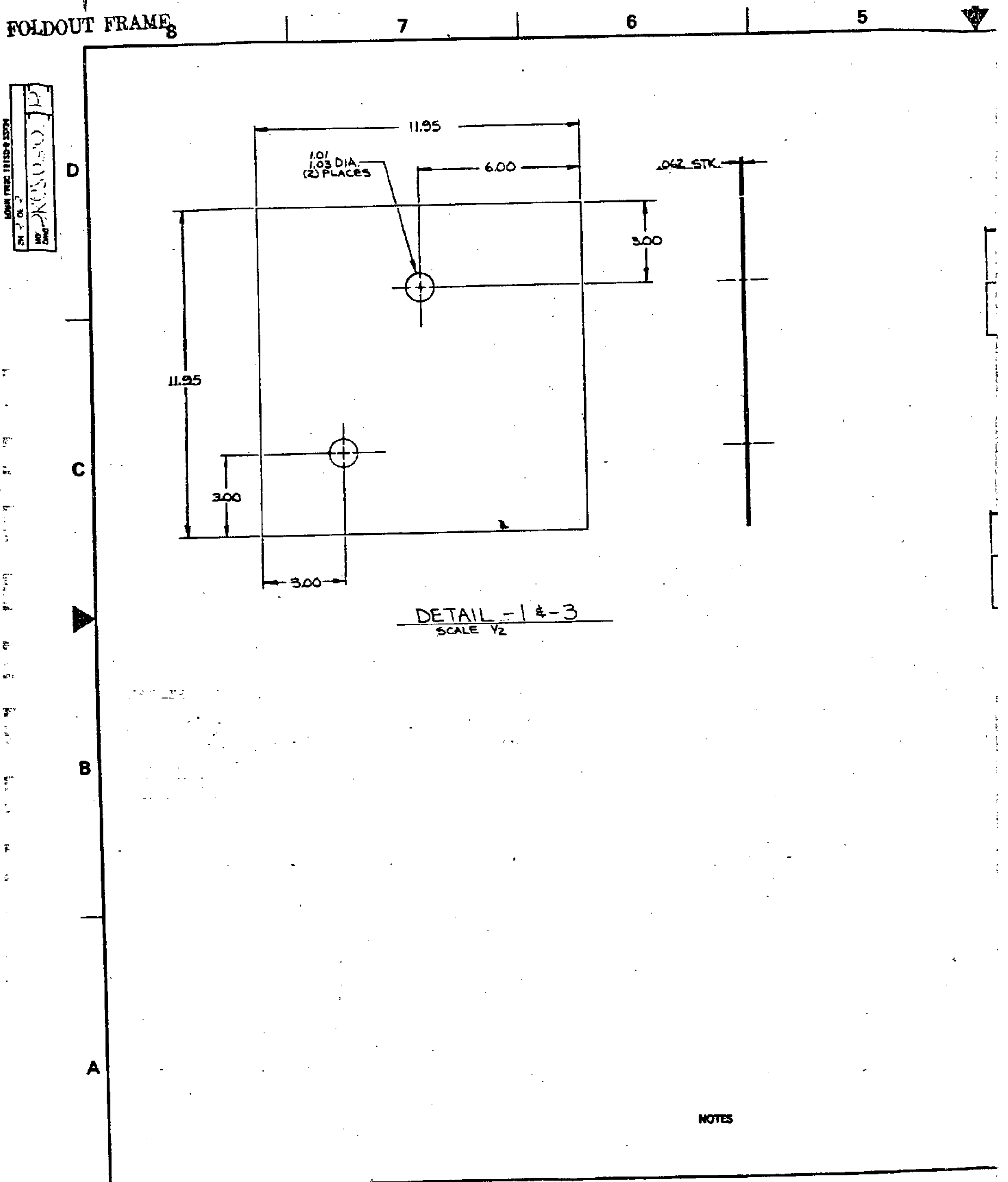

FORM LMSC 15120-6

Appendix E1

ENVIRONMENTAL TEST PLAN FOR PHASE III RSI PROTOTYPE PANEL

NAS 9-12856

National Aeronautics and Space Administration
Manned Spacecraft Center
Houston, Texas

Prepared by:

D. R. Elgin

D. R. Elgin
Thermal Protection System

Approved by:

R. D. Buttram

R. D. Buttram
Program Manager, NAS 9-12856

Kevin Forsberg

K. J. Forsberg, Manager
Thermal Protection System

ENVIRONMENTAL TEST PLAN FOR PHASE III
RSI PROTOTYPE PANEL

1. INTRODUCTION

Lockheed Missiles & Space Company, Inc. (LMSC) is delivering one prototype test panel for NASA/MSC evaluation as specified in Section 3.5.1 of the Statement of Work for Contract NAS 9-12856. This panel consists of an aluminum structure simulating the Space Shuttle Orbiter primary structure, four square feet of LI-900 silica rigid surface insulation (RSI) attached with the strain arrestor attachment system, instrumentation, and test fixture adaptor hardware. This document outlines the LMSC recommended environmental test program to be followed by MSC in evaluation of this panel. The objective of the test program is to perform a thermal/structural evaluation of the prototype panel to demonstrate the feasibility of the silica RSI for application on the Space Shuttle Orbiter Vehicle. The approach to meeting this objective is: (1) to evaluate reuse capabilities of the RSI material, (2) to evaluate strain isolation performance of the attachment concept, and (3) to compare LMSC analytical predictions with the NASA/MSC obtained experimental data.

2. DESIGN CRITERIA/CONDITIONS

The aluminum prototype panel is representative of primary structure in Area 2 on the orbiter vehicle lower surface as specified in the Phase II contract (NAS 9-12083). The panel design temperature limit of 250°F occurs in flight during critical load conditions. A maximum temperature of 300°F occurs after landing. Depending on orbit conditions, the initial temperature at start of reentry can vary from +250°F down to -250°F. The backface temperature history of the Area 2P aluminum structure is shown in Fig. 1 for two initial temperatures. In addition, the substrate load history is superimposed from start of reentry to touchdown at 3600 seconds. The -250°F cold soak condition has been used for the majority of the screening exercises. Other critical conditions at t = 1000 seconds and at touchdown have been considered in the design effort. For screening it has been shown that the $-250^{\circ}F$ cold soak condition results in stresses very close to the maximum values; therefore, in the interest of economy and schedule, it is suggested that the cooldown tests be performed without application of tensile loads.

The contract Phase II groundrules specify an adiabatic backface condition on the primary structure and a maximum backface temperature of $300^{\circ}F$. In addition to the pressure effects on thermal conductivity, the heat capacity of the attachment system and structure also effect the LI-900 sizing. Figure 2 shows the LI-900 thickness requirement versus attachment heat capacity for a family of maximum backface temperatures. As an example, the contract baseline (HMS/X-904) results in a heat capacity of 0.114 Btu/$^{\circ}F$, requiring a LI-900 thickness of 3.04 inches to limit the primary structure temperature to $300^{\circ}F$.

The LI-900 is sized for flight pressures assuming an adiabatic backface. To satisfy the test program objectives during the 1 atm tests, the modified test pulse shown in Fig. 3 is recommended. The load conditions can then be imposed for the same backface temperature conditions that would be obtained for flight conditions with an adiabatic backface.

To approach the adiabatic backface condition, it is suggested covering the substrate with about 2 to 3 in. of low density fibrous insulation (4 to 6 pcf) similar to Dynaflex or microquartz or its equivalent. Due to the massive end fixtures for the load tests which act as a heat sink and create a two dimensional conduction situation on the backface only the center area of the panel can be expected to approach the adiabatic backface condition.

The test program consists of subjecting the test panel to sequential and combined environment simulations of ascent acoustic loading, ascent mechanical loading, orbit cold soak, entry mechanical loading and heating, and cruise mechanical loading.

The aluminum panel is designed to carry primary structure loads with the pressure differential loads of secondary importance. Application of the pressure differential loads in the existing MSC tensile load/radiant heat facility would require extensive modifications which are not considered justified to perform the panel thermal/structural evaluations. Therefore, it is proposed that the mechanical loads on these panels be confined to tensile loads.

It is intended to subject the panel to a minimum of 25 and a maximum of 100 mission environment simulations.

3. PANEL DESCRIPTION

The prototype panel assembly design is shown on LMSC drawing SKW 111672, Fig. 4 (three sheets). The strain arrestor plate design is shown separately on SKW 111772, Fig. 5.

4. INSTRUMENTATION

The proposed instrumentation is also shown on SKW 111672. Two of the 12 x 12 x 3 in. LI-900 tiles are instrumented in depth with thermocouples. One of these tiles also has surface thermocouples. Both strain gages and thermocouples are located on the aluminum structure backface. Thermocouples are to be continuously recorded during all thermal tests; strain gages are to be continuously monitored during cold soak and mechanical tests. The instrumentation consists of:

7	– Pt - Pt 10 percent Rh T/C's – Surface and 0.25 in. depth
20	– Cr-Al T/C's at plugs
TBD	– Cr-Al T/C's on aluminum
TBD	– Unidirectional strain gages

In addition to the above instrumentation, LMSC requests that at least one GFE accelerometer be installed and monitored during acoustic testing at a location to be determined. One GFE deflectometer should monitor the deflection at the panel center point during mechanical load tests.

5. RECOMMENDED TEST PROGRAM

The prototype panel has been designed to interface with existing MSC test hardware.

5.1 TEST DESCRIPTION

The individual recommended tests are as follows:

5.1.1 Axial Load Test

a. Apply axial preload of 1000 lb.

b. Increase load at a rate of 500 lb/sec to 96,000 lb (full limit load) in 15,000 lb increments and hold load for sufficient time at each 15,000 lb increment for visual inspection of TPS. Maintain load for 10 minutes at 96,000 lb.

c. Reduce load to 1,000 lb over a period of not less than 1 minute.

d. Perform visual inspection of panel, record any anomalies, photograph.

5.1.2 Radiant Heat Test (1700°F, Atmospheric Pressure)

a. Apply axial preload of 1000 lb.

b. Increase RSI surface temperature to 1700°F over a period of 300 sec.

c. Maintain 1700°F surface temperature for 950 sec.

d. Decrease surface temperature to ambient over a period of 350 sec.

e. Allow panel to cool to ambient conditions.

f. Inspect panel, record any anomalies, photograph.

5.1.3 Radiant Heat Test (2300°F, Atmospheric Pressure)

a. Apply axial preload of 1000 lb.

b. Increase RSI surface temperature to 2300°F over a period of 500 sec.

c. Follow the atmospheric pressure heat pulse shown in Fig. 3.

d. Allow panel to cool to ambient conditions.

e. Inspect panel, record any anomalies, photograph.

5.1.4 Radiant Heat Test ($2300^{o}F$, Atmospheric Pressure + Axial Load, Maximum Bondline Temperature Condition)

a. Apply axial preload of 1000 lb.
b. Follow the atmospheric pressure heat pulse shown in Fig. 3.
c. Gradually apply load to obtain an axial load of 33,600 lb at 35 minutes from start of the temperature pulse.
d. Maintain 33,600 lb axial load for 10 minutes.
e. Increase load to 64,800 lb over a 30 sec period.
f. Maintain 64,800 lb load for 1 minute.
g. Decrease load to 33,600 lb over a 30 sec period.
h. At 50 minutes from start of temperature pulse, increase load to 96,000 lb over a 30 second period.
i. Maintain 96,000 lb load for 1 minute.
j. Reduce load to 1000 lb over a 1 minute period.
k. Allow panel to cool.
l. Inspect panel, record any anomalies, photograph.

5.1.5 Orbit Cooldown Cycle (Atmospheric Pressure)

a. Cool test article to $-250^{o}F$. (In about 5 hours, cooling from LI-900 surface).
b. Maintain specimen at $-250^{o}F$ for a test period of 90 minutes.
c. Allow panel to return to ambient temperature conditions.
d. Inspect panel, record any anomalies, photograph.

5.1.6 Radiant Heat Test ($2300^{o}F$, Reduced Pressure)

This portion of the test sequence will be performed in the radiant-vacuum test facility.

a. Depressurize the vacuum chamber to 0.1 psia.
b. Follow the flight heat pulse shown in Fig. 3.

c. Initiate pressurization of the vacuum chamber. Control a linear increase in pressure from 0.1 psia at 500 seconds into the heat pulse to 1.0 psi at 3000 seconds into the heat pulse. Control a linear increase in pressure from 1.0 psi at 3000 seconds into the heat pulse to 14.7 psi at 3600 seconds into the pulse.

d. Allow panel to cool to ambient conditions.

e. Inspect panel, record any anomalies, photograph.

5.1.7 Acoustic Test

a. Expose test panel to spectrum shown in Fig. 6 for a period of 150 seconds.

b. Inspect panel, record any anomalies, photograph.

5.2 TEST SEQUENCE

The recommended test sequence is shown in Table 1. This sequence accumulates 28 thermal cycles on the panel. Subsequent tests should initiate with test number 7.

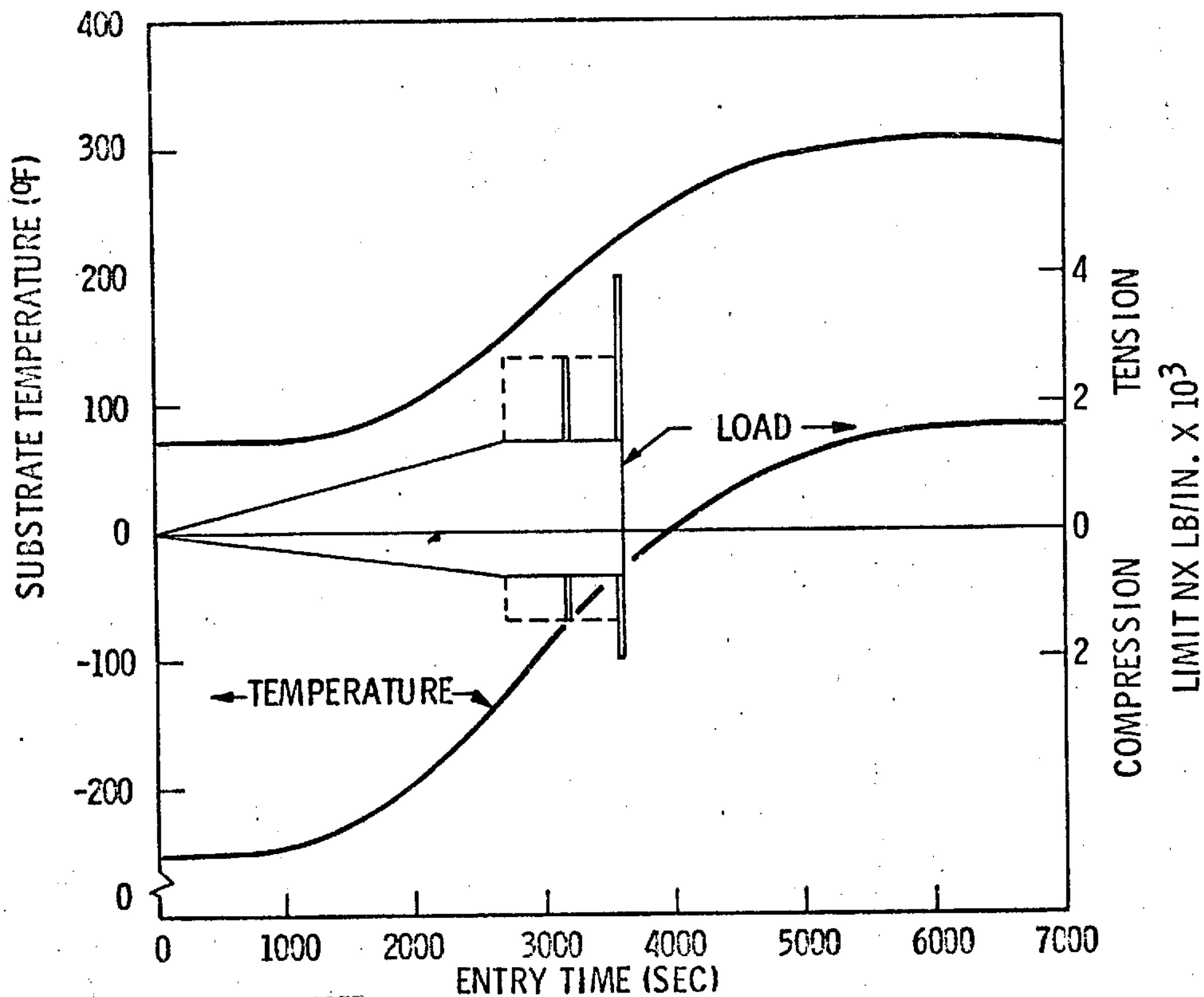

Area 2P Temperature/Load History

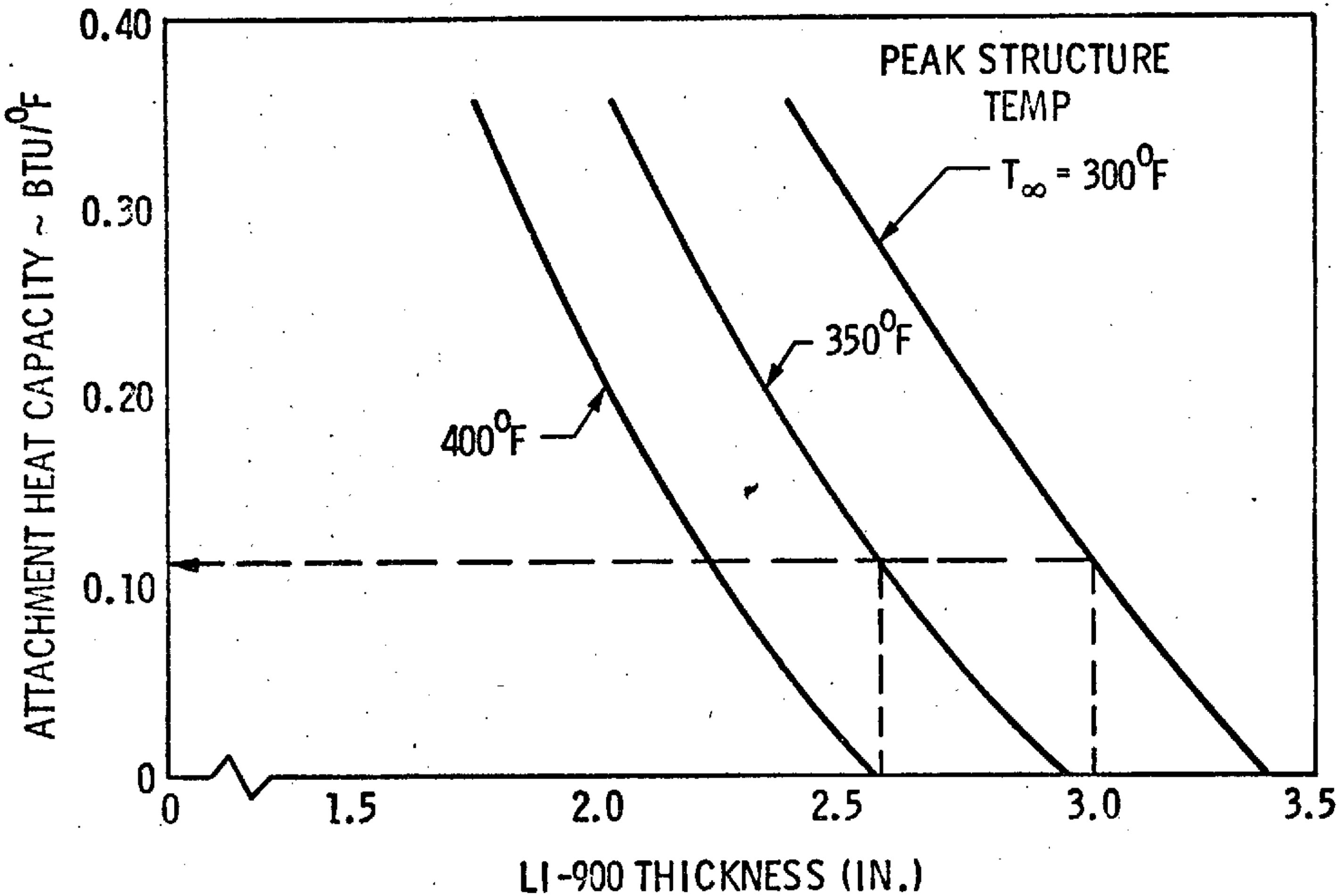

Fig. 2 Variation of LI-900 Thickness With Attachment Heat Capacity — Area 2P

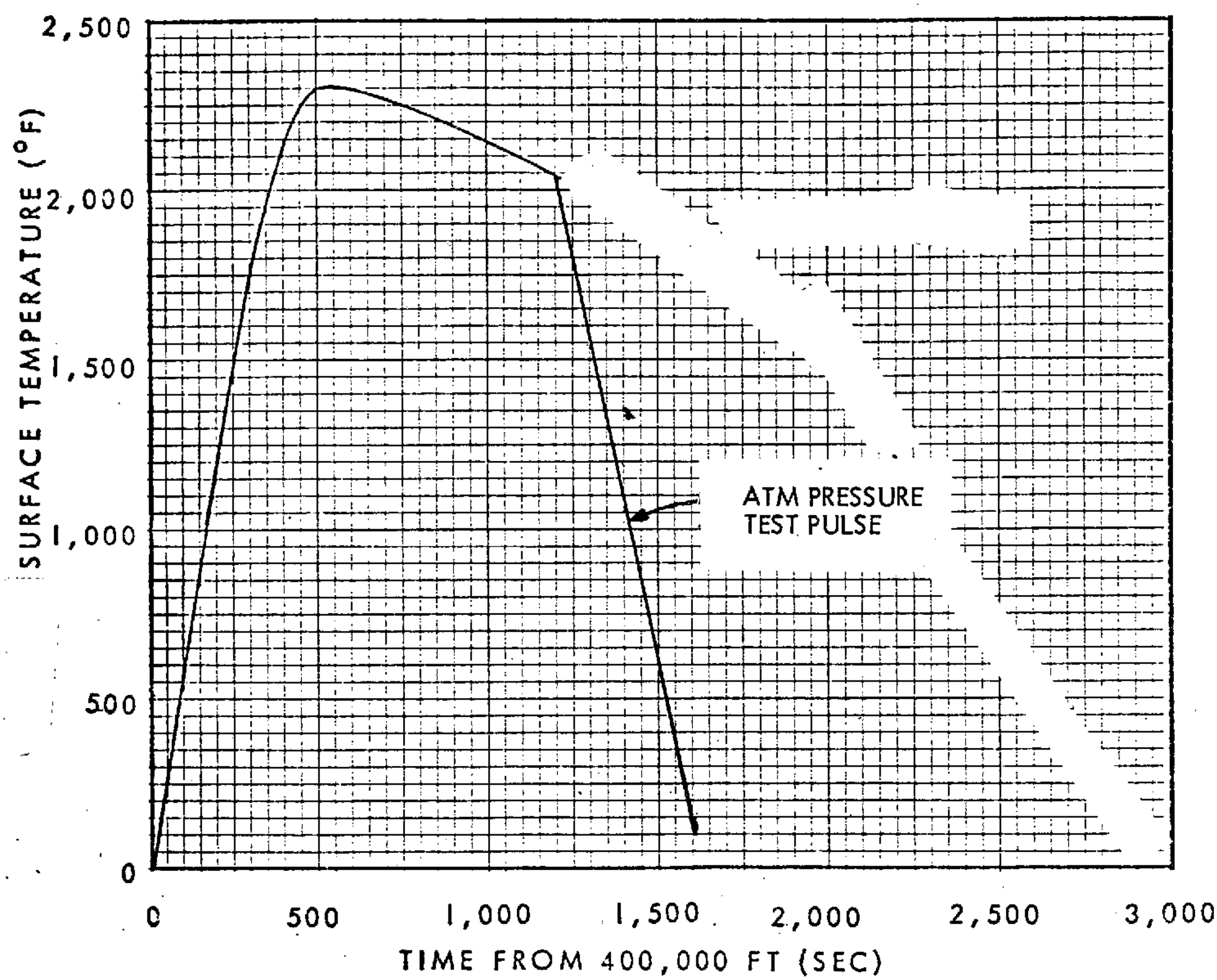

Test Temperature Profile – Area 2

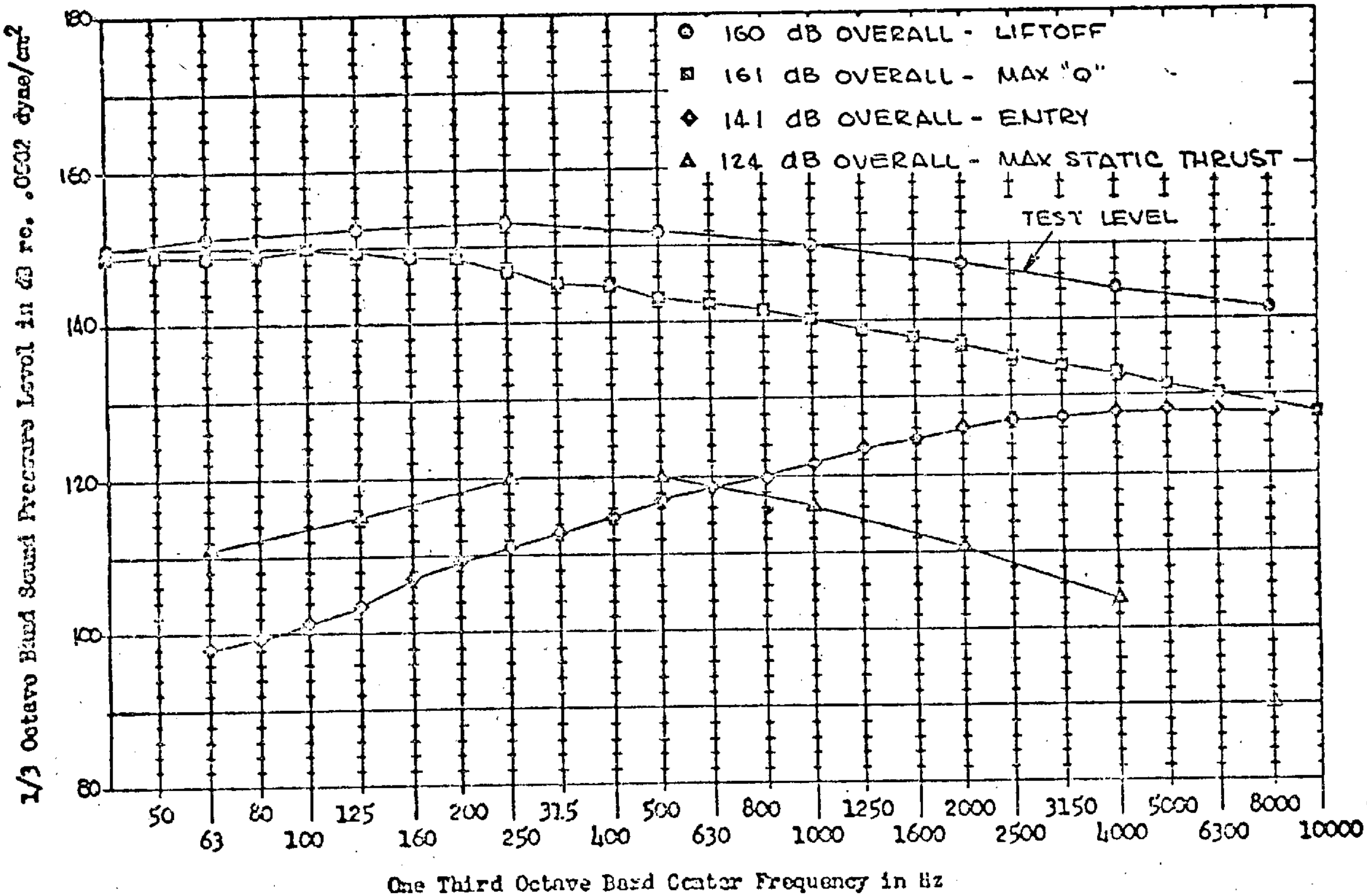

Acoustic Test Criteria